2020-09-23

Self-Recoverable Dual Physically Cross-Linked Hydrogels Incorporating Hydrophobic Interactions

Liu, Xinyao

UNIVERSITY OF CALGARY

Self-Recoverable Dual Physically Cross-Linked Hydrogels Incorporating Hydrophobic Interactions

by

Xinyao Liu

A THESIS

SUBMITTED TO THE FACULTY OF GRADUATE STUDIES

IN PARTIAL FULFILMENT OF THE REQUIREMENTS FOR THE

DEGREE OF MASTER OF SCIENCE

GRADUATE PROGRAM IN CHEMICAL ENGINEERING

CALGARY, ALBERTA

SEPTEMBER, 2020

Abstract

Over the past few years, self-recoverable hydrogels with desirable mechanical properties have attracted a lot of interests. However, the incorporating of hydrophobic force in hydrogel was not well studied to improve the mechanical properties of self-healing materials compared to electrostatic interactions and hydrogen bonding. In this study, a novel dual physically cross-linked (DPC) hydrogel with self-recoverability was mainly cross-linked and strengthened by hydrophobic interactions between the hydrocarbon chains C8 and C18, in addition to electrostatic and hydrogen bonding between N,N-dimethylacrylamide (DMAc) and cellulose nanocrystal (CNC). C18 alkyl chain was grafted to N-[3-(Dimethylamino)propyl] methacrylamide (DMAPMA) to obtain hydrophobic monomer DMAPMA-C18. Hydrophobic CNC-C8was obtained by grafting C8 to the surface using silane chemistry. Then the DPCCNC-g-DMAc-DMAPMA-C18 (CNC DPC) hydrogels and CNC-C8-g-DMAc-DMAPMA-C18 (CNC-C8 DPC) hydrogels were prepared. The optimum CNC-C8 DPC hydrogel with 0.0675 w/v % DMAPMA-C18 and 0.4 w/v % CNC-C8 possessed excellent elongation of 4267.85%±1445.58%, nominal stress of 331.05±32.06 kPa, true stress of 14463.99±2939.98 kPa, compressive tress of 2822.77 kPa at the strain of 90%, facile self-recovery with tetrahydrofuran on the cut surfaces, as well as high water absorption ability of 19.87±0.64 g/g with well-retained shape.

Keywords: Hydrogel; Self-Recoverability; Nanocellulose Crystal; Hydrophobic Force.

Preface

This thesis is original, unpublished, independent work by the author, Xinyao Liu, with the contribution of the individuals listed below.

The research shown in this thesis was conducted under the supervision of Dr. Qingye (Gemma) Lu and Dr. Jinguang Hu, both of which have made significant contributions to all areas of this project.

Acknowledgement

At first, I would like to strongly thank my supervisor Dr. Qingye (Gemma) Lu and co-supervisor Dr. Jinguang Hu for their helpful advice and supervision during all my research work periods. I feel fortunate to work on such an interesting project and obtained satisfying results at last.

I really appreciate that Dr. Hua Song and Dr. Ke (Duke) Du as members of my committee. for the great comments and feedback

Special thanks to Bo Yang and Lu Lai for all of their technical and experimental supports. I must be grateful to the technician in our laboratory, Ola Jabar, who provided me training to the devices in the common lab, which are actually useful in my experiments. I would like to thank Qing Wang for his suggestions in tensile test part. Big thanks to Xiao He and Mozhu Li for their advice on my writing work and the helps from Yulei Zhu and Xiaowei Sun on graphs drawing. I would like to acknowledge the University of Calgary service labs that assisted with several sample analysis and the funding sources (NSERC Discovery Grant，the Start-up fund from University of Calgary, URGC SEM faculty seed grant sponsored by NSERC, the Canada First Research Excellence Fund (CFREF) for its Global Research Initiative in Sustainable Low Carbon Unconventional Resources).Big thanks to all past and present group members in the Dr. Lu and Dr. Hu

group for the support throughout my time in the lab. I feel fortunate to have the opportunities to work with members of both groups who diversified my knowledge.

At last, I must give big thanks to my parents. I cannot finish the Master degree successfully here without the love and supports from them. They encourage me and are proud of me all the time. In addition, I would also like to thank my friends for their supports and comforts. Your encouragements are quite significant for me to study abroad alone as an international student.

Table of Contents

Abstract....ii

Preface iii

Acknowledgement....iv

Table of Contents vi

List of Tables....x

List of Figures xiii

List of Schemes....xx

List of Symbols, Abbreviations & Nomenclature....xxi

Chapter 1 Introduction....1

1.1 Background 1

1.2 Interactions in Dual Physically Cross-Linked Hydrogel 7

1.3 Research Gaps 10

1.4 Overview of Objectives and Thesis Outline 14

Chapter 2 Literature Review....16

2.1 Hydrogels 16

2.1.1 Hydrogels Tensile Properties Enhancement Methods....16

2.1.1.1 Chemical covalent bonds 16

2.1.1.2 Hydrogen bonds 17

2.1.1.3 Electrostatic interactions 17
2.1.1.4 Hydrophobic interactions 18
2.1.2 Self-Recoverable Hydrogel Materials 20
2.2 Cellulose Nanocrystals 23
2.2.1 Cellulose Nanocrystals Characteristics 23
2.2.1 Cellulose Nanocrystals in Hydrogels 25
Chapter 3 Materials and Experimental Methods 29
3.1 Materials 29
3.2 Fourier-Transform Infrared Spectroscopy (FT-IR) 29
3.3 Scanning Electron Microscope (SEM) 30
3.4 Tensile Test 30
3.5 Compression Test 32
3.6 Self-Recoverability Test 32
3.7 Swelling Test 33
3.8 Two-way ANOVA Analysis 37
Chapter 4 Preparation of Hydrophobic Monomer and CNC, and Synthesis of Hydrogels 39
4.1 Preparation of DMAPMA-C18 39
4.2 Preparation of CNC-C8 40
4.3 Synthesis of CNC DPC Hydrogels 44

4.4 Synthesis of CNC-C8 DPC Hydrogels 49

Chapter 5 Characterization and Performance Evaluation of DPC Hydrogels 51

5.1 FT-IR Analysis 51

5.2 Mechanical Measurements 53

5.2.1 Stress 53

5.2.1.1 Nominal Stress 53

5.2.2.1 True Stress 60

5.2.2 Strain 64

5.2.3 Compression Tests 70

5.2.4 Typical Stress-Strain Profiles 72

5.2.5 Self-Recoverability 73

5.3 Swelling Test 76

5.3.1 Water Absorption 76

5.3.2 Olive Oil Absorption 86

5.3.3 Chloroform Absorption 91

5.4 Two-way ANOVA Analysis 98

5.4.1 Test of the Effects of CNC/CNC-C8 and DMAPMA-C18 Contents on Stress 98

5.4.2 Test of the Effects of CNC/CNC-C8 and DMAPMA-C18 Contents on Strain 103

5.4.3 Test of the Effects of CNC/CNC-C8 and DMAPMA-C18 Contents on

Water Absorption 109

5.4.4 Test of the Effects of CNC/CNC-C8 and DMAPMA-C18 Contents on Olive Oil Absorption 115

5.4.5 Test of the Effects of CNC/CNC-C8 and DMAPMA-C18 Contents on Chloroform Absorption 120

5.5 SEM Analysis 127

Chapter 6 Conclusion and Future Work 128

6.1 Conclusion 128

6.2 Future Work 132

References 134

Appendix 154

List of Tables

Table 4. 1 The volumes of trichloro(octyl)silane to react with 3 g CNC at different C8 alkyl chains modification levels.....43

Table 5. 1 DPC hydrogel nominal stresses (kPa) at different CNC contents (w/v %) and DMAPMA-C18 contents (w/v %) 56

Table 5. 2 DPC hydrogel nominal stresses (kPa) at different CNC-C8 contents (w/v %) and DMAPMA-C18 contents (w/v %).....57

Table 5. 3 DPC hydrogel true stresses (kPa) at different CNC contents (w/v %) and DMAPMA-C18 contents (w/v %).....61

Table 5. 4 DPC hydrogel true stresses (kPa) at different CNC-C8 contents (w/v%) and DMAPMA-C18 contents (w/v %) 62

Table 5. 5 DPC hydrogel elongations (%) at different CNC contents (w/v %) and DMAPMA-C18 contents (w/v %).....67

Table 5. 6 DPC hydrogel elongations (%) at different CNC-C8 contents (w/v %) and DMAPMA-C18 contents (w/v %).....68

Table 5. 7 DPC hydrogel water absorption capacity (g/g) at different CNC contents (w/v %) and DMAPMA-C18 contents (w/v %).....81

Table 5. 8 DPC hydrogel water absorption capacity (g/g) at different CNC-C8 contents (w/v %) and DMAPMA-C18 contents (w/v %) 82

Table 5. 9 DPC hydrogel olive oil absorption capacity (g/g) at different CNC contents (w/v %) and DMAPMA-C18 contents (w/v %) 87

Table 5. 10 DPC hydrogel olive oil absorption capacity (g/g) at different CNC-C8

contents (w/v %) and DMAPMA-C18 contents (w/v %) 88

Table 5. 11 DPC hydrogel Chloroform Absorption Capacity (g/g) at different CNC Contents (w/v %) and DMAPMA-C18 contents (w/v %) 94

Table 5. 12 DPC hydrogel Chloroform Absorption Capacity (g/g) at different CNC-C8 contents (w/v %) and DMAPMA-C18 contents (w/v %)..... 95

Table 5. 13 CNC DPC hydrogels Minitab® 19 factor information for stress..... 99

Table 5. 14 CNC DPC hydrogels Minitab® 19 Two-way ANOVA results for stress. 99

Table 5. 15 CNC-C8 DPC hydrogels Minitab® 19 factor information for stress 101

Table 5. 16 CNC-C8 DPC hydrogels Minitab® 19 Two-way ANOVA results for stress..... 102

Table 5. 17 CNC DPC hydrogels Minitab® 19 factor information for strain..... 104

Table 5. 18 CNC DPC hydrogels Minitab® 19 Two-way ANOVA results for strain 104

Table 5. 19 CNC-C8 DPC hydrogels Minitab® 19 factor information for strain 106

Table 5. 20 CNC-C8 DPC hydrogels Minitab® 19 Two-way ANOVA results for strain..... 107

Table 5. 21 CNC DPC hydrogels Minitab® 19 factor information for water absorption 109

Table 5. 22 CNC DPC hydrogels Minitab® 19 Two-way ANOVA results for water absorption 110

Table 5. 23 CNC-C8 DPC hydrogels Minitab® 19 Factor Information outputs for water absorption 112

Table 5. 24 CNC-C8 DPC hydrogels Minitab® 19 Two-way ANOVA results outputs for water absorption 113

Table 5. 25 CNC DPC hydrogels Minitab® 19 factor information for olive oil absorption 115

Table 5. 26 CNC DPC hydrogels Minitab® 19 Two-way ANOVA results for olive oil absorption 116

Table 5. 27 CNC-C8 DPC hydrogels Minitab® 19 factor information for olive oil absorption 118

Table 5. 28 CNC-C8 DPC hydrogels Minitab® 19 Two-way ANOVA results for olive oil absorption 119

Table 5. 29 CNC DPC hydrogels Minitab® 19 factor information for chloroform absorption 121

Table 5. 30 CNC DPC hydrogels Minitab® 19 Two-way ANOVA results for chloroform absorption 122

Table 5. 31 CNC-C8 DPC hydrogels Minitab® 19 factor information for chloroform absorption 124

Table 5. 32 CNC-C8 DPC hydrogels Minitab® 19 Two-way ANOVA results for chloroform absorption 125

List of Figures

Figure 1. 1 Schematics of (a) single network (SN), (b) double network (DN), (c) triple network (TN) hydrogels and (d) dual physically cross-linked (DPC) hydrogels. 6

Figure 1.2 Schematics of three main physical interactions: (a) hydrogen bonding; (b) hydrophobic associations; (c) electrostatic interactions. 9

Figure 1. 3 Schematic of synthesizing (a) DMAPAMA-C18, (b) CNC-C8 (inset – CNC suspension in toluene), and (c) polymer P-DMAc-DMAPMA-C18; and interaction mechanism among (d) P-DMAc-DMAPMA-C18, (e) CNC-P-DMAc-DMAPMA-C18, and (f) CNC-C8-DMAc-DMAPMA-C18 hydrogels. 12

Figure 2.1 General concepts for self-healing process (Hager et al., 2010. Copyright permission license number: 4876821254963). a) The mechanical influence produces a crack on the material; b) detail crack view; c) the appearance of a "mobile phase"; (d) the crack is recovered by the "mobile phase"; (e) The immobilization material condition after finishing the self-healing process.....20

Figure 2.2 The mechanism sketch map of microcapsules helpingfor self-recoverability (Hager et al., 2010. Copyright permission license number: 4876821254963).....22

Figure 2. 3 Green material source of nanocellulose. 25

Figure 3.1 Shape conditions of hydrogels before and after water absorption process compared with a same coin: (a) initial wet DPC hydrogels before water absorption; (b) expanded wet DPC hydrogels after water absorption for 1 d; (c)

initial freeze-dried DPC hydrogels before water absorption; (d) expanded freeze-dried DPC hydrogels after water absorption for 1 day. 34

Figure 3.2 The shapes of freeze-dried samples after immersion in (a) water, (b) olive oil, and (c) chloroform for 24 hrs compared to a same coin. The insets in every picture show the initial shape of freeze-dried sample.The scale bars are 1 cm. 35

Figure 3.3 The shape of the freeze-dried samples after immersion in chloroform for (a) 80 mins and (b) 24 hrs, respectively. The inset in (a) shows the initial shape of freeze-dried sample. The scale bars are 1 cm. 37

Figure 4. 1 DMAPMA-C18 synthesis installation diagram. 40

Figure 4. 2CNC suspension conditions in different solvents: (a) CNC in acetone with sediments at the bottom, (b) CNC in toluene with sediments at the bottom, (c) CNC can be dispersed well in water, then (d) add acetone and (e) transfer CNC from the mixture solvent to toluene. 41

Figure 4. 3 Schematic of nanocellulose crystal (CNC). 42

Figure 4.4 Schematic of interactions in DMAc-DMAPMA-C18 polymers. 46

Figure 4.5 Schematic of interactions in CNC-DMAc-DMAPMA-C18 hydrogels ... 47

Figure 4.6 Schematic of interactions in CNC-C8-DMAc-DMAPMA-C18 hydrogels. 50

Figure 5.1FT-IR spectra of (a) CNC and CNC-C8 with different C8-modification level, and (b) monomer DMAPMA-C8, polymerized DMAc-DMAPMA-C8, CNC DPC hydrogel and CNC-C8 DPC hydrogel. 52

Figure 5.2 Hydrogel without DMAPMA-C18 monomers (a) could flow while being inverted and (b) Looks like glue. 53

Figure 5. 3 The nominal stress of the DPC hydrogels as a function of the dosage of DMAPMA-C18 with zero CNC or CNC-C8. 54

Figure 5. 4 Nominal tress of CNC or CNC-C8 DPC hydrogels as a function of the dosages of DMAPMA-C18 and (a) CNC or (b) CNC-C8. Each curve represents the changes as a function of DMAPMA-C18 content at constant dosage of CNC or CNC-C8. The points in red circles are the optimal stress values. 55

Figure 5. 5 The nominal stress of the DPC hydrogels as functions of the dosages of CNCand CNC-C8 at each DMAPMA-C18 contents of (a) 0.0225 w/v %, (b) 0.03375 w/v %,(c) 0.045 w/v %, (d) 0.05625 w/v %, (e) 0.0675 w/v %,(f) 0.07875 w/v %,(g) 0.09 w/v %, (h) 0.10125 w/v % and (i) 0.1125 w/v % separately. 58

Figure 5. 6 The(a) uniform hydrogel and (b) not uniform hydrogel. 59

Figure 5. 7 True stress of CNC or CNC-C8 DPC hydrogels as a function of the dosages of DMAPMA-C18 and (a) CNC or (b) CNC-C8. Each curve represents the changes as a function of DMAPMA-C18 content at constant dosage of CNC or CNC-C8. The points in red circles are the optimal stress values. 60

Figure 5. 8 The true stress of the DPC hydrogels as functions of the dosages of CNC and CNC-C8 at each DMAPMA-C18 contents of (a) 0.0225 w/v % , (b) 0.03375 w/v %, (c) 0.045 w/v %, (d) 0.05625 w/v % , (e) 0.0675 w/v %, (f) 0.07875 w/v %, (g) 0.09 w/v %, (h) 0.10125 w/v % and (i) 0.1125 w/v % separately. 63

Figure 5.9 The true stress of the DPC hydrogels as a function of the dosage of DMAPMA-C18. 64

Figure 5.10 The elongation of the DPC hydrogels as a function of the dosage of

DMAPMA-C18. 65

Figure 5. 11 The elongations of DPC hydrogels as a function of the dosage of DMAPMA-C18 and (a) CNC or (b) CNC-C8. Each curve represents the changes as a function of DMAPMA-C18 content at constant dosage of CNC or CNC-C8. The points in red circles are the optimal elongation values. 66

Figure 5. 12 The stress of the DPC hydrogels as a function of the dosages of CNC and CNC-C8 at each DMAPMA-C18 contents of (a) 0.0225 w/v %, (b) 0.03375 w/v %,(c) 0.045 w/v %, (d) 0.05625 w/v %, (e) 0.0675 w/v %,(f) 0.07875 w/v %,(g) 0.09 w/v %, (h) 0.10125 w/v % and (i) 0.1125 w/v % separately.....69

Figure 5. 13 The complete recovery of CNC-C8-P-DMAc-DMAPMA-C18 hydrogel from a pressing-releasing process.....71

Figure 5. 14 Compressive stress-strain curves for the optimal CNC DPC hydrogels and CNC-C8 DPC hydrogels. 72

Figure 5. 15 Typical nominal stress-strain profiles for (a) CNC DPC hydrogels, ...73

Figure 5.16 Photographs (a) and (b) demonstrating the self-healing behavior of CNC-P-DMAc-DMAPMA-C18 hydrogel with optimum contents of CNC and DMAPMA-C18 (a) cut into two hydrogel parts (b) self-recovered. Photographs (c-e) show the ability of hydrogel to withstand (c) twisting, (d) stretching, and (e) knotting. 74

Figure 5. 17 The (a) stress and (b) strain self-recovery ratios of CNC DPC hydrogels and CNC-C8 DPC hydrogels with different DMAPMA-C18 contents.....75

Figure 5. 18 Typical stress-strain curves for self-repaired (a) CNC DPC hydrogel and (b) CNC-C8 DPC hydrogel with optimum content of DMAPMA-C18 and CNC or CNC-C8. 76

Figure 5. 19 Water absorption capacities for (a) wet and (b) freeze-dried CNC DPC hydrogels. 77

Figure 5. 20 Water absorption ability in hours of freeze-dried (a) CNC-P-DMAc-DMAPMA-C18, (b) CNC-C8-P-DMAc-DMAPMA-C18, (c) CNC-P-DMAc-2 DMAPMA-C18 and (d) CNC-C8-P-DMAc-2 DMAPMA-C18 hydrogels. 78

Figure 5. 21 Water absorption ability in days of freeze-dried (a) CNC-P-DMAc-DMAPMA-C18, (b) CNC-C8-P-DMAc-DMAPMA-C18, (c) CNC-P-DMAc-2 DMAPMA-C18 and (d) CNC-C8-P-DMAc-2 DMAPMA-C18 hydrogels. 79

Figure 5. 22 Water absorption capacity of the DPC hydrogel as a function of the dosage of (a) CNC or (b) CNC-C8 and DMAPMA-C18. The points in red circles are the optimal water absorption capacity values. 83

Figure 5. 23 Water absorption capacity of the DPC hydrogels as functions of the dosages of CNC and CNC-C8 at constant dosage of DMAPMA-C18 (a) 0.0225 w/v % , (b) 0.03375 w/v %, (c) 0.045 w/v %, (d) 0.05625 w/v % , (e) 0.0675 w/v %, (f) 0.07875 w/v %, (g) 0.09 w/v %, (h) 0.10125 w/v % and (i) 0.1125 w/v %. 84

Figure 5. 24 Water absorption capacity of DPC hydrogels as a function of the dosage of DMAPMA-C18 85

Figure 5. 25 Water absorption capacities cycling tests. 86

Figure 5. 26 Olive oil absorption capacity of DPC hydrogel as a function of the content of (a) CNC or (b) CNC-C8 and DMAPMA-C18. The points in red circles are the optimal olive oil absorption capacity values. 89

Figure 5. 27 Olive oil absorption capacity of the DPC hydrogels as a function of the dosages of CNC and CNC-C8 at each DMAPMA-C18 contents of (a) 0.0225 w/v % , (b) 0.03375 w/v %, (c) 0.045 w/v %, (d) 0.05625 w/v % , (e) 0.0675 w/v %, (f) 0.07875 w/v %, (g) 0.09 w/v %, (h) 0.10125 w/v % and (i) 0.1125 w/v % separately. 90

Figure 5. 28 Olive oil absorption capacity of DPC hydrogel with different contents of DMAPMA-C18 91

Figure 5. 29 Chloroform absorption capacities for wet and freeze-dried CNC DPC hydrogels at 1 DMAPMA-C18 after ten minutes. 92

Figure 5. 30 The increase of chloroform absorption capacities for CNC DPC hydrogel with the increase of time. 93

Figure 5. 31 Chloroform absorption capacity of DPC hydrogel as a function of the dosage of (a) CNC or (b) CNC-C8 and DMAPMA-C18. The points in red circles are the optimal chloroform absorption capacity values. 96

Figure 5. 32 Chloroform absorption capacity of the DPC hydrogels as a function of the dosages of CNC and CNC-C8 at each DMAPMA-C18 contents of (a) 0.0225 w/v % , (b) 0.03375 w/v %, (c) 0.045 w/v %, (d) 0.05625 w/v % , (e) 0.0675 w/v %, (f) 0.07875 w/v %, (g) 0.09 w/v %, (h) 0.10125 w/v % and (i) 0.1125 w/v %. 97

Figure 5. 33 Chloroform capacity of the DPC hydrogels as a function of the dosage of DMAPMA-C18. 98

Figure 5. 34 CNC DPC hydrogels Minitab® 19 main effects plots for stress. 100

Figure 5. 35 CNC-C8 DPC hydrogels Minitab® 19 main effects plots for stress. .. 103

Figure 5. 36 CNC DPC hydrogels Minitab® 19 main effects plots for strain. 105

Figure 5. 37 CNC-C8 DPC hydrogels Minitab® 19 main effects plots for strain ... 108

Figure 5. 38 CNC DPC hydrogels Minitab® 19 main effects plots for water absorption. ... 111

Figure 5. 39 CNC-C8 DPC hydrogels Minitab® 19 main effects plots for water absorption ... 114

Figure 5. 40 CNC DPC hydrogels Minitab® 19 main effects plot outputs for olive oil absorption. ... 117

Figure 5. 41 CNC-C8 DPC hydrogels Minitab® 19 main effects plots for olive oil absorption ... 120

Figure 5. 42 CNC DPC hydrogels Minitab® 19 main effects plots for chloroform absorption. ... 123

Figure 5. 43 CNC-C8 DPC hydrogels Minitab® 19 main effects plots for chloroform absorption. ... 126

Figure 5. 44 SEM graphs for freeze-dried DPC hydrogels cutting surface. ... 127

List of Schemes

Scheme 4.1 Synthesis of DMAPMA-C18. 39

Scheme 4. 2 Synthesis of CNC-C8. 43

Scheme 4. 3 Synthesis of DMAc-DMAPMA-C18 polymer. 46

Scheme 4. 4 Interactions in DMAc-DMAPMA-C18 polymers. 47

Scheme 4.5 Synthesis of CNC-DMAc-DMAPMA-C18 DPC hydrogels. 48

Scheme 4. 6 Synthesis of CNC-C8-DMAc-DMAPMA-C18 DPC hydrogels 49

List of Symbols, Abbreviations & Nomenclature

18C-Br - 1-Bromooctadecane

3D - Three-dimensional

ANOVA-Analysis of variance

CNC - Cellulose nanocrystal

CNC DPC hydrogel - CNC-g-DMAc-DMAPMA-C18 hydrogel

CNC-C8 DPC hydrogel - CNC-C8-g-DMAc-DMAPMA-C18 hydrogel

CNF - Cellulose nanofibril

DMAc - N,N-dimethylacrylamide

D. I. water - Deionized water

DMAPMA - N-[3-(Dimethylamino)propyl]methacrylamide

DN - Double network

DPC hydrogel - Dual physically cross-linked hydrogel

E. Coli - *Escherichia coli*

FT-IR - Fourier-transform infrared spectroscopy

KPS - Potassium persulfate

LB - Luria-Bertani

NC - Nanocomposite

PAA - Poly acrylic acid

PAM - Polyacrylamide

Q-TCNCS - Quaternary ammonium tundish cellulose nanocrystals

SEM - Scanning electron microscope

SN - Single network

THF - Tetrahydrofuran

Chapter 1 Introduction

1.1 Background

Hydrogels are three-dimensional (3D) cross-linking structure soft materials with a lot of polymer chains (Yuan et al., 2016). As most of its components is water (Z. Zhao, Fang, Rong, & Liu, 2017), hydrogels are usually quite hydrophilic (F. Li, Su, Wang, Wu, & Wang, 2010). The cross-linked networks make hydrogels able to swell and keep a great amount of water inside it without damages to their shapes. They are in a combination condition of solids and liquids (H. Li, Choi, Rutland, & Atkin, 2020). For liquids properties, solvents could diffuse into hydrogels like dispersing in liquid system. For solids properties, the shape of hydrogels would be damaged after being pressed by force and get recovered after releasing the stress(Gong, 2006). The “soft and wet” water containing hydrogel characteristics are approved to be similar to those of living tissues (Akay et al., 2013; Loessner et al., 2016), therefore they would have wide applications in wet environments including artificial muscles and tissues, medical deliveries and so on (Q. Chen et al., 2015; Rao et al., 2018). However, hydrogels used in these fields generally face stress bearing and physical damages problems, so ideal tensile properties and self-healing abilities would be significant (T. L. Sun et al., 2013).

There are usually not enough energy bearing structures in traditional hydrogels (Akay et al., 2013). Therefore, when there appears a pressing or stretching force to hydrogels, they

are definitely easy to break (C. H. Yang et al., 2013). But the promising application areas for hydrogel materials should be like artificial muscles and tissues as mentioned above. They need to play roles like the real muscles and tissues in bodies. If they are so brittle and weak, it would not be reliable for them to have applications as biomaterials. In another word, the poor mechanical properties and self-healing abilities would limit the applications fields of hydrogel materials (J. Y. Sun et al., 2012). If we want to use them as artificial muscles and tissues and for other wider applications, it would be significant to improve the physical capacities and self-healing abilities of hydrogel materials(Yuan et al., 2016).

There are so many methods applied to classify different types of hydrogel materials. One conventional classification is to itemize hydrogels into chemically cross-linking hydrogels and physically cross-linking hydrogels (Seiffert & Sprakel, 2012). Chemically cross-linking hydrogels are composed of chemical rigid bonding which are not reversible while physical cross-linked hydrogels are usually combined with non-covalent physical forces such as electrostatic interactions, hydrophobic forces, hydrogen bonding and so on(X. Yang, Zhang, & Zhang, 2012).When there are pressures or forces applied to hydrogels, the physical interactions could break at first and then get reversed by themselves. The actions do not need any extra energy and would be simple to realize. In contrast, chemical bonds would be hard to recover after being broken. For this reason, we could say that the physical interactions in physically cross-linked hydrogels form a

dynamic system, which could be helpful for hydrogels to dissipate energies and get revised when forces applied to hydrogel materials (Iyer et al., 2013; X. Zhao, 2014). Therefore, physically cross-linked hydrogels are commonly with better mechanical characteristics than chemically cross-linked hydrogels (Busseron, Ruff, Moulin, & Giuseppone, 2013; C. J. Wu, Gaharwar, Chan, & Schmidt, 2011).

Another way to distinguish different types of hydrogel materials is based on the network structures. Hydrogels could be divided into single network (SN), double network (DN) and triple network (TN) hydrogels. SN hydrogels are usually composed of only one type of polymer compositions to form a rigid skeleton as shown in **Figure 1.1a**, which is also the typical conventional hydrogel network structure. The rigid polymer structure is not ductile and reversible. In addition, the SN hydrogel condition is similar to liquids and the polymers inside are usually not uniform, so they are generally weak, brittle and usually not with ideal tensile properties(Gong, 2010).

A modified hydrogel structure called DN hydrogel structure was produced (Gong, Katsuyama, Kurokawa, & Osada, 2003), which was composed of two polymer monomers. One is used to form a rigid skeleton in hydrogels with the similar roles of the polymer molecules in SN hydrogels. The other one is flexible and stretchable, which could be entangled with the rigid skeleton as shown in **Figure 1.1b**. The rigid skeleton was synthesized before the ductile polymer monomers in the DN hydrogel synthesis process, so the rigid skeleton was called the first network while the other one is the second

network (Gong et al., 2003). The DN hydrogel structure could play a useful role in dissipating stresses and forces applied to hydrogels (Gong, 2014). It was proved that the tensile strength and elongation values of DN hydrogels were improved a lot compared with that of SN hydrogels (Fung & Skalak, 1982; Gong, 2010). DN hydrogels have attracted a great amount of attentions because of the significant improvement in tensile properties than traditional hydrogel materials (Haque, Kurokawa, & Gong, 2012).

TN hydrogel structure is similar to DN hydrogel structure. The first network is still a rigid chemical skeleton. The second network and the third network are both polymers added into the system to enhance the physical characteristics, which are combined with physical interactions including hydrogen bonding and hydrophobic interactions. The physical bonding could also help to improve the seal-healing abilities of hydrogel materials (Y. Wang et al., 2018). **Figure 1.1c** showed the schematics of TN hydrogel structures. Because of the TN hydrogel structures are with one more ductile physically cross-linked polymer molecules than DN hydrogels, the TN hydrogels could bear more energy and have stronger physical bonding for self-recovering than DN hydrogels. In general, TN hydrogels are with more optimal mechanical and self-healing capacities than DN hydrogels (Xuefei Li, Qin, Zhang, & Guo, 2019). TN hydrogel structure is a chemical-physical cross-linking structure. Studies showed that the chemical-physical cross-linking structure could efficiently improve hydrogel mechanical properties (W. Sun et al., 2016; S. Wu, Dong, Li, Wang, & Cao, 2017; D. Zhao et al., 2016).

All of the SN, DN and TN hydrogels are with a rigid first network structure. When there are pressing or stretching forces applying to the SN, DN and TN hydrogels, once the chemical bonds are broken, the hydrogels would also be broken and hard to dissipate energy and heal the cracks (Na et al., 2006; Naficy, Spinks, & Wallace, 2014). Dual physically cross-linked (DPC) hydrogel structures are with no irreversible chemical bonding as shown in **Figure 1.1d**. There are only two ductile polymer molecules inside. This is a full physical cross-linking network structure (Y. Hu et al., 2016). When the DPC hydrogels are stretched, all the polymer monomers could move flexibly without any limits from rigid chemical skeleton like an elastic. When the stretching force is removed, the DPC hydrogel shape would get recovered easily compared to SN, DN and TN structures with the existence of rigid chemical bonding. The condition would be similar for pressing forces applying to DPC hydrogels. In addition, the physical forces between polymer monomers like hydrogen bonding, electrostatic interactions and hydrophobic associations could also help for shape recovery and self-healing process. It was estimated that the hydrogels combined of only physical interactions would have better mechanical and self-recoverable performances than those with rigid chemical bonding (Xuefeng Li, Yang, Zhao, Long, & Zheng, 2017; X. H. Wang et al., 2018).

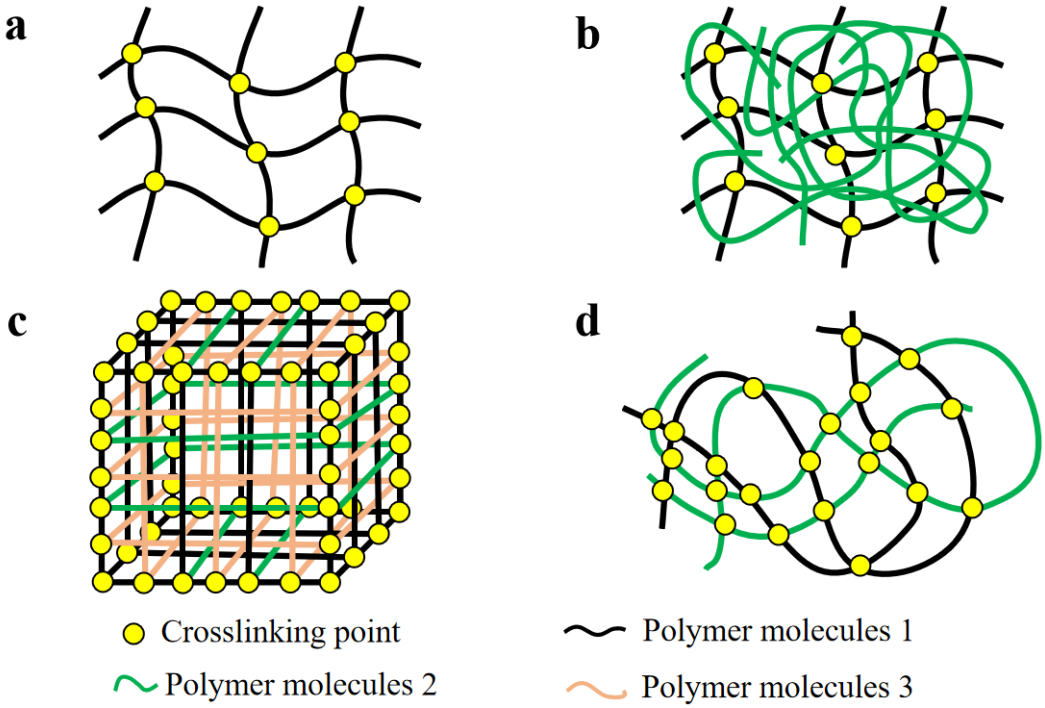

Figure 1. 1 Schematics of (a) single network (SN), (b) double network (DN), (c) triple network (TN) hydrogels and (d) dual physically cross-linked (DPC) hydrogels.

If hydrogels are with ideal self-recoverability and high mechanical strengths at the same time, they could have wider possible applications areas (Hager et al., 2010), so that they could be reused for many times to save the costs. However, because of the existence of rigid chemical bonding in traditional hydrogels, they are generally easy to be broken and have actually weak self-healing abilities (J. Y. Sun et al., 2012).One promising method to solve this problem is to introduce physical force into hydrogel networks to substitute for the rigid covalent bonds in traditional hydrogel materials (Q. Chen et al., 2015).Although the physical bonding may be broken under external stress, they could still have the abilities to get self-recovered after the stress removed.

1.2 Interactions in Dual Physically Cross-Linked Hydrogel

The physical interactions inside DPC hydrogels could efficiently help to improve the mechanical properties and self-healing abilities of hydrogel materials (Ashton & Stewart, 2015; Fan, Shi, Lian, Li, & Yin, 2013; Wei, Wang, Su, Wang, & Qiu, 2015). The physical non-covalent interactions mainly include hydrogen bonding, hydrophobic interactions, electrostatic interactions and so on (Seiffert & Sprakel, 2012; J. Yang, Han, Xu, & Sun, 2014).

Hydrogen bonding is not like a chemical bond. Hydrogen bonding could be divided into two categories: intermolecular hydrogen bonding and intra molecular hydrogen bonding. Intermolecular hydrogen bonding appears between different molecules while intra molecular hydrogen bonding is formed between different parts on one same molecule (Pethes, Bakó, & Pusztai, 2020). To be specific for the hydrogen bonding formation process, a hydrogen atom is combined with an atom with rich electrons, like oxygen (O), nitrogen (N) and fluorine (F), by chemically rigid covalent bond at first. Then if the hydrogen atom is getting close to another electron rich atom, there would appear an interaction between the electron rich atom and the hydrogen atom (Weinhold & Klein, 2014). For example, the schematic of hydrogen bonding between two H_2O molecules is shown in **Figure 1.2a**. The two atoms with rich electron are both oxygen atoms. The hydrogen bonding could be written as "O-H⋯O". The "-" refers to the covalent bond and the "⋯" refers to the hydrogen bond (Arunan et al., 2011).

Materials without polarities could gather together in aqueous solution. This phenomenon is probably because of hydrophobic association (Chandler, 2005).Hydrophobic association effects are a type of reversible physical interactions (Miquelard-Garnier, Demeures, Creton, & Hourdet, 2006). One important factor for the hydrophobic forces formation is hydrophobe. Hydrophobes are difficult to solute insolvent water. They are hydrophobic. Hydrophobes are generally with no polarities. Materials with long hydrophobic carbon chains are a common type of hydrophobes (Akhavan, Jarvis, & Majewski, 2013). Water is with bent shape and polar covalent bonds, so it is defined as polar materials (Jane Reece et al., 2011). Materials which could be easily dissolved in water are hydrophilic substances, which are usually with high polarities. As shown in **Figure 1.2b**, the red areas with hydrophobes are hydrophobic regions and the blue areas are hydrophilic regions. When it is put in dry environmental conditions, the polymer body could be stretched naturally. But once it is immersed into aqueous solutions, the hydrophilic regions are going to get close to the water solvent while the hydrophobic regions are going to escape from it. As a result, the polymer would gather together with hydrophobic groups in the central area and the hydrophilic groups distributed at the outside of the polymer. The hydrophobic effects could not only make the hydrophobic groups gather together but also push the hydrophilic groups gather together (Smulders, Zarra, & Nitschke, 2013). Hydrogen bonding usually take places between hydrophilic groups with high polarities (Chandramouli et al., 2015). From this point of view, we

could say that the hydrophobic force is helpful to enhance hydrogen bonding (Yao et al., 2018).

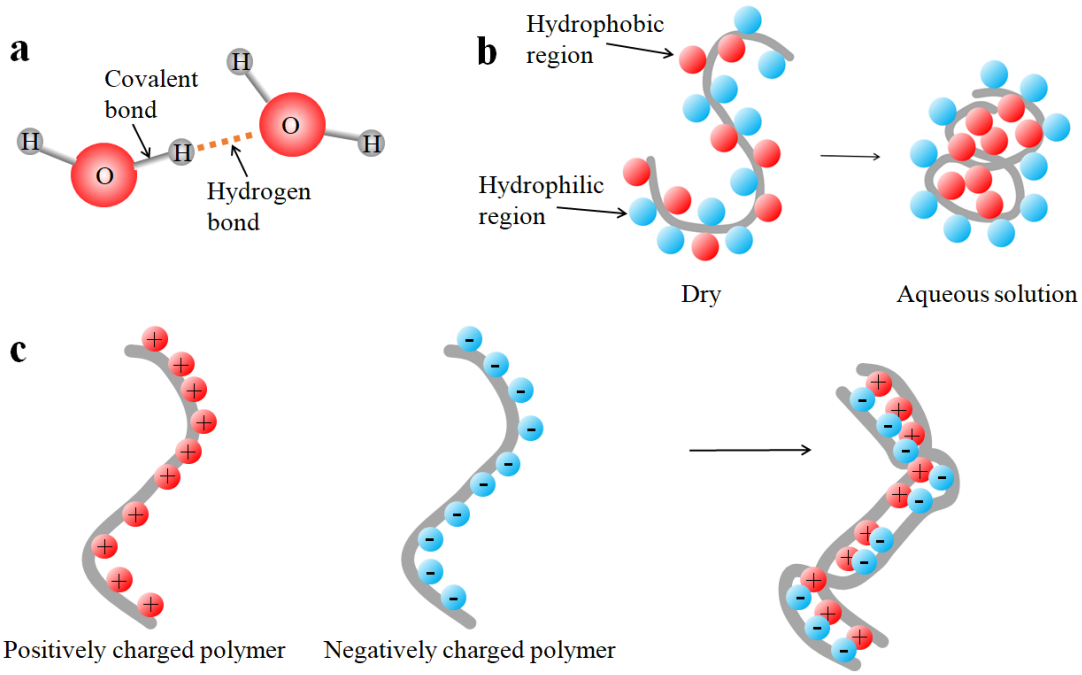

Figure 1.2 Schematics of three main physical interactions: (a) hydrogen bonding; (b) hydrophobic associations; (c) electrostatic interactions.

Electrostatic interaction exists between charged objects, normally called electrostatic double layer forces in aqueous solution. It is attractive between positively charged and negative charged objects. Cationic polymer carries positive charges in water and electrically attracts to positively charged species, while anionic polymer carries negative charges in water and electrically attracts to negatively charged species. The schematic of the interactions are shown in **Figure 1.2 c**.The electrostatic interactions could make the hydrogel structures tighter and thus improve the mechanical properties of hydrogel

materials (J. Yang et al., 2014).

1.3 Research Gaps

It is very important but challenging to design the hydrogels to have high mechanical properties and ideal self-recovery abilities at the same time (Hager, Greil, Leyens, Van Der Zwaag, & Schubert, 2010). Due to the presence of rigid covalent bonds in SN, DN and TN hydrogels, they are easy to be broken under forces. Therefore, fully physically cross-linking hydrogel network would be a promising research area (Q. Chen et al., 2015).

Hydrophobic forces is one type of physical interaction forces in hydrogels (Tuncaboylu, Sari, Oppermann, & Okay, 2011). Even if the hydrophobic associations are broken, they could still be self-recovered and be formed as before. So they could help with energy dissipation under stress and reversible abilities after broken (Mihajlovic et al., 2017). Therefore, hydrophobic interactions could also help to improve the crack resistance and self-healing capacities of hydrogel materials (Hao & Weiss, 2011). In addition, the hydrophobic force could also make hydrogen bonding gather tightly and improve the hydrogel mechanical capacities and self-healing abilities (Yao et al., 2018). However, there are not a lot of research focused on the effects of hydrophobic forces on hydrogel mechanical and self-resemble properties. It would be promising to study on the hydrophobic force effects on hydrogel physical characteristics and self-recoverability improvements.

In addition to the method of improving the hydrogel mechanical properties by changing the hydrogel network structures from chemically cross-linking networks to physically cross-linking networks, nanocomposite (NC) hydrogels would be another useful method to enhance the hydrogel tensile capacities (Haraguchi & Takehisa, 2002; Shi, Wang, Guo, Zhong, & Xie, 2015; T. Wang et al., 2014; D. Xu et al., 2015). Nanocellulose, clay, graphene oxide and other inorganic nanoparticles are all ideal nanocomposites to NC hydrogels synthesis(J. Wang, Lin, Cheng, & Jiang, 2012; Zhong, Liu, & Xie, 2015).Cellulose is a kind of the most abundant and popular material resources in nature (Moon, Martini, Nairn, Simonsen, & Youngblood, 2011). Cellulose nanocrystals (CNCs) could be generally obtained from cellulose acid hydrolysis (Sir ó & Plackett, 2010). As a type of inorganic nanoparticle, CNCs are with ideal mechanical properties itself and could help to enhance NC hydrogels tensile characteristics (Habibi, Lucia, & Rojas, 2010).

A possible proposal is to introduce CNCs into DPC hydrogel systems, where would form a DPC and NC combination hydrogel system. The DPC hydrogel mechanical properties could be enhanced to a higher level. Besides, if the CNC could be modified by hydrophobic groups and hydrogen bonding could be introduced, the new DPC hydrogel could be promising to show excellent physical capacities and self-recoverable abilities.

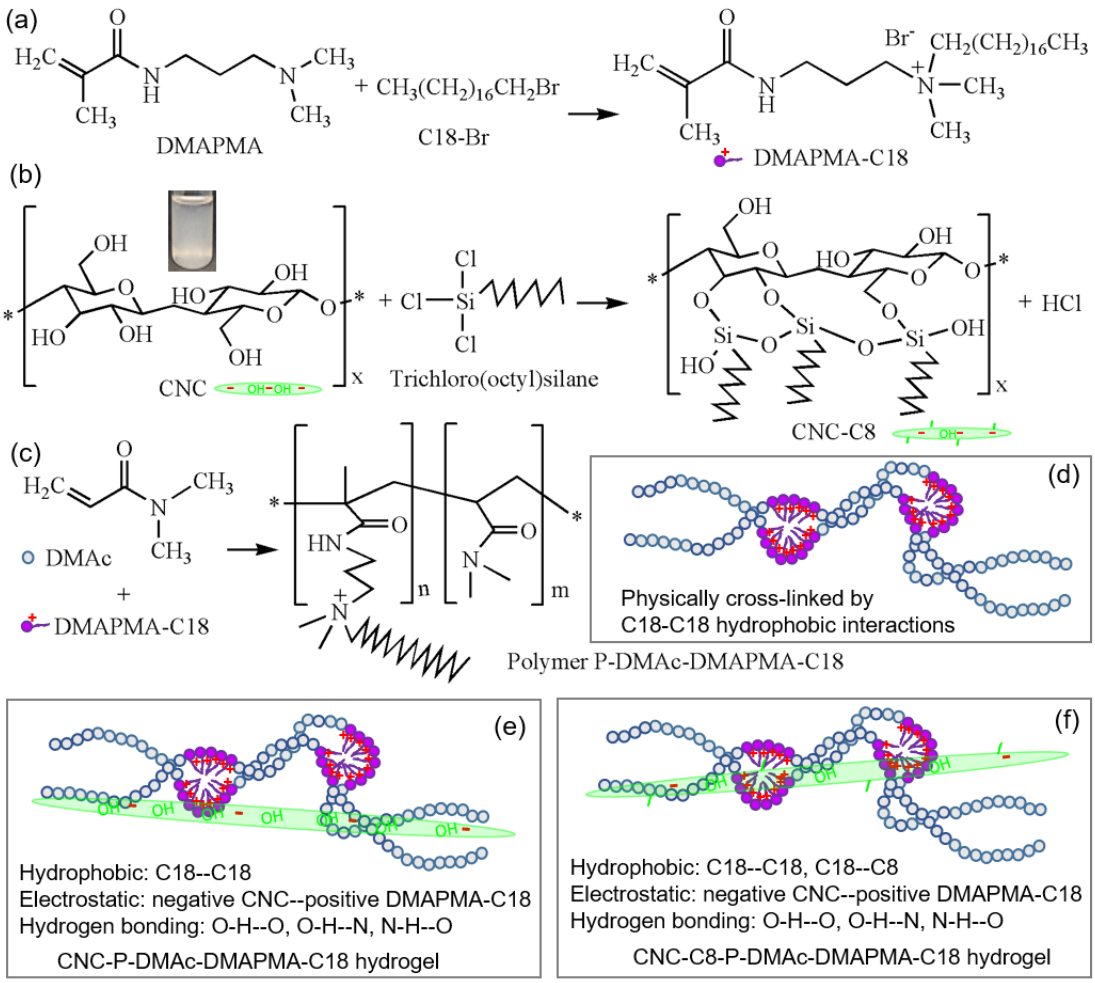

Figure 1. 3 Schematic of synthesizing (a) DMAPAMA-C18, (b) CNC-C8 (inset – CNC suspension in toluene), and (c) polymer P-DMAc-DMAPMA-C18; and interaction mechanism among (d) P-DMAc-DMAPMA-C18, (e) CNC-P-DMAc-DMAPMA-C18, and (f) CNC-C8-DMAc-DMAPMA-C18 hydrogels.

As for traditional hydrogels, they could not contain ideal tensile strength and strain at the same time. For traditional hydrogel structures with rigid bonds, they are with high mechanical stress (usually over 1-2 MPa) and low elongation values (less than 1000%). The DPC hydrogels in this study are like long polymer chains get entangled with each

other as well as CNC and connected with flexible physical bonds. When it was stretched, the changes of hydrogel shapes would not lead to many breaks of rigid bonds, so the stress could be contained well. During the stretching process, the reversible and flexible physical interactions could help for keep the complete structure no broken, which could help for the ideal elongation values of DPC hydrogel materials. Thus the mechanical strength and elongations could get improved a lot at the same time compared with the traditional hydrogel materials.

In this study, C18 alkyl chain was grafted to N-[3-(Dimethylamino)propyl] methacrylamide (DMAPMA) to obtain hydrophobic monomer DMAPMA-C18 (**Fig. 1.3a**). Hydrophobic CNC-C8 was obtained by grafting C8 to the surface using silane chemistry (**Fig. 1.3b**). Then block polymer hydrogel DMAc-g-DMAPMA-C18physically cross-linked by hydrophobic interactions between C18 chains was synthesized using monomers N,N-dimethylacrylamide (DMAc) and DMAPMA-C18 initiated by potassium persulfate (KPS) (**Fig. 1.3c** and **Fig. 1.3d**). Different dosages of CNC and CNC-C8 were added into the polymerization process, respectively, to create dual physically cross-linked CNC-g-DMAc-DMAPMA-C18 (CNC DPC) and CNC-C8-g-DMAc-DMAPMA-C18 (CNC-C8 DPC) hydrogels, respectively. The CNC and CNC-C8 reinforced hydrogels were expected to have good self-recoverability and high tensile strength, considering available physical attractions among the system, hydrophobic interactions between C18 chains, electrostatic attraction between negatively charged CNC and positively charged

DMAPMA-C18, hydrogen bonding among O-H---O, O-H--N, N-H--O (**Fig.1.3e**), and extra hydrophobic interaction between C18 and C8 chains in CNC-C8 reinforced hydrogels (**Fig. 1.3f**).

1.4 Overview of Objectives and Thesis Outline

In this study, a type of DPC hydrogel was synthesized using hydrophobic monomers DMAPMA-C18 and DMAc forming the first physically cross-linked network, and CNC and hydrophobically-modified CNC introduced to form a the second physically interacted structure. The overall objective of this study is to evaluate the effects of hydrophobic forces and different dosages of cellulose nanocrystal addition on mechanical properties of DPC hydrogels. For this purpose, the specific objectives are developed as follows:

1. Evaluate the feasibility of hydrophobic forces and CNC addition in the DPC hydrogels to enhance mechanical properties including stress and strain, and obtain the optimal dosages of hydrophobic monomers addition and CNC addition.

2. Apply hydrophobic modifications to CNC and further evaluate the optimum modified CNC-C8 contents for DPC hydrogels with optimal mechanical characteristics.

3. Investigate the self-recoverable ability of CNC and CNC-C8 DPC hydrogels to find the optimal conditions for self-healing.

4. Explore the swelling capacities of DPC hydrogels in water, olive oil and chloroform with different dosages of hydrophobic DMAPMA-C18 monomers and CNC or hydrophobic modified CNC-C8 contents.

In this thesis, Chapter 1 provides a background related to the study and discussed the current issues, objectives and outline of the thesis. Chapter 2 is a literature review of contents related to this study of hydrogel materials and CNC, reported the four main types of forces and interactions appearing in hydrogel materials for tensile properties enhancement, self-recoverable hydrogel materials as well as the characteristics and applications of cellulose nanocrystals. Then Chapter 3 introduces the detailed materials and experimental methods used in this study. Afterwards, Chapter 4 and 5 are the main parts to address the above objectives in the study. Chapter 4 depicts preparation process for the hydrophobic monomers DMAPMA-C18 and hydrophobic CNC-C8 in detail as well as the CNC DPC hydrogels and CNC-C8 DPC hydrogels synthesis method. Chapter 5 is the Fourier-transform infrared spectroscopy (FT-IR) characterization and DPC hydrogels performance evaluation part, including the results of FT-IR test, tensile test, self-healing ability test, swelling test, Two-way ANOVA analysis and scanning electron microscope (SEM) analysis. The contents in this study are also prepared to be written in a technical paper for publication. Finally, Chapter 6 summarizes the conclusions of this study and future work.

Chapter 2 Literature Review

2.1 Hydrogels

2.1.1 Hydrogels Tensile Properties Enhancement Methods

Currently, there are four main forces applied to improve hydrogel tensile strength and elongation values, which are chemical covalent bonds, hydrogen bonds, electrostatic interactions and hydrophobic associations.

2.1.1.1 Chemical covalent bonds

A covalent bond usually appears between two atoms which share an electron pair (House & House, 2010; Lewis, 1916). Covalent bonds are usually strong and could improve the hydrogel mechanical properties efficiently (H. Chen et al., 2015). However, as they are not reversible and cannot recover after broken, the hydrogels with covalent bonds are usually weak and brittle (Naficy et al., 2014).

Chemical covalent bonds usually show obvious effects on the improvements of stresses and elongations of self-recoverable materials. Dai et al. studied that the length of side chains would play a role in improving the mechanical strengths and self-recoverability of hydrogels (Dai et al., 2015). N-acryloyl glycinamide can be initiated to form poly (N-acryloyl glycinamide) (Seuring &Agarwal, 2010).

2.1.1.2 Hydrogen bonds

Hydrogen bonds are a type of physical force (J. Yang et al., 2014). They are weaker than chemical covalent bonds but they are reversible and could self-heal after being broken. In a hydrogen bonding, a hydrogen atom is combined with an atom with rich electrons by chemically rigid covalent bond. Then there would appear an interaction between another electron rich atom and the hydrogen atom (Weinhold & Klein, 2014).

Compared with chemical bonds, hydrogen bonds would not play an effect in mechanical property improvements as significantly as chemical bonds, but they would be quite helpful for self-recovery abilities (Burattini et al., 2010). The hydrogen bonds are reversible and could be self-resemble after being broken (L. Li et al., 2017).

Ji hyung Ryu et al. studied the microstructures, thermal properties and mechanical performances of CNF (cellulose nanofibrils) /PAM (polyacrylamide) composite films (Ryu, Koo Han, Lee, & Jeong, 2019). Li Bengang et al. proposed a simple method to prepare CNC-g-PAM/PAA(poly acrylic acid) nanocomposite hydrogels with mechanical toughness and self-healing abilities (B. Li et al., 2018).

2.1.1.3 Electrostatic interactions

Electrostatic interactions would also play a role not only in enhancing hydrogel mechanical strengths but also help in self-recovery abilities (T. L. Sun et al., 2013). Zhang Tiantian et al. reported the preparation of double cross-linked nanocomposite

hydrogels by introducing quaternary ammonium tundish cellulose nanocrystals (Q-TCNCS) into chemically-cross-linked PAA network (Zhang, Cheng, Ye, & Chang, 2017). Tao Linsun et al. reported the formation of tensile viscoelastic hydrogels with various mechanical performances from polymers containing randomly dispersed cationic and anionic repetitive groups (T. L. Sun et al., 2013). Strong bonds are eternally cross-linked with significant tensile while the reversible weak bonds are broken and re-formed to dissipate energy. The mechanical performances of DPC hydrogel materials could be easily adjusted by changing the concentrations of clay andiron ions molar ratio. The ideal DPC hydrogel has high tensile strength (about 84.37 kPa) and high elongation (around17 times).

2.1.1.4Hydrophobicinteractions

When a polymer is with both hydrophilic regions and hydrophobic region and immersed into aqueous solution, the hydrophobic regions are prone to gather together at the central area to escape the water molecules outside while the hydrophilic regions would like to stay outside and are going to get close with water molecule (Chandler, 2005). Hydrophobic force is also a physical transient interchain interaction, which could also self-recovered after being broken like hydrogen bonding. In addition, it was approved that the hydrophobic interactions could help to enhance hydrogen bonding strength (Yao et al., 2018).

Hydrophobic force is also a type of reversible physical interactions (Jiang et al., 2009). Although hydrophobic forces would also be a type of worth studying physical effects on the enhancement of physical and self-healing properties (K. Xu et al., 2013), there are not many studies on the effects of hydrophobic forces for mechanical properties improvement for now. Kun Xu et al. has synthesized a dimethyldodecyl (2-acrylamideorthyl) ammonium bromide surfactant monomer (K. Xu et al., 2013). The resulting optimal gels possessed optimal mechanical properties of 250 kPa for tensile strength, 14 MPa for compressive strength and 1850% for elongation at break. Marko Mihajlovic et al. studied on a hydrophilic poly (ethylene glycol) and hydrophobic dimer fatty acid building blocks (Mihajlovic et al., 2017). The final hydrogel samples are mechanically quite stable and tough with a tensile toughness of 4.12 MJ/M^3. Currently, there are not a lot of work focused on the hydrophobic association effects on hydrogel mechanical properties and self-healing abilities improvements. It would be a promising area to study in the future for the hydrogel materials with ideal toughness, processability and easy to preparing properties (Miquelard-Garnier et al., 2006).

In addition to above-mentioned four types of interactions forces, physical entanglement may also get involved to improve the mechanical performances. Nanocomposite (NC) hydrogels could improve the tensile properties by entangling flexible inorganic nanoparticles into hydrogel structures (J. Wang et al., 2012), which is a typical mechanical property enhancement method by physical entanglement. The physical

associations between ductile polymers and inorganic nanocomposite particles could help to improve the hydrogel physical characteristics (Haraguchi & Takehisa, 2002).

2.1.2 Self-Recoverable Hydrogel Materials

In order to guarantee both the structure and functional integrity for hydrogel materials, it is significant to make sure their self-recovery ability (Yu, Chen, Xu, & Liu, 2016). Self-recoverability is the action to heal exterior mechanical harms. It generally exists in nature. Self-healing abilities not only appear at the single molecules level (like DNA repairing) but also at the macroscopic level (like broken bones merging). But most of artificial materials are usually not with the property. Self-recoverability has tremendous importance especiallyfor materials in regions with long-standing poor accessibility. Self-recovery materials are also important for surface coatings which are vulnerable to damage (Hager et al., 2010). Self-recoverable artificial materials have wide potential application areas and have developed rapidly in recent years (Phadke et al., 2012). For these reasons, self-recovery functions have attracted great attentions and can be widely used in fields such as soft robots and tissue engineering.

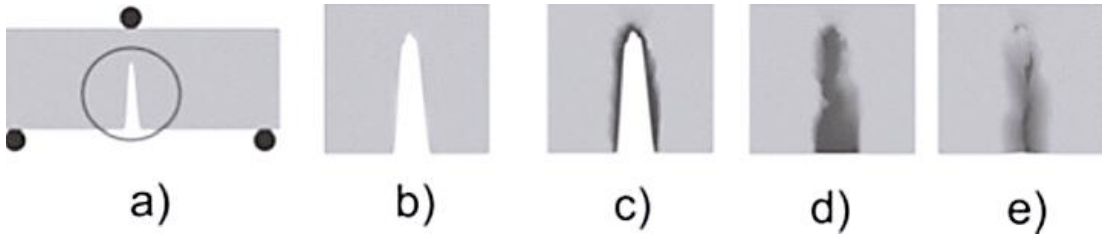

Figure 2.1 General concepts for self-healing process (Hager et al., 2010. Copyright

permission license number: 4876821254963). a) The mechanical influence produces a crack on the material; b) detail crack view; c) the appearance of a “mobile phase”; (d) the crack is recovered by the “mobile phase”; (e) The immobilization material condition after finishing the self-healing process.

Self-recoverable materials could be classified into two types: Non-autonomic and autonomic. Non-autonomic self-recoverable materials would need outside stimuli, such as high temperature while autonomic self-recoverable materials would not require one. In another word, the stimuli for autonomic self-healing materials is the damage itself (Hager et al., 2010). All types of autonomic self-healing materials including metals, ceramics and polymers rely on the same general principle shown in **Figure 2.1** in which there forms a mobile phase to heal the damage.

Currently, polymers are the most popular self-healing materials to study the self-recovery abilities (Hager et al., 2010). Microcapsules full of monomers which could be released after the crack appear on the materials were used to help rebind the non-autonomic self-recoverable polymer materials (White et al., 2001). The mechanism graph is shown in **Figure 2.2**.

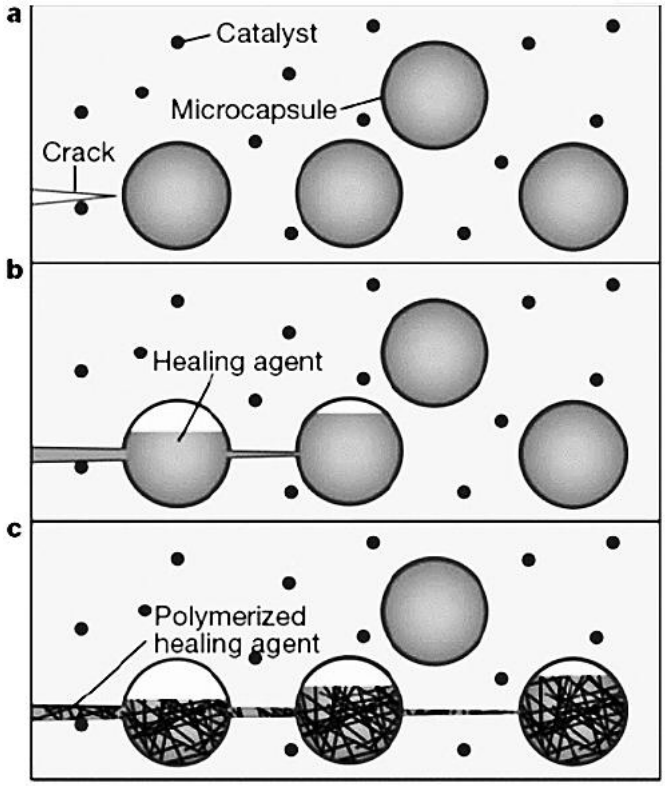

Figure 2.2 The mechanism sketch map of microcapsules helpingfor self-recoverability(Hager et al., 2010. Copyright permission license number: 4876821254963).

Great efforts are made to improve the microcapsules, such as polymer coatings, glass hollow embedding, biomimetic and so on (Hager et al., 2010). Finally, there appeared a type of filled microcapsules with a recovery agent released (Kolmakov et al., 2010). The concept is still not mature for now. Combining the natural self-healing capabilities to the generic self-recovery abilities (White et al., 2001). Currently, most of the latest self-resemble materials are produced according to the inspirations from nature.

Nevertheless, the initial properties of engineered materials have to be considered seriously when copy the natural models (Amendola & Meneghetti, 2009; Van Der Zwaag, Van Dijk, Jonkers, Mookhoek, & Sloof, 2009; Youngblood & Sottos, 2008). Currently, it is still challenging to keep the initial characteristics after the negative mechanical effects on the materials. The mature microcapsules would become a promising method to deal with this issue in the future (Odom et al., 2010).

2.2 Cellulose Nanocrystals

2.2.1 Cellulose Nanocrystals Characteristics

Nanocellulose is the most sufficient natural organic source. It is with a wide range of applications including composite materials, coatings, textiles, construction, drug delivery, personal caring and so on (Habibi et al., 2010; Klemm et al., 2011; Lee et al., 2012; Moon et al., 2011). As a newly appeared nanomaterial type, nanocellulose materials have attracted great attentions (Blanco et al., 2018).

It was proven that the nanocellulose materials are usually hydrophilic. They could be used in both hydrophilic materials, such as hydrogels (De France, Hoare, & Cranston, 2017). , Because the nanocellulose materials are generally flexible, ductile and with ideal mechanical properties, they could be used in hydrogels to help improve the hydrogel tensile properties efficiently (Plackett, Letchford, Jackson, & Burt, 2014). Nanocellulose materials are usually with outstanding surface area to volume ratios. Therefore when they

are added into hydrogels materials, there would be more associations formed with the polymer chains and monomers inside, making the hydrogels cross-linked more tightly to thus enhance the mechanical characteristics.

CNCs are generally derived from some cellulose sources in nature including plants by hydrolysis process (De France et al., 2017). Fortunately, the extracting process of CNCs could perfectly keep their intact crystalline structure, which is with high tensile property and could help to enhance hydrogel mechanical properties. As it is shown in **Figure 2.3,** nanocellulose including CNCs could be extracted from the green natural plants resources and could be used to produce aerogels and hydrogels. When the materials are decomposed, the CNCs could still be beneficial for plant growths in nature as a form of nutrition. It was estimated that the nanocellulose materials could be used as enhancement fillers in composite materials with better ecological compatibilities than other fillers like silicate and clay (Tingaut, Zimmermann, & Sèbe, 2012). Due to the increased environmental concerns about the usages of petroleum-based products and chemicals, nanocellulose as a type of environmental-friendly green materials with renewable and abundance properties would be worthy to study (Thomas et al., 2018).

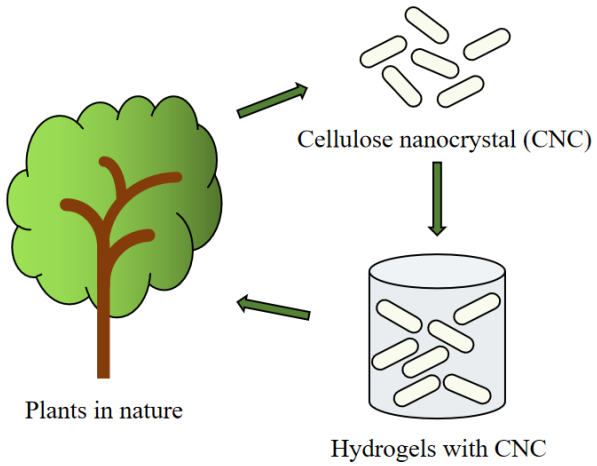

Figure 2. 3 Green material source of nanocellulose.

2.2.1 Cellulose Nanocrystals in Hydrogels

Polymer nanocomposites are generally with outstanding mechanical, optical and electronic capacities (J. Yang et al., 2013). They have attracted great attentions and developed rapidly in recent years. Nanocomposite (NC) hydrogels are usually composed of nanoparticles and polymer chains (Y. Hu et al., 2016).

It is significant to understand the mechanical properties enhancement mechanism with nanoscale particles added in polymer materials (J. Yang et al., 2013). These nanocomposites are ideal substance used to form nanocomposite (NC) hydrogels because they are generally flexible and stretchable (Tamesue et al., 2013; J. Wang et al., 2012). The physical forces between nanocomposites and polymer chains could help to improve the tensile strength, elongation values and self-recoverable abilities of NC hydrogels because they are reversible (Haraguchi & Takehisa, 2002; C. Li, Mu, Lin, & Ngai, 2015).

The physical forces could get self-recovered after being broken. Thus, the roles of nanoparticles in NC hydrogels are not only physical cross-linkers but also mechanical properties enhancers. Due to the existence of nanocomposites fillers, the mechanical properties including tensile strength and elongations as well as the self-healing abilities of NC hydrogels is generally better than that of chemically cross-linking hydrogels. It was estimated that the change of nanocomposite contents in NC hydrogel materials could help to control the number of inside cross-linking dots, so that the tensile strength and elongations could be adjusted accordingly (X. Hu et al., 2011).

CNC, as a type of nanocomposite materials, could be used to enhance the hydrogel mechanical properties as well (Plackett et al., 2014). CNC content is one important factor for hydrogel tensile capacities improvement. It was approved that once the CNC content is over 10 wt %, the CNCs would be transferred into an aggregated phase (Ureña-Benavides, Ao, Davis, & Kitchens, 2011) and cannot play a good role in physical properties enhancement. In addition, they are easy to be entangled with each other, they are not suitable to form single component gels alone (De France et al., 2017). Therefore, it would not be reliable to increase hydrogel mechanical strength only by the addition of CNCs. Other measures should be taken by combining CNCs with other substance to improve the hydrogel mechanical properties.

There have been a great number of studies focused on hydrogels reinforced by CNC. Jun

Yang et al. explored the interactions and morphologies of CNC/poly (acrylic acid) nanocomposite hydrogels (J. Yang et al., 2013). It turned out that the CNC aspect ratio values and nonpermanent interactions between CNC and matrix have effects on the nanocomposite physical properties. The dynamic mechanical analysis results showed that the chain mobility around CNC surfaces is decreased obviously, which is a new understanding of CNC enhancement mechanism. Bengang Li et al. presented self-healing nanocomposite hydrogel materials with ideal tensile strengths and physical properties enhanced by surface-modified CNCs (B. Li et al., 2018). CNCs were modified with PAM at first to produce monomer CNC-g-PAM. The roles of CNC-g-PAM monomers are not only nanofillers but also the cross-linkers with hydrogen bonds. The dual physically cross-linked CNC-g-PAM/PAA hydrogel materials could have excellent self-recoverable abilities as well. Amir Khabibullin et al. reported a type of hydrogel material composed of CNCs and graphene quantum dots (Khabibullin et al., 2017). Graphene quantum dots and CNCs are both negatively charged, but they could still gathered together because hydrogen bonds and hydrophobic forces could be more significant than the electrostatic repulsion. The physically cross-linked hydrogel products are also with ideal mechanical performances. Overall, it is worthy to study on CNCs used as hydrogel mechanical and self-healing properties enhancement agents.

In addition, there also appeared some methods to prepare functional cellulose-based composite materials (Lin, Huang, & Dufresne, 2012), such as modifying CNCs with

hydrophobic carbon chains (Gousse, Chanzy, Excoffier, Soubeyrand, & Fleury, 2002).The hydrophobic interactions could act as physical cross-linkers to help improve the tensile strength and elongation values. Therefore the hydrogels materials could get improved in this way when the hydrophobic modified CNCs were added into hydrogel materials.

Chapter 3 Materials and Experimental Methods

3.1 Materials

N,N-Dimethylacrylamide (DMAc), 1-Bromooctadecane (18C-Br, ⩾97.0%), Potassium persulfate (KPS), N-[3-(Dimethylamino)propyl] methacrylamide (DMAPMA, 99%), Trichloro(octyl)silane (97%), Toluene (99.8%), Imidazole, Diethyl ether (⩾99.0%), Chloroform (⩾99.8%), Tetrahydrofuran (THF, ⩾99.0%) were from Sigma-Aldrich, Acetone (⩾99.5%) from Innova chemical, Cellulose nanocrystals (CNC, Alberta Innovates Technology Futures) were produced through an acid hydrolysis process with a rigid rod-like structure (a length in the range of 100-200 nm, a diameter in the range of 5-15 nm, a density of 1.6 g/cm^3). Kingscote 506250-RF4 Fluorescent RED Leak Tracer Dyewas from Cole-Parmer. Olive oil was purchased from superstore market. Water used was from Milli-Q water (Millipore deionized with a resistivity of 18.2 MΩ·cm, D.I. water).

3.2 Fourier-Transform Infrared Spectroscopy (FT-IR)

Fourier-transform infrared spectroscopy (FTIR) is a chemical analysis method which is commonly used to obtain emission or absorption infrared spectrum of samples (Griffiths & De Haseth, 2006). The components of samples could be analyzed based on the wave numbers and area of each infrared spectrum peak (Berthomieu & Hienerwadel, 2009).

The chemical compositions of the materials were characterized on an FT-IR spectrometer (Perkin Elmer Frontier L1280044). The range was 400-4000 cm^{-1} and the resolution was4 cm^{-1}. To be specific, at first, the sample plate was cleaned with tissues and the background data was collected. Then a little amount of samples were applied to the sample plate and scanned to collect the sample data with background subtraction.

3.3 Scanning Electron Microscope (SEM)

Scanning electron microscope (SEM) could be used to image sample surfaces by a focused electron beam (Idris & El-Zahhar, 2019). The mechanism of SEM is mainly the interactions between sample atoms and beam electrons. The signals with certain intensity produced from the interactions could be used to detect the sample surface topography and components. The SEM image was collected on a Phenom ProX Desktop scanning electron microscope (Thermo Fisher Scientific, USA). At first, free-dried hydrogel samples were cut into small pieces and mounted rigidly on a specimen holder using a conductive adhesive. Then the holder with samples was put into the SEM sample chamber for SEM characterizations.

3.4 Tensile Test

The main mechanical properties of hydrogels include tensile stress and elongation at break. During the tensile test process, the hydrogel was stretched at a stable speed until

break.

Elongation is also called strain in the unit of %. It shows how many times the sample could be pulled and stretched compared to the initial condition. The elongation value was calculated from the position data recorded by the testing machine. It was obtained by dividing the difference between the final position at break and the initial position by the initial position data. Assume L_0 is the initial length of sample, L is the length of sample at t time, strain = $\frac{L-L_0}{L_0}$. Elongation could show how flexible or stretchable the samples are.

Stress is a measurement for tensile strength. The higher the stress value is, the tougher the sample with stronger mechanical strength (Y. Hu et al., 2016). The tensile stress in this study mainly include nominal stress and true stress. The optimal nominal stress results data is the maximum stress applied to the sample cutting surface before break. It was calculated from the pulling force decided by the cutting surface area in kPa. Assume A_0 is the initial cutting surface area, F is the force applied to samples at t time. Then $nominal\ \ stress = \frac{F}{A_0}$, The true stress considered the changes of cutting surface areas during pulling process. Then $true\ \ stress = \frac{F}{\frac{A_0 \times L_0}{L}} = \frac{FL}{A_0 L_0} = \frac{nomimal\ \ stress \times L}{L_0}$. Because strain = $\frac{L-L_0}{L_0} = \frac{L}{L_0} - 1$, the relationship between nominal stress and true stress is as below: $true\ \ stress = nominal\ \ stress \times (strain + 1)$.

The mechanical property of the hydrogels was tested on a universal material testing machine (eXpert 7600, ADMET) at room temperature with a speed of 30 mm min^{-1}. The diameter of each hydrogel samples was all4 mm. The initial lengths of the hydrogel

samples for the tensile test between the two clamps were recorded separately every time. Each sample was produced and tested in at least three replicates to calculate the mean value for stress (kPa) and elongation (%).

3.5 Compression Test

The compression tests for DPC hydrogel samples were conducted with SHIMADZU AGS-X universal testing machine. The load cell is 5 kN. The samples were in the shape of cylinders with 24 mm for diameter and 14 mm for thickness. The compression speed for crosshead was 10 mm/min and the initial cross section was 490 mm^2. The strain range for the compression tests was 0-90%.

3.6Self-Recoverability Test

The DPC hydrogels in this study is a type of non-automatic self-healing material (Hager et al., 2010). The modest external trigger for DPC hydrogels self-healing process is THF. The hydrogels were cut in two equal-volume parts with an extremely sharp knife. Three drops of THF were daubed between the two cut surfaces and then the two parts were connected tightly together with plastic wrap at room temperature overnight. The plastic wrap was used to keep the water inside the hydrogels during self-healing process and to make sure the hydrogels are in same conditions as the one before self-healing process. THF is a solvent with polarity and could mix readily with water in hydrogels (Gessner &

Mayer, 2000). So the cutting surfaces of two hydrogels could be deformed and mixed together under the effects of THF. The self-healing process was also repeated for the time period of 2 hours, the hydrogels cannot be self-recovered well and would be extremely easy to be broken while stretching. When the self-healing process was conducted for more than one day, the self-healing ratios of CNC DPC hydrogels seem similar to the one get self-healed after overnight. Therefore, overnight would be a proper time period selected for self-healing process.

3.7 Swelling Test

Polymer hydrogel is a type of three-dimensional network "soft-wet" materials with a lot of hydrophilic polymeric materials, which could absorb and retain a great amount of deionized water (water) with structural integrity (Gribova, Crouzier, & Picart, 2011; J. Hu, Zhang, & Liu, 2012; Y. Li, Rodrigues, & Tomás, 2012). Therefore, it is important to study the physical or chemical cross-linking measures to keep the three-dimensional network hydrogel structures in aqueous solution (Bardajee, Pourjavadi, Ghavami, Soleyman, & Jafarpour, 2011).

The swelling or absorption performance of the hydrogels were evaluated in water, chloroform and olive oil. For a typical absorption experiment, one block of sample was weighed at first and then immersed into 50 mL solvent in a sealed centrifuge tube. The weight in grams of the block was recorded as a function of time. The absorption capacity

(g/g) was calculated through the difference between the initial weight (g) and the later recorded weight (g) at every recorded day divided by the initial weight (g). Each experiment was repeated for three times.

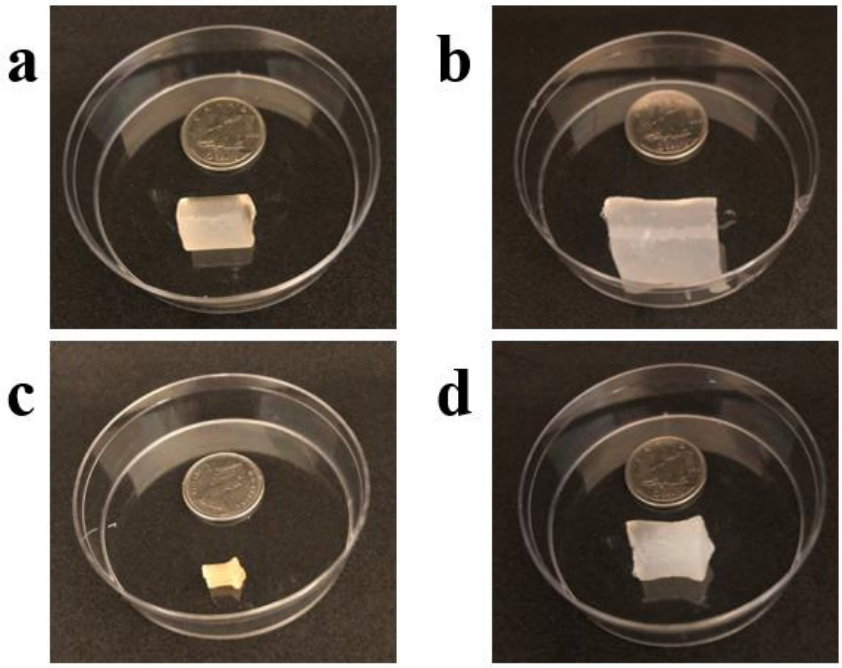

Figure 3.1 Shape conditions of hydrogels before and after water absorption process compared with a same coin: (a) initial wet DPC hydrogels before water absorption; (b) expanded wet DPC hydrogels after water absorption for 1 d; (c) initial freeze-dried DPC hydrogels before water absorption; (d) expanded freeze-dried DPC hydrogels after water absorption for 1 day.

As shown in **Figure 3.1**, samples at two different conditions were used, initial as-prepared hydrogel and freeze-dried one. The samples could expand a lot but remain in a similar shape to the initial condition, not broken or fragile after 1 d even more than 30 d

in water. The initial as-prepared one is already composed of a great amount of water. So freeze-dried sample would show better water absorption capacities. Almost no absorption was observed with initial as-prepared hydrogel in chloroform for 80min or olive oil for 5 min, indicating the stability of hydrogel in oils. Thus most absorption experiments were done with freeze-dried samples.

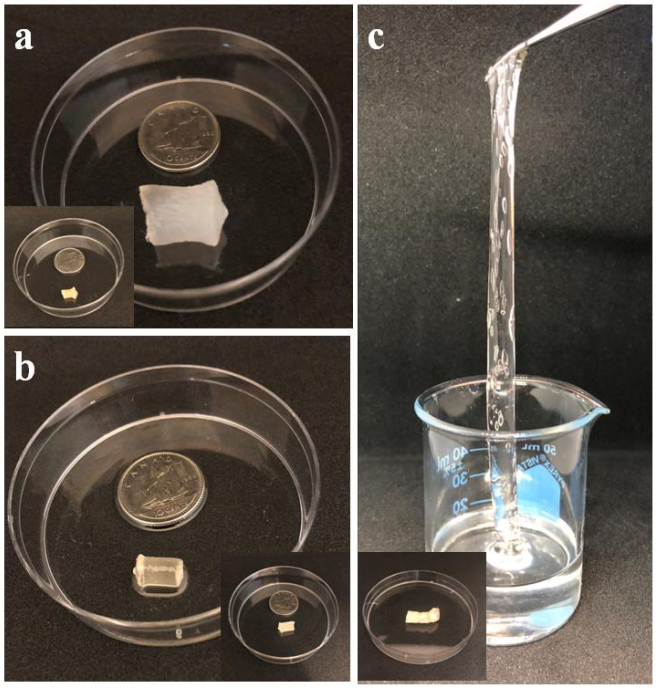

Figure 3.2 The shapes of freeze-dried samples after immersion in (a) water, (b) olive oil, and (c) chloroform for 24 hrscompared to a same coin. The insets in every picture show the initial shape of freeze-dried sample.

To estimate the testing time period, the shape and weights were monitored with the increase of time by putting the freeze-dried samples in water, olive oil and chloroform, respectively. Conditions of freeze-dried samples after being immersed for 24 hrs are

shown in **Figure 3.2**.The samples in water were with similar shapes but have expanded a lot in the volume compared with the initial conditions. The samples in olive oil were with similar shapes as before and almost did not expand compared with the initial conditions. Both of the samples in water and olive oil would not be broken even after a 30-d immersion period.

The water absorption capacities increased a lot during the first seven days, especially during the first day. After the seventh day, the water absorption capacities increased very slowly. So the time period for water absorption tests was selected as seven days.

The water absorption recycle test was conducted. The time period for water absorption recycle test was selected as 24 hrs for each cycle. One block of DPC hydrogel was immersed into water for 24 hrs and the weight was recorded. The hydrogel was freeze-dried and the weight of the sample after freeze-drying was recorded again. Then the freeze-dried sample was used to absorb water again and its weight was recorded after 24 hrs water absorption. The water absorption process was repeated for five times in the recycle tests.

The samples were proven to be saturated after being immersed in the olive oil for 5 mins based on the weight measurements. So the time period selected for olive oil swelling test was 5 mins.

The samples immersed in chloroform are broken after 24 hrs as shown in **Figure 3.2 c.**

So the time period should be selected as at the time the hydrogel shapes were not broken, which should be less than the time period of one day. According to the records in **Figure 3.3**, 80 mins was selected as a proper time period for chloroform absorption tests.

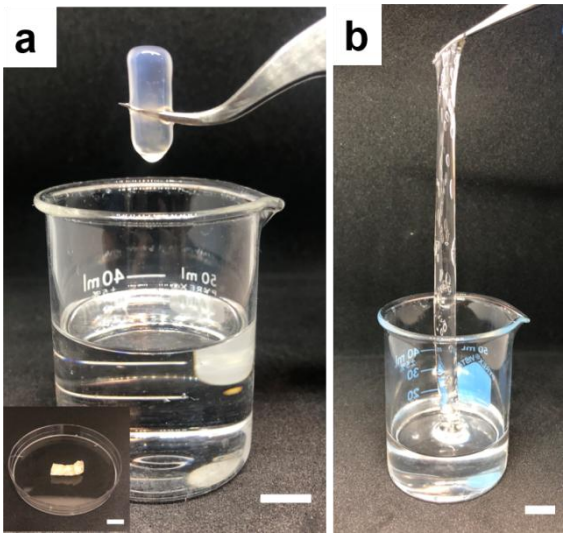

Figure 3.3 The shape of the freeze-dried samples after immersion in chloroform for (a) 80 mins and (b) 24 hrs, respectively. The inset in (a) shows the initial shape of freeze-dried sample. The scale bars are 1 cm.

3.8 Two-way ANOVA Analysis

Analysis of variance (ANOVA) is a very useful and common method to analysis datasets. It is used to compare the variances of group means. One-Way ANOVA and Two-way ANOVA are the two popular types of ANOVA. The main difference is that One-Way ANOVA is usually at groups with only one variable or factor while Two-way ANOVA is at groups with two. One-Way ANOVA is a hypothesis based test, the null hypothesis of which is there is no difference between the groups. It is mainly used to compare the

equalities between the means. However, the Two-way ANOVA is mainly used to test the interactions of two independent factors (assume factor A and factor B). The null hypothesizes are as follows: (1) There is no difference between factor A groups. (2) There is no difference between factor B groups. (3) There is no interaction between factor A and factor B (Levine, Ramsey, & Smldt, 2001).

There are two independent factors in this study, which are DMAPMA-C18 contents and CNC (CNC-C8) contents. So Two-way ANOVA was selected to analyze the data. Minitab® 19 was used as the statistical software for Two-way ANOVA analysis.

Chapter 4 Preparation of Hydrophobic Monomer and CNC, and Synthesis of Hydrogels

4.1 Preparation of DMAPMA-C18

The first step was the synthesis of DMAPMA-C18, which could play a part in hydrophobic interactions. The preparation of DMAPMA-C18 is summarized in **Scheme 4.1**.8.5g (0.05 mol) N-[3-(Dimethylamino)propyl] methacrylamide (DMAPMA) and 20g (0.06 mol) 1-Bromooctadecane(C18-Br) were added into 40 mL anhydrous acetone and mechanically stirred at 300 rpm under 55^{o}Cunder nitrogen protection. The synthesis installation diagram is shown in **Figure 4.1**. After 30 hrs, 50 mL absolute diethyl ether was added to make the products DMAPMA-C18 separated out as the phase of white sediments, which were washed for three times by filtration with absolute diethyl ether and then put into the vacuum chamber overnight to obtain the final dry DMAPMA-C18 products.

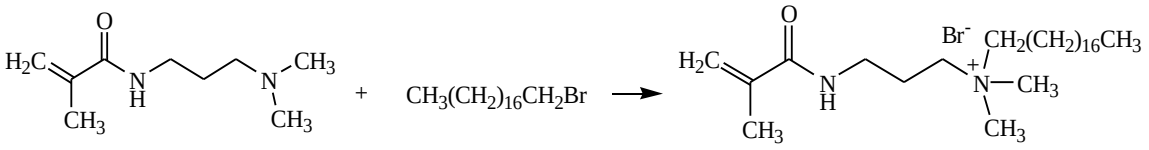

Scheme 4.1 Synthesis of DMAPMA-C18.

One of the drawbacks of DMAPMA-C18 products is they are a type of surfactant which

would produce a great number of bubbles when put in water. The bubbles could make the hydrogels inhomogeneous and reduce the mechanical strengths as well as elongations. A good solution for this problem is to stir DMAPMA-C18 in water overnight in advance before the synthesis process of hydrogels, which could reduce the bubbles obviously and help to form ideal DPC hydrogels.

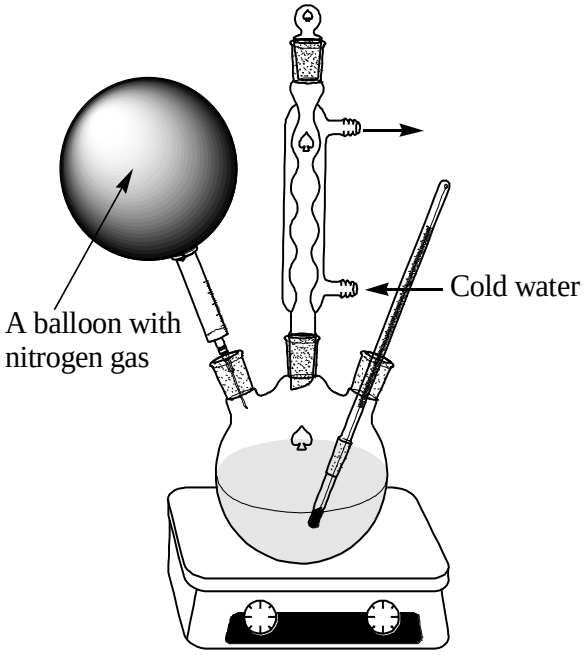

Figure 4. 1 DMAPMA-C18 synthesis installation diagram.

4.2 Preparation of CNC-C8

In order to prepare substantially chemically stable suspensions, longer alkyl moieties like C8 were selected because they are less reactive and could produce more stable hydrophobic silylated CNC whiskers.

The synthesis should be conducted in non-polar solvent such as toluene to avoid the

hydrolyzation of chlorine groups on trichloro(octyl)silane. However, there are so many polar hydroxyl groups on the surface of CNC which could make iteasily well dispersed in polar water while hard to be uniformly dispersed in toluene which is of no polarity. Therefore, one crucial part of CNC-C8 preparation is to transfer the solvent from water to toluene.

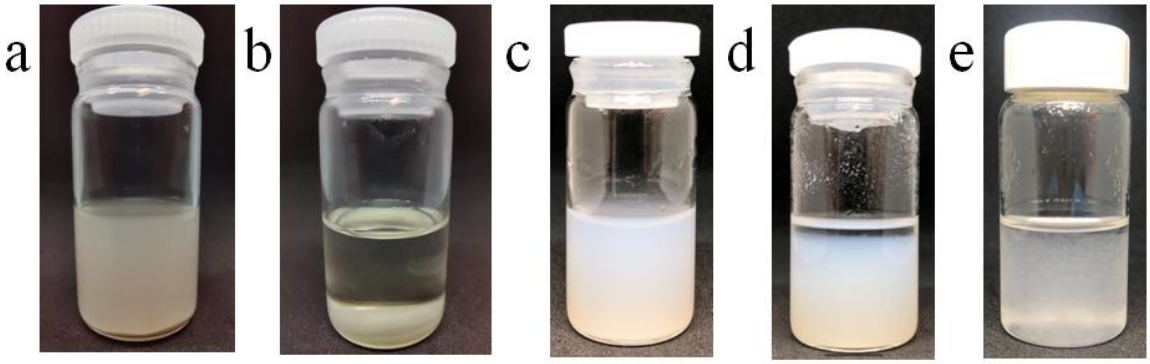

Figure 4. 2 CNC suspension conditions in different solvents: (a) CNC in acetone with sediments at the bottom, (b) CNC in toluene with sediments at the bottom, (c) CNC can be dispersed well in water, then (d) add acetone and (e) transfer CNC from the mixture solvent to toluene.

Before CNC-C8 synthesis process, we transferred the solvent from water to acetone which has medium polarity, then to toluene with no polarities. The CNC suspension conditions in different solvents are shown in **Figure 4.2**. In the vial (a), CNC would be precipitated at the bottom when it was added in acetone directly. Similarly, in the vial (b), CNC would also be precipitated when it was added in toluene directly. As this synthesis should be conducted in the non-polar toluene, we disperse 3g CNC uniformly in 100

mL water under ultrasonic at first (c), then add 1000mL acetone into it to form a jelly-like system (d). The solvent of a mixture water and acetone could be almost removed after filtration. Then 300 mL toluene was added gradually with stirring by a glass rob into the rest “wet” CNC to make it uniformly dispersed at last (e). A water content of around 1% (v/v) should be measured in the final suspension (Gousséet al., 2002).

The next goal is to synthesize CNC-C8 with different C8 alkyl chains modification levels (5%, 10%, 15% and 20%). We need to do calculations at first.

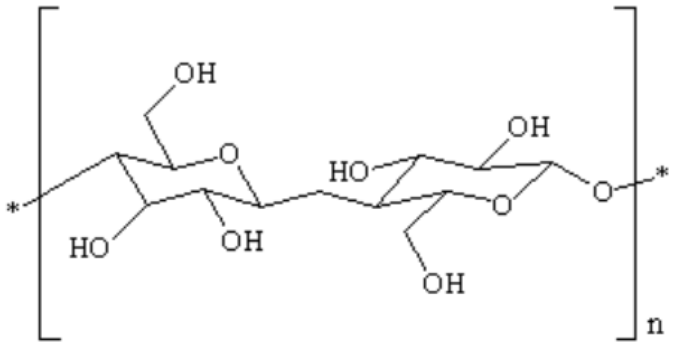

Figure 4. 3 Schematic of nanocellulose crystal (CNC).

From **Figure 4.3** we could see that CNC could be written as $(C_6H_{10}O_5)_n$ (Phanthong et al., 2018). For each $(C_6H_{10}O_5)$ unit, the weight is $12\times6+1\times10+16\times5=162$ (g/mol). As each $(C_6H_{10}O_5)$ unit contains three hydroxyl groups there are $(1\div162)\times3=0.0185$ (mol) hydroxyl groups in 1g CNC .

Trichloro(octyl)silane is 247.67 g/mol, density $\rho=1.07$ g/mL. Assume one mole of hydroxyl group reacts with one mole of trichloro(octyl)silane, the volume for

trichloro(octyl)silane to react with 3 g CNC should be 0.0185×3×247.67÷1.07=12.846 (mL) if it is going to obtain a 100% level of C8 alkyl chains modification. At 5% alkyl chains modification level, the trichloro(octyl)silane volume should be 12.846×5%=0.642 (mL). According to the calculation results, the volume amounts of trichloro(octyl)silane added at different modification levels are listed in **Table 4.1.**

Table 4. 1 The volumes of trichloro(octyl)silane to react with 3 g CNC at different C8 alkyl chains modification levels

C8 alkyl chains modification level (%)	5	10	15	20	100
Volumes of trichloro(octyl)silane	0.642	1.285	1.927	2.569	12.846

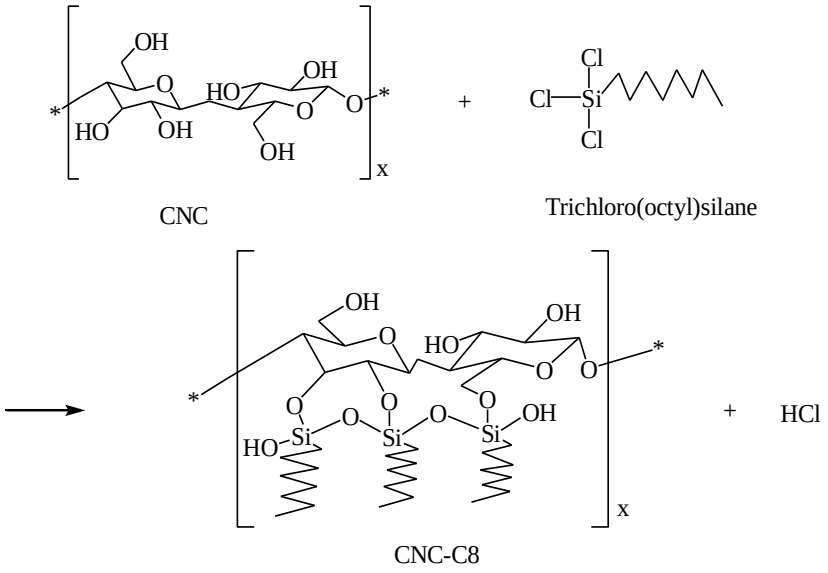

Scheme 4. 2 Synthesis of CNC-C8.

The preparation of CNC-C8 is summarized in **Scheme 4.2**. In order to synthesis 5% (10%, 15%, 20%) C8 alkyl chains modification level of CNC-C8 products, 0.642 mL (1.285 mL,

1.927 mL, 2.569 mL) trichloro(octyl)silane was added into 3 g transferred CNC in 300 mL toluene to stir at 300rpm at room temperature. After 16 hrs, a mixture of 20 mL THF and 5 mL methanol was added to stop the reaction. Then THF was used to wash the products for three times with centrifugation at the 12000 rpm for 10 min. The clear waste liquid was poured out and the white solids were put into the vacuum chamber overnight to obtain the final dry CNC-C8 products.

4.3 Synthesis of CNC DPC Hydrogels

Monomer DMAPMA-C18 is a type of surfactant which would produce a great number of bubbles in water. The bubbles could make the hydrogels inhomogeneous and reduce the mechanical strengths as well as elongations. To obviously reduce the bubbles, different dosages of 1.89 g, 2.835 g, 3.78 g, 4.725 g, 5.67 g, 6.615 g, 7.56 g, 8.505 g and 9.45 g DMAPMA-C18 in 42 mL water was prepared separately with magnetic stirring at 300 rpm at room temperature overnight in advance before the hydrogel preparation.

We assume that 1.89 g DMAPMA-C18 in 42 mL water could produce the CNC DPC hydrogels with 1 unit of DMAPMA-C18, denoted as 1 DMAPMA-C18. Then the dosage of 2.835 g, 3.78 g, 4.725 g, 5.67 g, 6.615 g, 7.56 g, 8.505 g and 9.45 g DMAPMA-C18 in 42 mL water could produce CNC DPC hydrogels with 1.5 DMAPMA-C18, 2 DMAPMA-C18, 2.5 DMAPMA-C18, 3 DMAPMA-C18, 3.5 DMAPMA-C18, 4 DMAPMA-C18, 4.5 DMAPMA-C18 and 5 DMAPMA-C18, respectively, which also

means the DMAPMA-C18 contents in the final CNC DPC hydrogel products are 0.0225 w/v %, 0.03375 w/v %, 0.045 w/v %, 0.05625 w/v %, 0.0675 w/v %, 0.07875 w/v %, 0.09 w/v %, 0.10125 w/v % and 0.1125 w/v %, respectively, corresponding to the dosages of 1.89 g, 2.835 g, 3.78 g, 4.725 g, 5.67 g, 6.615 g, 7.56 g, 8.505 g and 9.45 g DMAPMA-C18 in 42 mL water in the preparation part as well. Different dosages of 0.06 g, 0.12 g, 0.18 g and 0.24 g CNC were added to 15 mL water separately corresponding to 0.2 w/v %, 0.4 w/v %, 0.6 w/v % and 0.8 w/v % CNC contents in final DPC hydrogels, which were dispersed well with a sonicator (QSONICA, Q500). 0.1g KPS was dissolved into 10 mL water to use as the initiator for polymer hydrogel synthesis.

For the example of the synthesis of CNC DPC hydrogels with CNC content of 0.2w/v % and 1 DMAPMA-C18, 5 mL CNC suspension (0.06g in 15 mL water) was added into 5 mL 1 DMAPMA-C18 solution which was stirred overnight in advance in a 50 mL beaker. Then 2 mL DMAc was added into it and nitrogen was blow into the solution for ten minutes to remove oxygen. After that, 0.8 mL 1 w/v % KPS solution was added into the solution and shaken slowly until uniform. Then the whole solution was transferred into a custom 1 mL-volume syringe into oven at 65^{o}Cfor four hrs. The final physically cross-linked CNC DPC hydrogel products could be obtained.

The general schematic illustration of the fabrication of DPC hydrogels without CNC addition is shown in **Scheme 4.3.** As shown in the schematic of DMAc-DMAPMA-C18

polymer interactions in **Figure 4.4** and **Scheme 4.4, t**he hydrophobic force between C18 chains on the polymers could make polymers physically cross-linked.

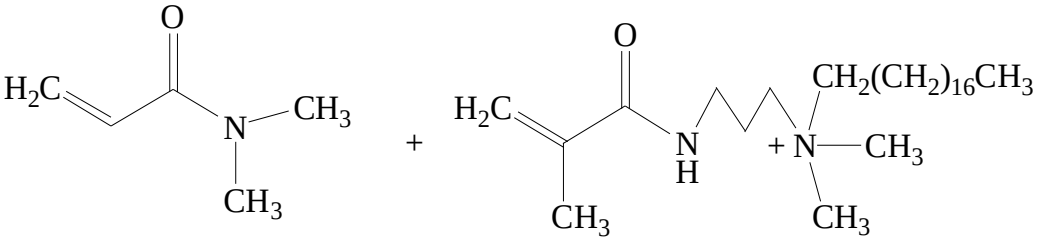

DMAc DMAPMA-C18

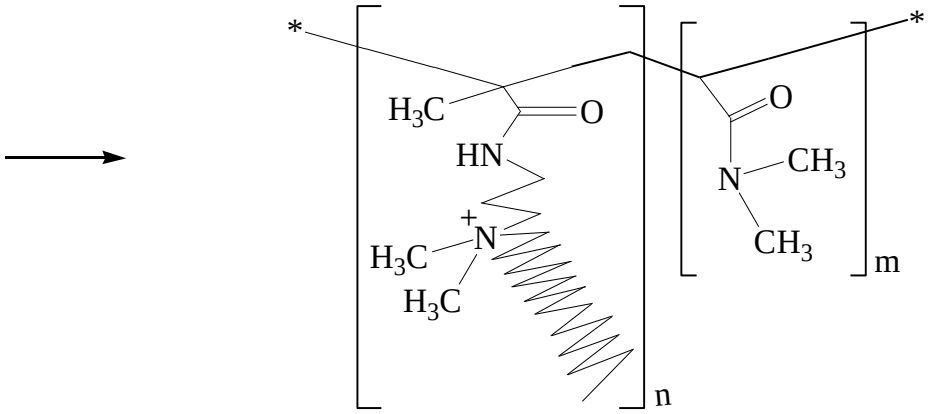

DMAc-DMAPMA-C18 polymer

Scheme 4. 3 Synthesis of DMAc-DMAPMA-C18 polymer.

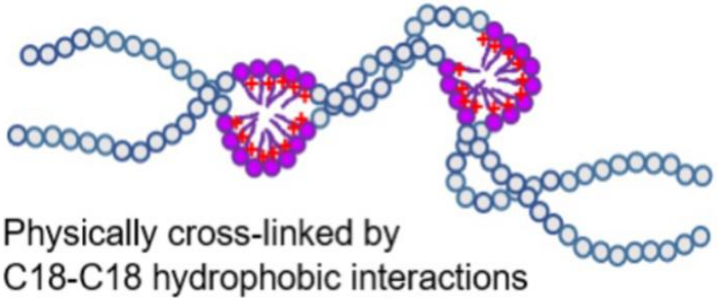

Figure 4.4 Schematic of interactions in DMAc-DMAPMA-C18 polymers.

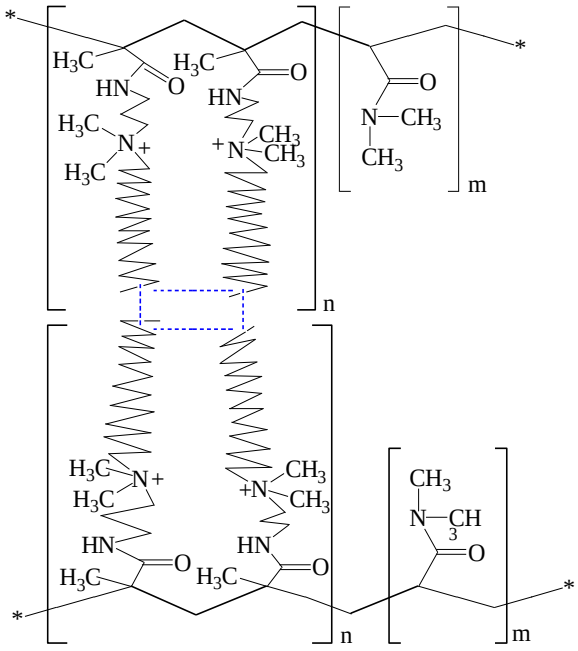

Scheme 4. 4 Interactions inDMAc-DMAPMA-C18 polymers.

The same procedure was followed for the preparation of other dosages of DMAPMA-C18 and CNC contents, except that bulk solution preparation used different dosages of DMAPMA-C18 contents in 42 mL water and different CNC contents

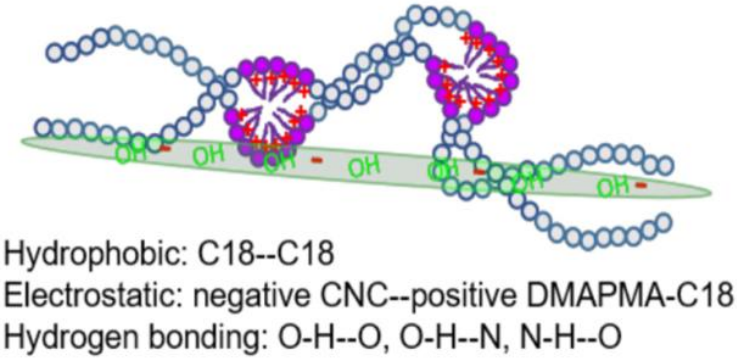

Figure 4.5 Schematic of interactions in CNC-DMAc-DMAPMA-C18 hydrogels.

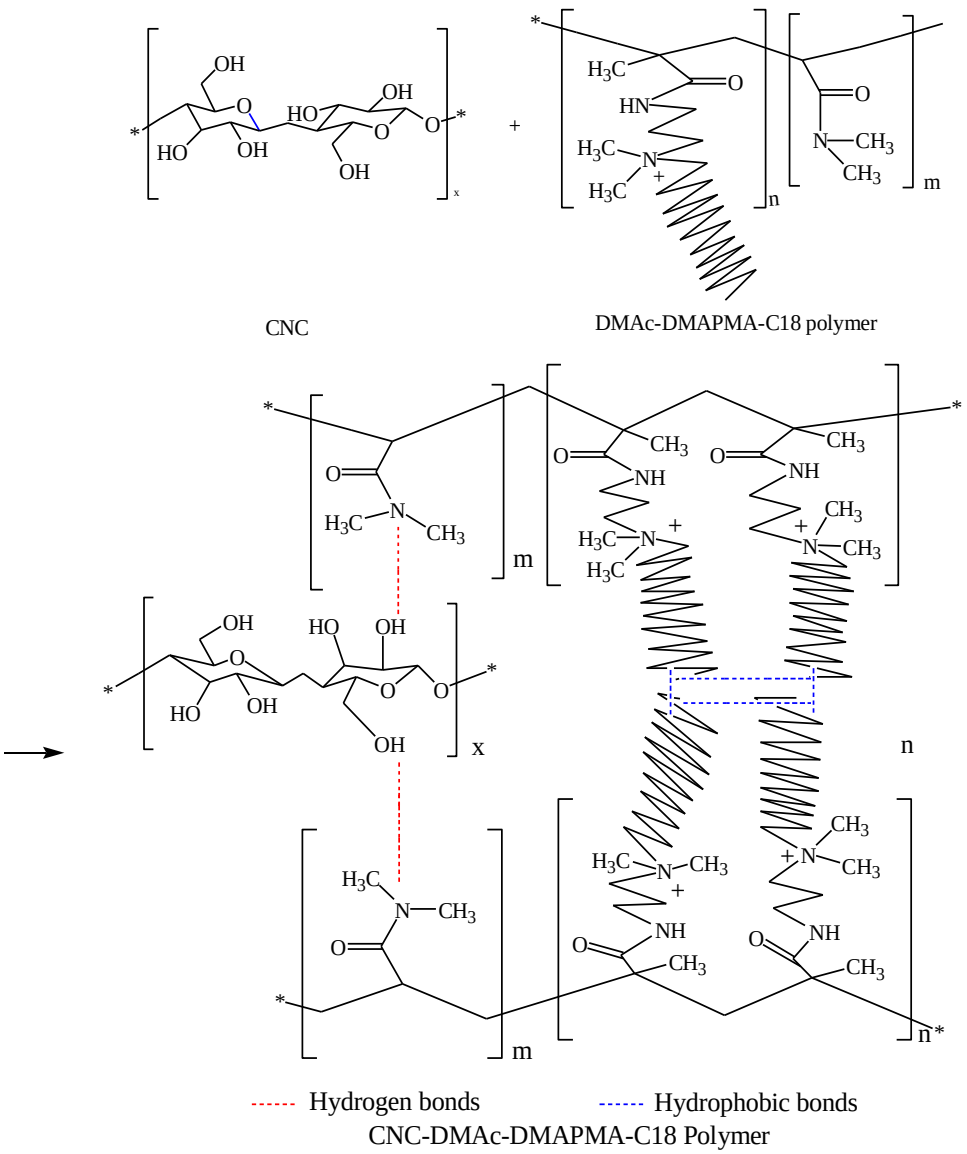

Scheme 4.5 Synthesis ofCNC-DMAc-DMAPMA-C18 DPC hydrogels.

As shown in the schematic of interactions in CNC-DMAc-DMAPMA-C18 DPC hydrogels in **Figure 4.5** and **Scheme 4.5**，hydrophobic interactions between C18-C18 chains, electrostatic interactions between negative charges on CNC and positive charges on DMAc-DMAPMA-C18 polymer, as well as hydrogen bonding in the system could exist and contribute to the formation of double physically cross-linked hydrogel network**.**

4.4 Synthesis of CNC-C8 DPC Hydrogels

Similar procedure was followed for preparing the CNC-C8 DPC hydrogels as CNC DPC hydrogel. As shown in the interactions in **Figure 4.6** and synthesis process in **Scheme 4.6**, besides the forces mentioned in the CNC DPC hydrogel system, there were also hydrophobic forces between C18 and C8 chains, making the hydrophobic forces stronger in total.

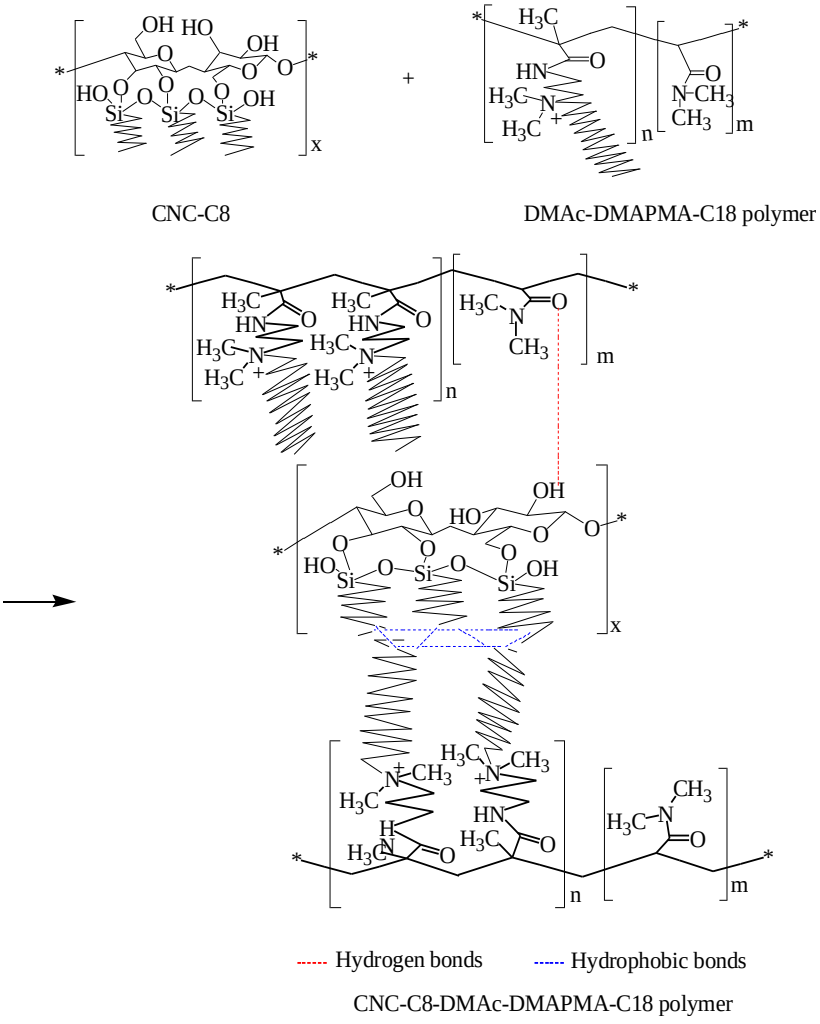

Scheme 4. 6 Synthesis of CNC-C8-DMAc-DMAPMA-C18 DPC hydrogels.

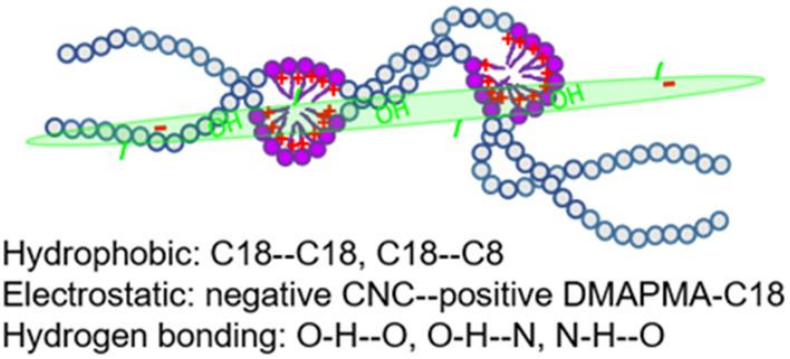

Figure 4.6 Schematic of interactions in CNC-C8-DMAc-DMAPMA-C18 hydrogels.

Chapter 5 Characterization and Performance Evaluation of DPC Hydrogels

5.1 FT-IR Analysis

As shown in **Figure 5.1a**, the peak at 1430 cm^{-1} refers to the CH_2 groups and double peaks at 1032 cm^{-1} and 1057 cm^{-1} refer to the C-O stretching of the CNC molecule. All these peaks were observed in the spectra of CNC and hydrophobized CNC (CNC-C8), confirming the common CNC structure of these cellulose nanocrystal. With the hydrophobic modifications on CNC molecule, new peaks were observed in the spectra of CNC-C8. The peak at 3340 cm^{-1} results from the stretching of O-H bond in the Si-OH (Gousséet al., 2002).From the spectrum results we can see that with the increase of trichloro(octyl)silane modification level, the peaks corresponding to SiO-H bonds would become more obvious. Nevertheless the intensity of the double-peak is not very strong so there is little probability of Si-OH polymerization reactions, leading to just mere influence on the final products. The characteristic peaks at 826 cm^{-1} and 759 cm^{-1} account for the Si-OH bending vibration and Si-O-Si symmetric stretching vibration, respectively. It is interesting to note that the characteristic peak at 2892 cm^{-1} (CH stretching) for CNC split into two individual peaks at 2914 cm^{-1} and 2847 cm^{-1} at the spectra of hydrophobic modified CNC-C8, indicating the modification of C8 chain onto the CNC molecule. Besides, the intensity of Si-O related peaks such as 3340 cm^{-1}, 1580 cm^{-1}, 826 cm^{-1} and

759 cm^{-1} increased with the growing content of C8, further confirming the successful hydrophobization of CNC using hydrocarbon C8 chain.

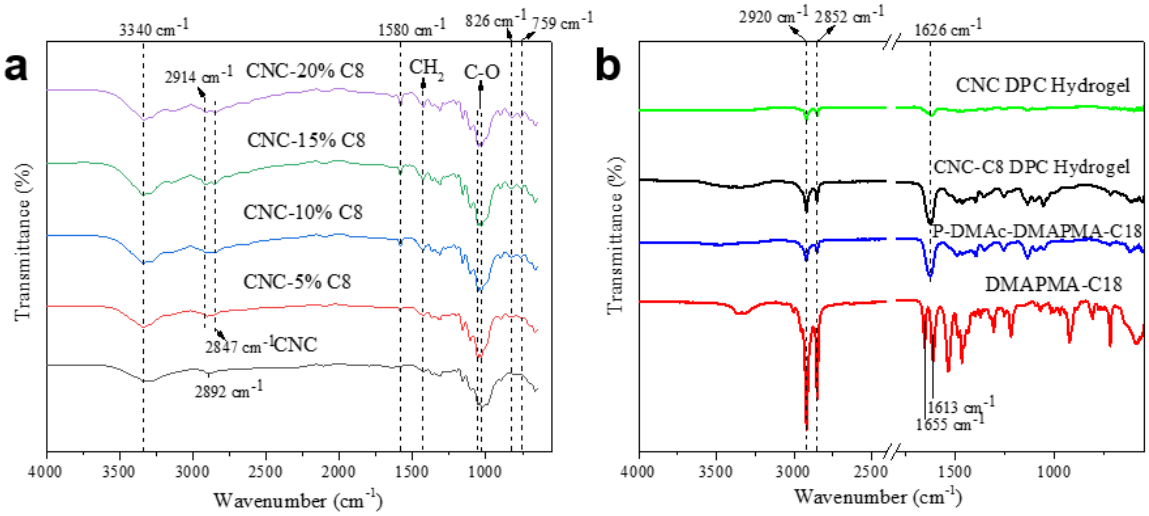

Figure 5.1 FT-IR spectra of (a) CNC and CNC-C8 with different C8-modification level, and (b) monomer DMAPMA-C8, polymerized DMAc-DMAPMA-C8, CNC DPC hydrogel and CNC-C8 DPC hydrogel.

Figure 5.1b shows the spectra of CNC DPC-hydrogel, CNC-C8 DPC-hydrogel and monomer DMAPMA-C18. The characteristic peaks at 2920 cm^{-1} and 2852 cm^{-1} are all observed in the spectra of these three materials, which represent the CH stretching vibration. It is worthy to notice that the peaks at 1613 cm^{-1} and 1655 cm^{-1} observed in the spectrum of monomer DMAPMA-C18 disappeared in the spectra of polymerized DMAc-DMAPMA-C18 and hydrogels. It is because the peak at 1613 cm^{-1} refers to the symmetric stretch vibration of the C=C group and the peak at 1655 cm^{-1} is attributed to C=O stretching vibration. The C=C groups were eliminated, and the peak attributed to

C=O moved to the new peak at 1626 cm^{-1} after polymerization of DMAPMA-C18. Such observation confirms the polymerized DMAPMA-C18 in the hydrogel.

5.2 Mechanical Measurements

5.2.1 Stress

5.2.1.1 Nominal Stress

Introducing hydrophobic monomer DMAPMA-C18 creates the first layer of physically crosslinking to form a hydrogel system.

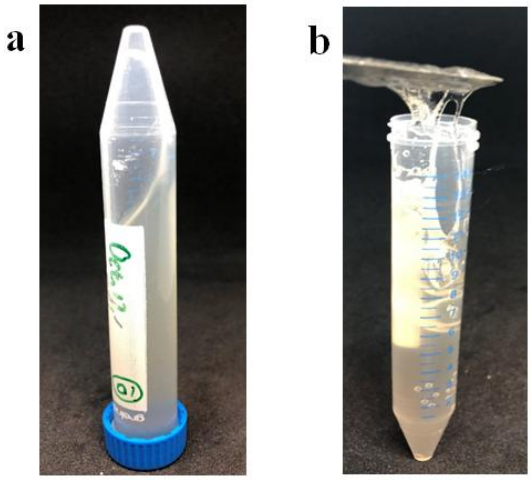

Figure 5.2 Hydrogel without DMAPMA-C18 monomers (a) could flow while being inverted and (b) Looks like glue.

Figure 5.2 showed the conditions of hydrogels without DMAPMA-C18 additions. In **Figure 5.2 a**, when the centrifuge tube was inverted, the hydrogel could flow under gravity and without rigid shape. As shown in **Figure 5.2 b**, the hydrogel product looks

like glue and was almost with no mechanical strengths. Therefore, DMAPMA-C18 monomers are essential for DPC hydrogel synthesis.

When the CNC or CNC-C8 is not added to the system, the optimal DMAPMA-C18 dosage for the hydrogel was 3 DMAPMA-C18 (0.0675 w/v %) with a nominal stress of 130.2±2.38 kPa as shown in **Figure 5.3**. When the DMAPMA-C18 content is higher than 0.0675 w/v %, the stress decreased. The main reason is the hydrophobic force became so strong when the hydrophobic monomer contents were very high, which led to the entanglements of polymer chains. Therefore, the hydrogel system was proven to be not uniform, which would be easy to be broken when external forces were applied.

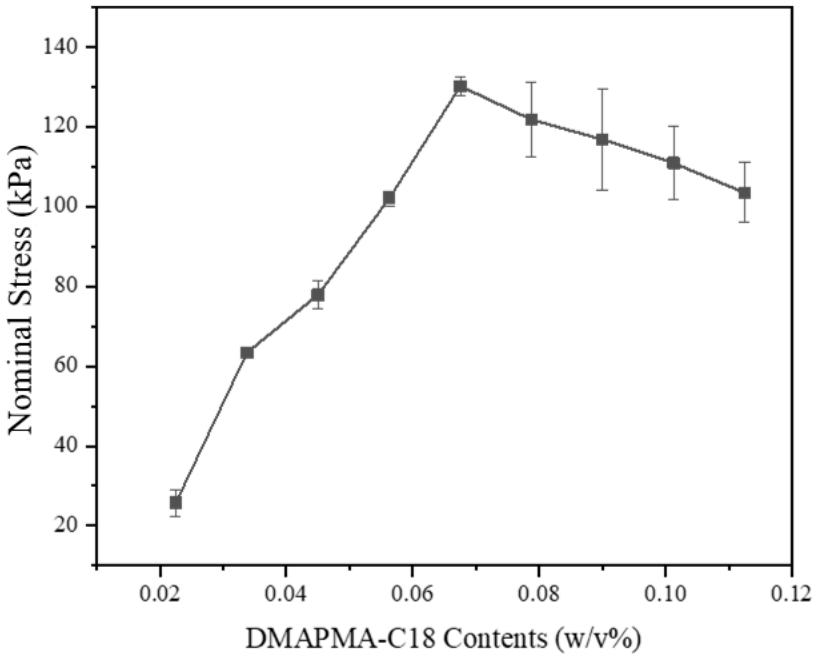

Figure 5. 3 The nominal stress of the DPC hydrogels as a function of the dosage of DMAPMA-C18 with zero CNC or CNC-C8.

With further inclusion of CNC or CNC-C8, the stress of the hydrogel will increase due to the reinforcement effects from the second layer of physically cross-linking into the system. As shown in **Figure5.4,**the changes of tensile strengths of CNC DPC hydrogels and CNC-C8 DPC hydrogels areas a function of the dosages of DMAPMA-C18 and CNC or CNC-C8 contents. Each line in **Figure 5.4 a** and **Figure 5.4 b** represents the changes as a function ofDMAPMA-C18 content at constant dosage of CNC or CNC-C8.Under different DMAPMA-C18 contents dosages, the final average DPC hydrogel stresses at different CNC and CNC-C8 contents are shown in **Table 5.1** and **Table 5.2** respectively.

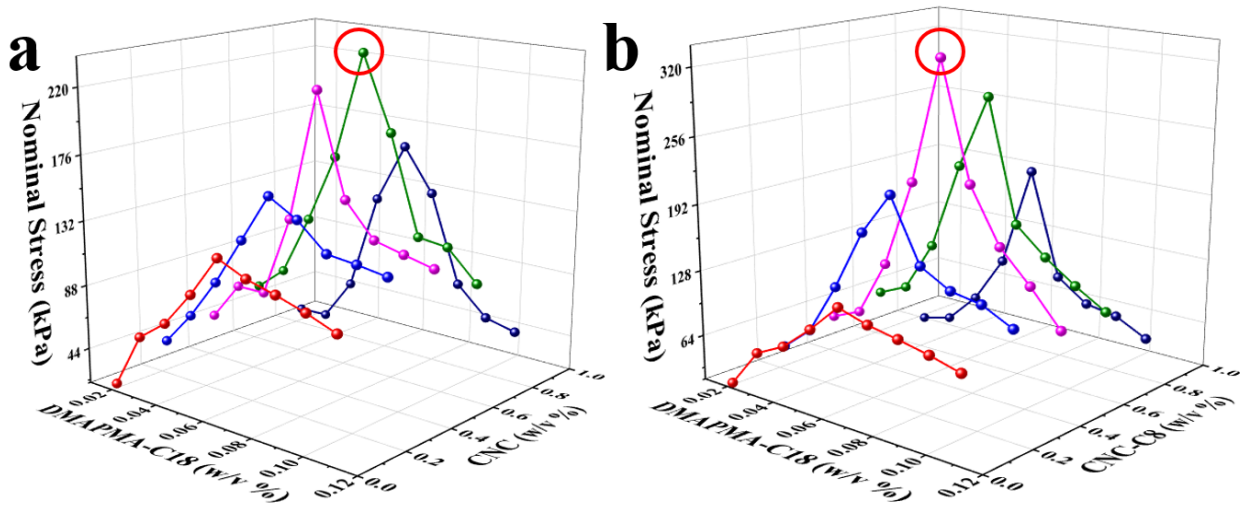

Figure 5. 4 Nominal tress of CNC or CNC-C8 DPC hydrogels as a function of the dosages of DMAPMA-C18 and (a) CNC or (b) CNC-C8. Each curve represents the changes as a function of DMAPMA-C18 content at constant dosage of CNC or CNC-C8. The points in red circles are the optimal stress values.

Table 5. 1DPC hydrogel nominal stresses (kPa) at different CNC contents (w/v %) and DMAPMA-C18 contents (w/v %)

Nominal Stress (kPa) / DMAPMA-C18 Content (w/v %)	CNC Content (w/v %)				
	0	0.2	0.4	0.6	0.8
0.0225	25.72	43.13	49.5	**59.92**	30.97
0.03375	63.38	66.22	75.63	**76.16**	31.57
0.045	77.9	94.1	75.9	**117.9**	60.13
0.05625	102	127	131.5	**165.3**	127.35
0.0675	130.2	159.85	220	**238.1**	168.09
0.07875	121.8	148.8	152.4	**188.2**	139.02
0.09	116.8	**131.5**	130.2	122.39	79.21
0.10125	110.9	**129.4**	125.3	119.95	60.33
0.1125	103.47	**126.45**	120.65	100.05	55.39

For the CNC DPC hydrogels, the optimum average nominal stress is 238.1±8.48 kPa at 0.6 w/v % CNC content and 0.0675 w/v% of 3 DMAPMA-C18. Generally at constant dosage of DMAPMA-C18, the stress increased with the increasing dosage of CNC from 0.0 w/v % to 0.6 w/v %, and decreased when CNC content was higher than 0.6 w/v %. Similarly, a peak-shaped relationship is observed between the stress and DMAPMA-C18

content at constant dosage of CNC, positive effects on the nominal stress with DMAPMA-C18 addition before the dosage of 0.0675 w/v% while negative after that.

Table 5. 2 DPC hydrogel nominal stresses (kPa) at different CNC-C8 contents (w/v %) and DMAPMA-C18 contents

(w/v %)

Nominal Stress (kPa) / DMAPMA-C18 Content (w/v %)	CNC-C8 Content (w/v %)				
	0	0.2	0.4	0.6	0.8
0.0225	25.72	43.71	56.73	**65.22**	20.4
0.03375	63.38	67.6	69.25	**78.23**	27.96
0.045	77.9	117.9	124.7	**128.1**	57.28
0.05625	102	176.85	210.9	**214.21**	103.57
0.0675	130.2	217.7	**331.05**	285.7	201.75
0.07875	121.8	158.75	**219.95**	168.3	100.72
0.09	116.8	142.9	**167.8**	142.85	80.25
0.10125	110.9	**138.1**	137.98	122.11	75.34
0.1125	103.47	**123.7**	104.1	104.3	60.23

For the CNC-C8 DPC hydrogels, the optimum nominal stress is 331.05±32.06 kPa at 0.4 w/v % CNC-C8 and 0.0675 w/v % DMAPMA-C18, higher than that for CNC DPC

hydrogels (238.1±8.48 kPa). In this case, the CNC-C8 DPC hydrogels could reach a higher nominal stress value with same DMAPMA-C18 content but lower CNC-C8 content (0.4 w/v %) compared to CNC DPC hydrogel with 0.6 w/v % CNC. This is due to the extra hydrophobic interactions introduced into the system

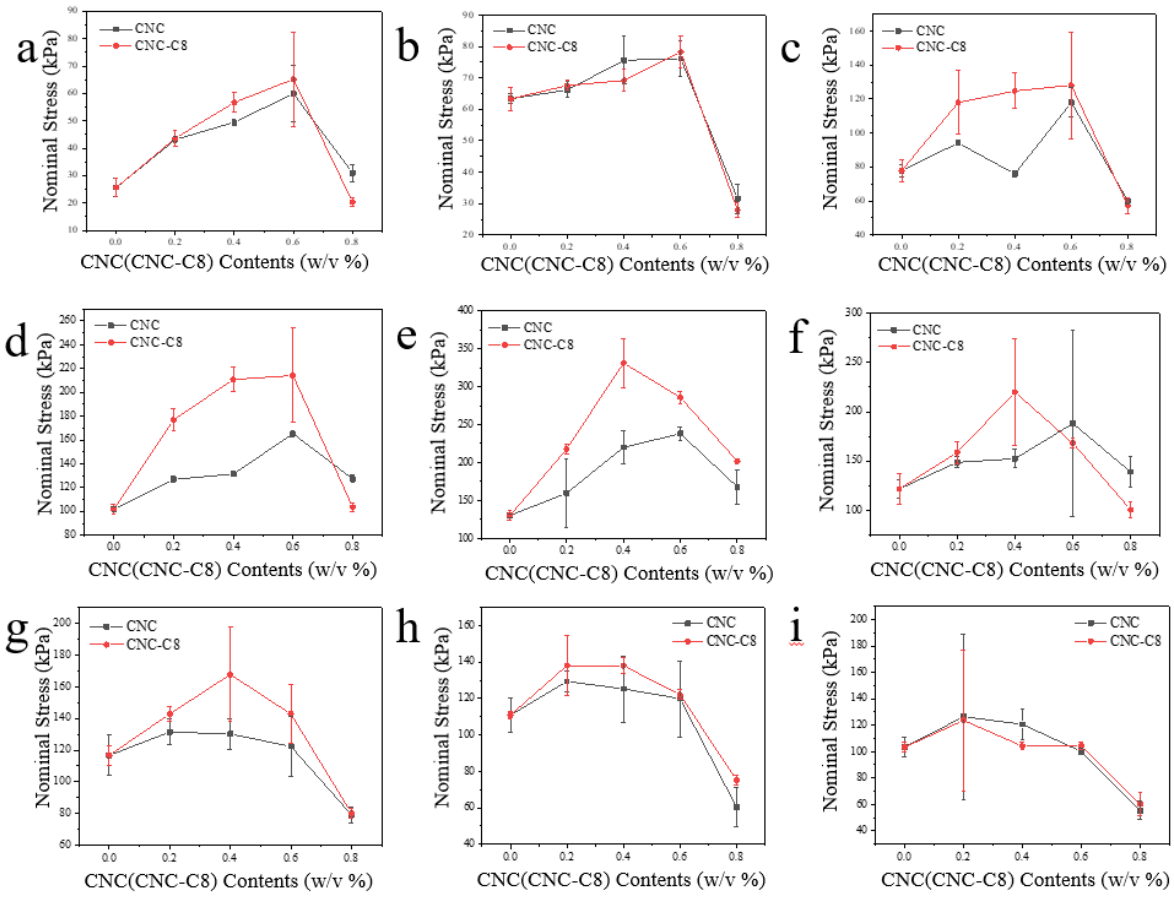

Figure 5. 5 The nominal stress of the DPC hydrogels as functions of the dosages of CNC and CNC-C8 at each DMAPMA-C18 contents of (a)0.0225 w/v % ,(b)0.03375 w/v %,(c)0.045 w/v %,(d) 0.05625 w/v % , (e)0.0675 w/v %,(f)0.07875 w/v %,(g)0.09 w/v %, (h)0.10125 w/v % and (i) 0.1125 w/v % separately.

Generally speaking, similar to CNC DPC hydrogels, the addition of CNC-C8 and DMAPMA-C18 both showed a positive effect at first and then show a negative effect after the optimal CNC-C8 content of 0.4 w/v % and DMAPMA-C18 content of 0.0675 w/v %.

Figure 5.5 showed the stress of the DPC hydrogels as a function of the dosages of CNC and CNC-C8 at each DMAPMA-C18 contents. The stress of CNC (or CNC-C8) DPC hydrogels decreases after the optimum values with the addition of CNC (CNC-C8).

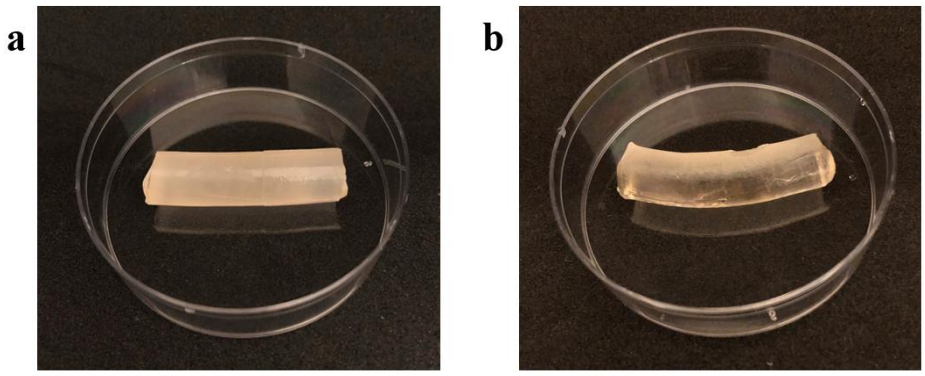

Figure 5. 6 The (a) uniform hydrogel and (b) not uniform hydrogel.

With the increasing dosage of CNC (or CNC-C8), the water solvent tends to be saturated and the CNC (or CNC-C8) would gather together with each other because of the hydrogen bonds between the hydroxyl groups on the surface of CNC (and the hydrophobic forces between C8 chains), making CNC (or CNC-C8) difficult to disperse well in water at the first step. The hydrogel products would be inhomogeneous and thus be prone to break easily under stress. Such effects are more obvious for CNC-C8 than

CNC DPC hydrogel, because of the strong hydrophobic interactions in CNC-C8. The stresses of CNC-C8 inhomogeneous hydrogels are even less than that of CNC inhomogeneous hydrogels products at the relatively high CNC (or CNC-C8) contents. **Figure 5.6** shows the pictures of uniform hydrogel in this study and not uniform with high CNC or CNC-C8 contents.

5.2.2.1 True Stress

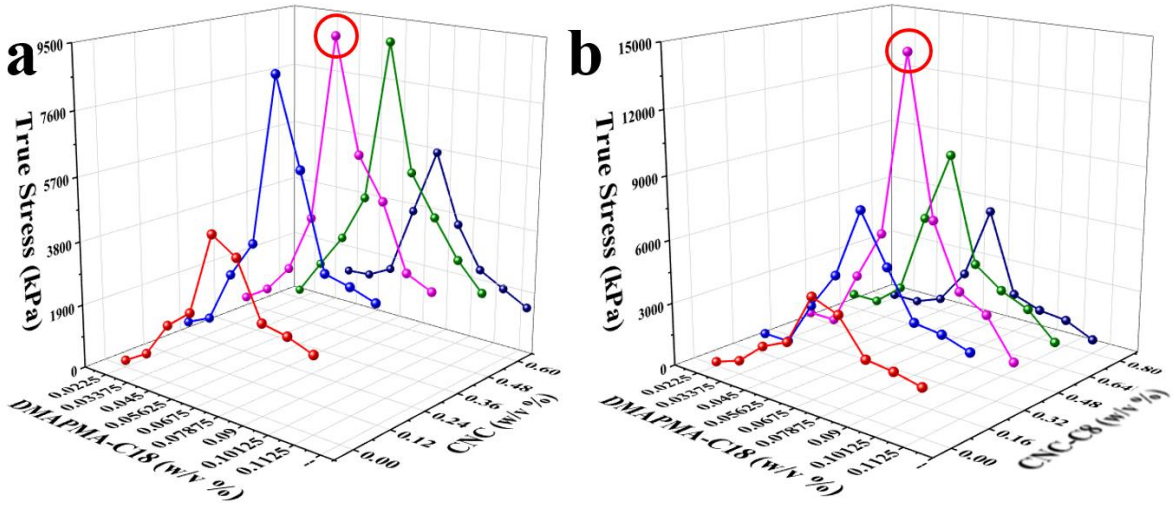

Figure 5. 7 True stress of CNC or CNC-C8 DPC hydrogels as a function of the dosages of DMAPMA-C18 and (a) CNC or (b) CNC-C8. Each curve represents the changes as a function of DMAPMA-C18 content at constant dosage of CNC or CNC-C8. The points in red circles are the optimal stress values.

Similar to nominal stress, as shown in **Figure5.7,** the changes of true stress of CNC DPC hydrogels and CNC-C8 DPC hydrogels are as a function of the dosages of

DMAPMA-C18 and CNC or CNC-C8 contents.

Each line in **Figure 5.7 a** and **Figure 5.7 b** represents the true stress changes as a function of DMAPMA-C18 content at constant dosage of CNC or CNC-C8.Under different DMAPMA-C18 contents dosages, the final average DPC hydrogel stresses at different CNC and CNC-C8 contents are shown in **Table 5.3**and **Table 5.4**respectively.

Table 5. 3 DPC hydrogel true stresses (kPa) at different CNC contents (w/v %) and DMAPMA-C18 contents (w/v %)

True Stress (kPa) / DMAPMA-C18 Content (w/v %)	CNC Content (w/v %)				
	0	0.2	0.4	0.6	0.8
0.0225	202.13	643.79	736.54	**888.24**	286.32
0.03375	642.09	982.02	1207.33	**1379.62**	342.35
0.045	1712.34	2539.26	2071.07	**2435.72**	735.18
0.05625	2297.03	3669.05	3842.72	**3920.18**	2917.96
0.0675	4742.35	8702.65	**9425.81**	8921.34	5033.96
0.07875	4273.88	**6143.29**	6078.24	5033.79	2804.32
0.09	2651.32	3356.17	**4852.39**	3790.22	1472.09
0.10125	2506.83	**3173.69**	2895.34	2634.95	1045.01
0.1125	2231.01	**2918.96**	2538.23	1802.36	621.59

Table 5. 4 DPC hydrogel true stresses (kPa) at different CNC-C8 contents (w/v%) and DMAPMA-C18 contents (w/v %)

True Stress (kPa) / DMAPMA-C18 Content (w/v %)	CNC-C8 Content (w/v %)				
	0	0.2	0.4	0.6	0.8
0.0225	202.13	687.99	882.06	**1012.96**	165.01
0.03375	642.09	1102.36	1204.37	**1220.96**	263.95
0.045	1712.34	2781.66	**3433.09**	2036.18	636.57
0.05625	2297.03	4573.23	5814.03	**5869.24**	2296.82
0.0675	4742.35	7902.88	**14463.99**	9205.43	5812.67
0.07875	4273.88	5601.32	**7025.84**	4206.33	1905.79
0.09	2651.32	3412.06	**4006.29**	3251.19	1436.97
0.10125	2506.83	3241.98	**3267.14**	2683.32	1282.99
0.1125	2231.01	**2816.92**	1426.17	1452.68	672.34

For the CNC DPC hydrogels, the optimum average true stress is 9425.81±5122.15kPa at 0.4 w/v % CNC content and 0.0675 w/v% of 3 DMAPMA-C18. For the CNC-C8 DPC hydrogels, the optimum true stress is 14463.99±2939.98kPa at 0.4 w/v % CNC-C8 and 0.0675 w/v % DMAPMA-C18, higher than that for CNC DPC hydrogels. In this case, the CNC-C8 DPC hydrogels could reach a higher true stress value with same

DMAPMA-C18 content (0.0675 w/v %) and CNC-C8 content (0.4 w/v %) of CNC DPC hydrogels with optimal true stress values, which is similar to the results of nominal stress values.

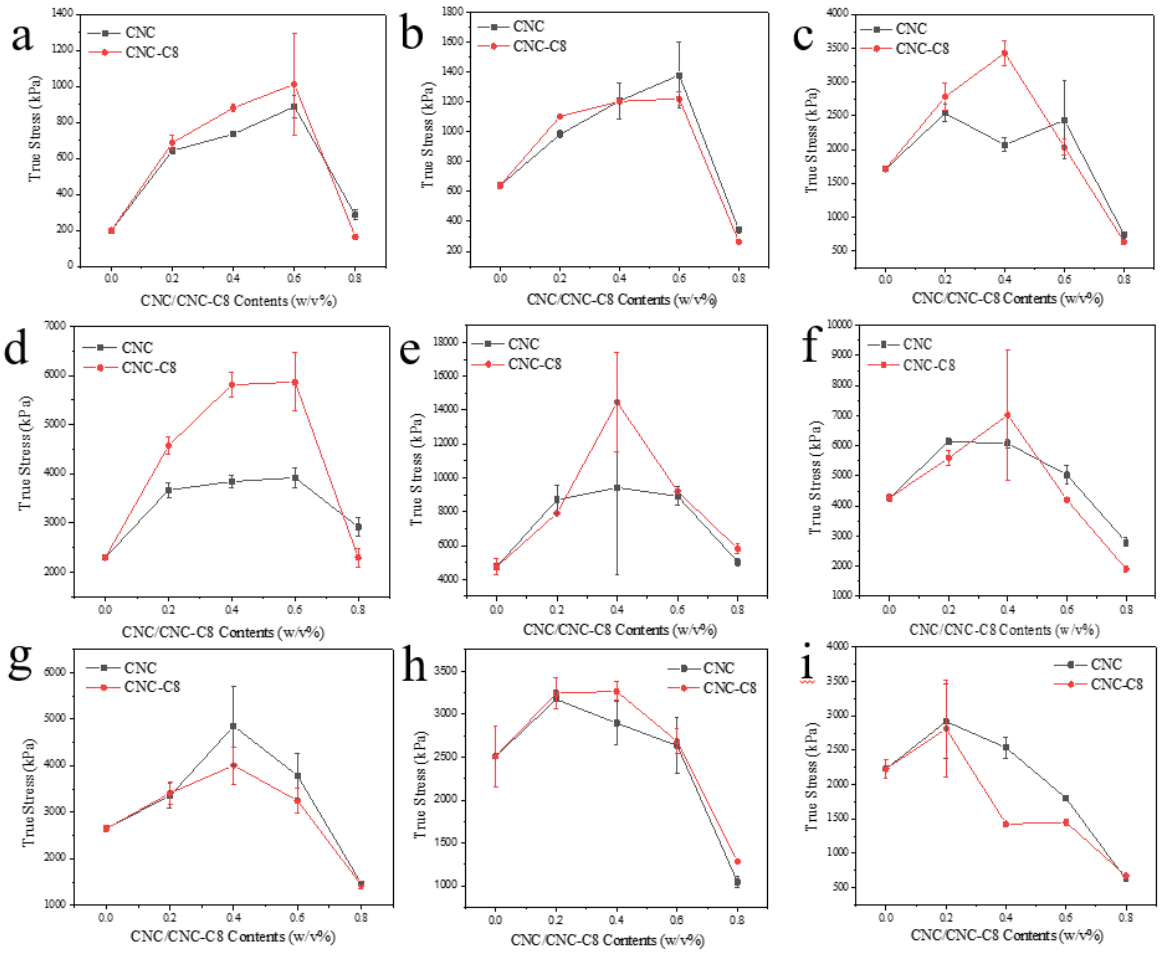

Figure 5. 8 The true stress of the DPC hydrogels as functions of the dosages of CNC and CNC-C8 at each DMAPMA-C18 contents of (a)0.0225 w/v % , (b)0.03375 w/v %, (c)0.045 w/v %, (d) 0.05625 w/v % , (e)0.0675 w/v %, (f)0.07875 w/v %, (g)0.09 w/v %, (h)0.10125 w/v % and (i) 0.1125 w/v % separately.

Similar to nominal stress, the true stress values with error bars at each DMAPMA-C18

content dosages are shown in **Figure 5.8** as well.

When the CNC or CNC-C8 is not added to the system, the optimal DMAPMA-C18 dosage for the hydrogel was 3 DMAPMA-C18 (0.0675 w/v %) with a true stress of 4742.35±476.17 kPa as shown in **Figure 5.9**. When the DMAPMA-C18 content is higher than 0.0675 w/v %, the stress decreased.

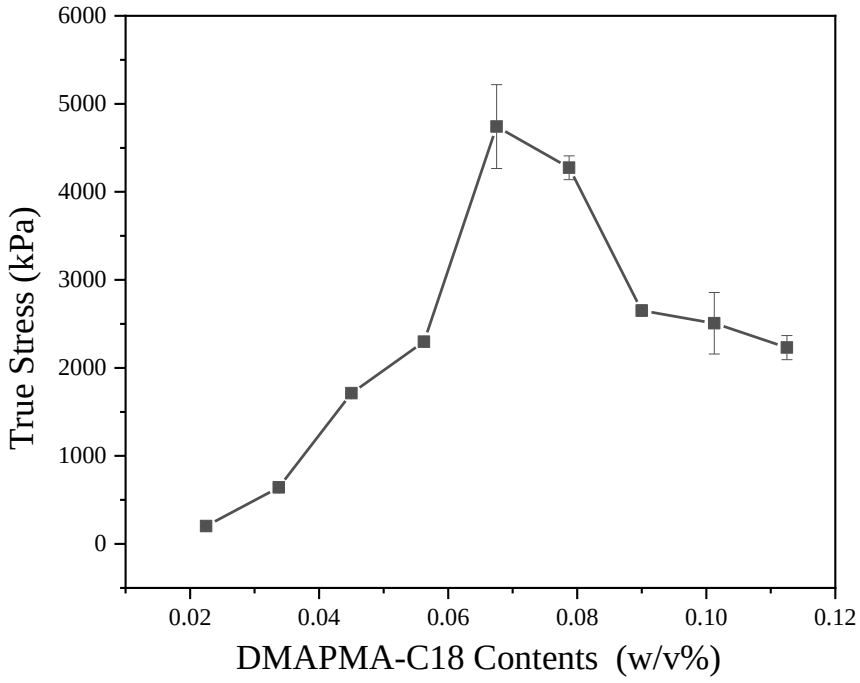

Figure 5.9 The true stress of the DPC hydrogels as a function of the dosage of DMAPMA-C18.

5.2.2 Strain

Similar to the observations for the stress, when the CNC or CNC-C8 is not added to the physically cross-linked hydrogels, the optimal DMAPMA-C18 dosage for elongation was

0.0675 w/v % with an elongation of 3530.94±281.08% as shown in **Figure 5.10**. The incorporating of hydrophobic monomer DMAPMA-C18 enhances the mechanical properties of the hydrogel system.

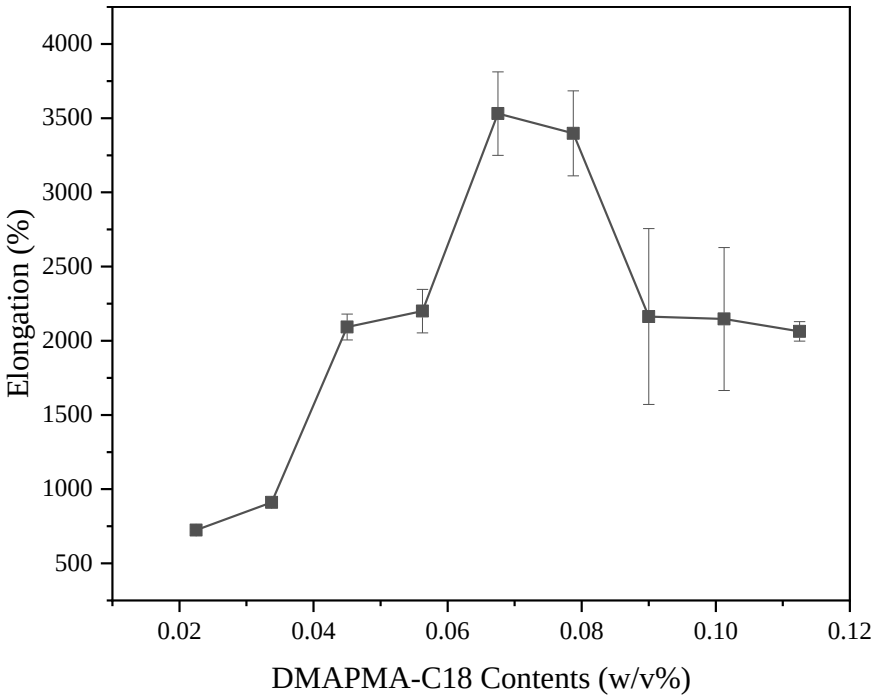

Figure 5.10 The elongation of the DPC hydrogels as a function of the dosage of DMAPMA-C18.

Figure 5.11 shows the elongation behaviors of the DPC hydrogels as a function of the dosage of DMAPMA-C18 and CNC or CNC-C8. It was found that the DPC hydrogels formed with CNC or CNC-C8 showed similar trends in the change of elongation behaviors by adjusting the content of CNC or CNC-C8. The optimal average elongation was 5352.29±1427.07 % for the CNC DPC hydrogel with 0.0675 w/v %DMAPMA-C18 content and 0.2 w/v % CNC content, and 4267.85±1445.58% for CNC-C8 DPC

hydrogels with 0.0675 w/v %DMAPMA-C18 and 0.4 w/v % CNC-C8, respectively.

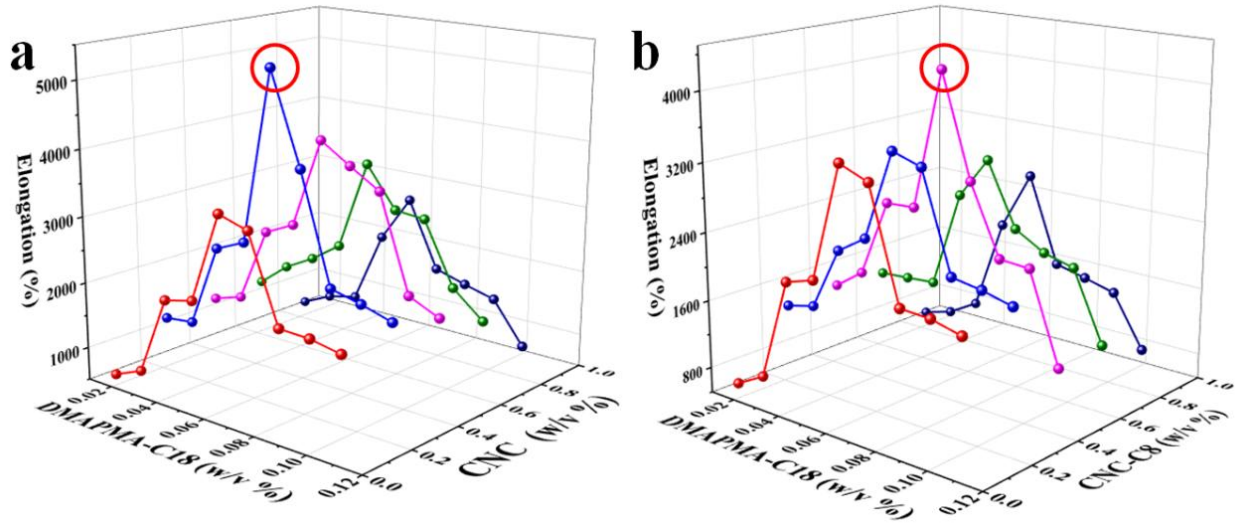

Figure 5. 11 The elongations of DPC hydrogels as a function of the dosage of DMAPMA-C18 and (a) CNC or (b) CNC-C8.Each curve represents the changes as a function of DMAPMA-C18 content at constant dosage of CNC or CNC-C8. The points in red circles are the optimal elongation values.

Generally, the addition of CNC contents could help with enhancing the elongations from 0.0 w/v % to 0.2 w/v % contents. After the CNC content is more than 0.2 w/v %, the CNC addition shows negative effects on tensile strengths of CNC DPC hydrogels. Similarly, as for the influences of DMAPMA-C18 contents on stresses, we could see that there are positive effects of DMAPMA-C18 contents addition before 0.0675 w/v %while negative effects after that.

Table 5. 5 DPC hydrogel elongations (%) at different CNC contents (w/v %) and DMAPMA-C18 contents (w/v %)

Elongation (%) / DMAPMA-C18 Content (w/v %)	CNC Content (w/v %)				
	0	0.2	0.4	0.6	0.8
0.0225	724.29	1321.81	1367.24	**1386.02**	785.36
0.03375	911.16	1375.35	1505.34	**1740.14**	993.27
0.045	2092.54	2610.1	**2631.1**	1981.44	1100.72
0.05625	2199.7	2802.62	**2839.51**	2287.26	2197.26
0.0675	3530.94	**5352.29**	4178.83	3641.98	2887.01
0.07875	3397.54	**4033.49**	3887.84	3036.44	1890.85
0.09	2163.33	2456.1	**3610.9**	2993.98	1753.96
0.10125	2146.49	**2349.74**	2205.11	2065.53	1632.02
0.1125	2063.21	**2214.74**	1997.84	1678.66	1011.38

The data of DPC hydrogel elongations at different CNC (CNC-C8) contents and DMAPMA-C18 contents are shown in **Table 5.5.** Similarly, the data of DPC hydrogel elongations at different CNC-C8 contents and DMAPMA-C18 contents are shown in **Table 5.6**. For each DMAPMA-C18 content and CNC-C8 content combination, every

experiment was repeated for three times and the elongation was measured for three times accordingly as well.

Table 5. 6 DPC hydrogel elongations (%) at different CNC-C8 contents (w/v %) and DMAPMA-C18 contents (w/v %)

Elongation (%) / DMAPMA-C18 Content (w/v %)	CNC-C8 Content (w/v %)				
	0	0.2	0.4	0.6	0.8
0.0225	724.29	1437.73	**1483.25**	1441	722.57
0.03375	911.16	1521.99	**1724.92**	1466.36	821.68
0.045	2092.54	2257.64	**2637.3**	1494.48	1021.35
0.05625	2199.7	2476.29	**2659.11**	2639.4	2106.73
0.0675	3530.94	3511.61	**4267.85**	3118.97	2779.68
0.07875	3397.54	**3404.98**	3095.27	2387.07	1782.06
0.09	2163.33	2296.48	**2302.15**	2187.78	1697.81
0.10125	2146.48	2241.81	**2280.17**	2096.14	1605.34
0.1125	2063.21	**2155.65**	1253.79	1288.54	1009.23

For the CNC DPC hydrogels, the optimum strain is 5352.29±1427.07 %, which is higher than the optimal strain of 4267.85±1445.58% for CNC-C8 DPC hydrogels. According to the experiments records, when the DMAPMA-C18 content is less than 0.045 w/v %, the CNC-C8DPChydrogels would show a better optimal elongation value than the CNC DPC

hydrogels. When the DMAPMA-C18 content is higher than 0.045 w/v %, the optimal elongation values of CNC DPC hydrogels would be higher than that of CNC-C8DPChydrogels.

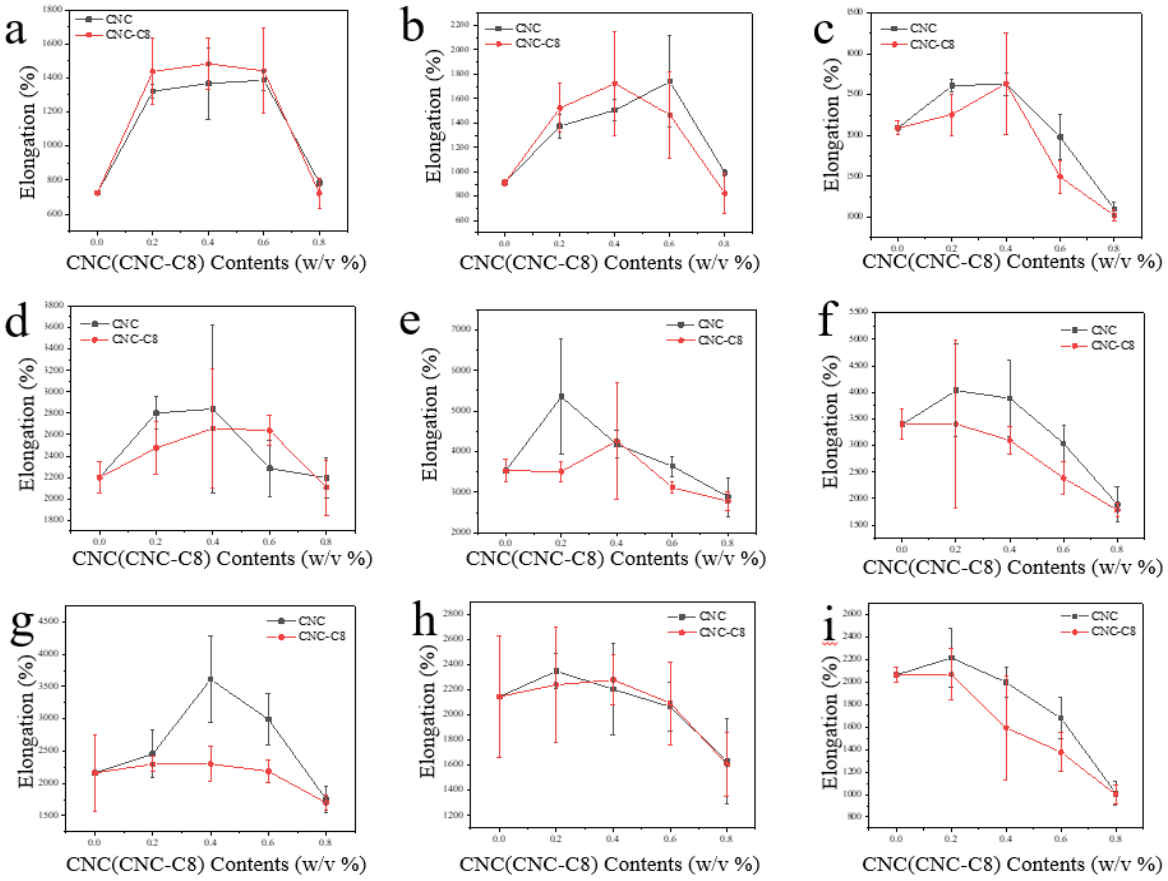

Figure 5. 12 The stress of the DPC hydrogels as a function of the dosages of CNC and CNC-C8 at each DMAPMA-C18 contents of (a) 0.0225 w/v % , (b) 0.03375 w/v %, (c) 0.045 w/v %, (d) 0.05625 w/v % , (e) 0.0675 w/v %, (f) 0.07875 w/v %, (g) 0.09 w/v %, (h) 0.10125 w/v % and (i) 0.1125 w/v % separately.

Similar to the impact on stress, the decreases on elongation at high CNC (or CNC-C8)

dosage are due to the inhomogeneity of the hydrogel products resulting from the strong interactions in CNC (or CNC-C8) at high dosage and less uniform dispersion in the hydrogel. Overall, the optimal DMAPMA-C18 and CNC-C8 content for CNC-C8 DPC hydrogels are 0.0675 w/v % and 0.4 w/v %, respectively, for maximum strain (331.05±32.06 kPa) and elongation (4267.85±1445.58%). For CNC DPC hydrogels, the optimal stress and elongation values did not appear at a same DMAPMA-C18 content and CNC content combination. The optimal DMAPMA-C18 content is also selected as 3 DMAPMA-C18 (0.0675 w/v %). As for the optimal CNC content, the one to obtain the optimal stress value is 0.6 w/v % (238.1±8.48 kPa) and the one to obtain the optimal elongation value is 0.2 w/v % (5352.29±1427.07 %).

According to the experiments results, the change of DAMPMA-C18 contents would play a more important role on tress and elongation values than CNC or CNC-C8 contents, indicating the importance of building the first layer structure cross-linked by hydrophobic forces. Overall, the type of CNC-C8 DPC hydrogel (3 DMAPMA-C18 and 0.4 w/v % CNC-C8) would be selected as the most optimal one in all the 90 types of DPC hydrogels.

5.2.3 Compression Tests

With the optimum contents of CNC-C8 and DMAPMA-C18 in the hydrogel, the CNC-C8 DPC hydrogel could completely recover after a pressing-releasing process, as

shown in **Figure 5.13.**

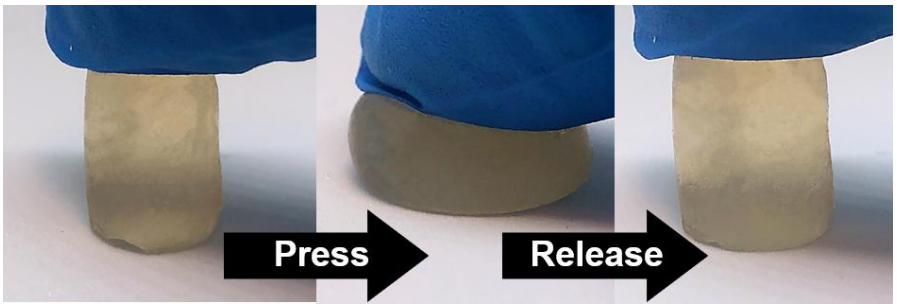

Figure 5. 13 The complete recovery of CNC-C8-P-DMAc-DMAPMA-C18 hydrogel from a pressing-releasing process.

The compressive stress-stain curves for the optimal CNC DPC hydrogels at 0.6 w/v% CNC and 3 DMAPMA-C18 contents as well as the optimal CNC-C8 DPC hydrogels at 0.4 w/v% CNC-C8 and 3 DMAPMA-C18 contents are shown in **Figure 5.14**. For the two types of optimal DPC hydrogel samples, the compressive press increased steadily before around 55% of strain and grew rapidly after that. In general, the compressive stress of CNC DPC hydrogel is higher than that of CNC-C8 DPC hydrogels. Both of the two types of optimal DPC hydrogel samples could stand at least 90% of strain and the optimal compressive stress for the CNC DPC hydrogelwas1605.21 kPa while for the CNC-C8 DPC hydrogel was 2822.77 kPa at the strain of 90%.

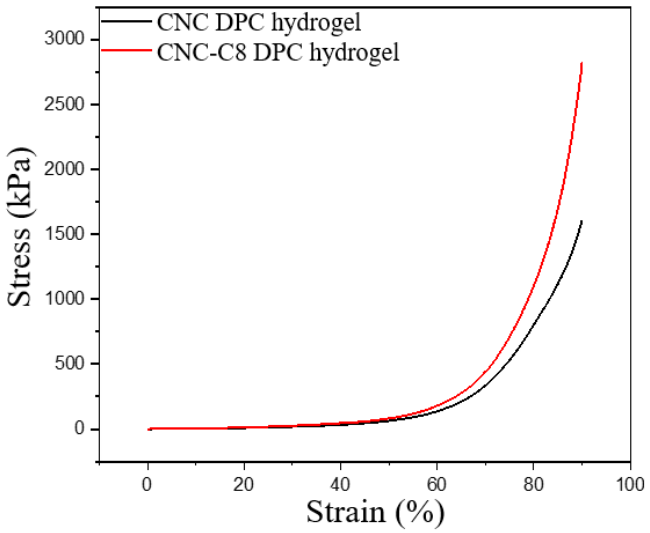

Figure 5. 14 Compressive stress-strain curves for the optimal CNC DPC hydrogels and CNC-C8 DPC hydrogels.

5.2.4 Typical Stress-Strain Profiles

The typical stress-strain profiles for CNC DPC hydrogels and CNC-C8 DPC hydrogels are shown in **Figure 5.15.** The optimum CNC DPC hydrogels and CNC-C8 DPC hydrogels types were selected among the three repeated experiments with the optimal stresses and elongations at the certain DMAPMA-C18 content and CNC or CNC-C8 content values. Obviously, the optimum stress and strain for CNC DPC hydrogels are 208.6 kPa and 6896.49% separately at 3 DMAPMA-C18 (0.0675 w/v %) content and 0.2 w/v % CNC content. CNC-C8 DPC hydrogels with 3 DMAPMA-C18 (0.0675 w/v %) and 0.4 w/v % CNC-C8 showed the optimal stress of 294.8 kPa and strain of 5909.64%. The stress and strain performances of 3 DMAPMA-C18 (0.0675%) are both much higher than that of DPC hydrogels with other DMAPMA-C18 contents.

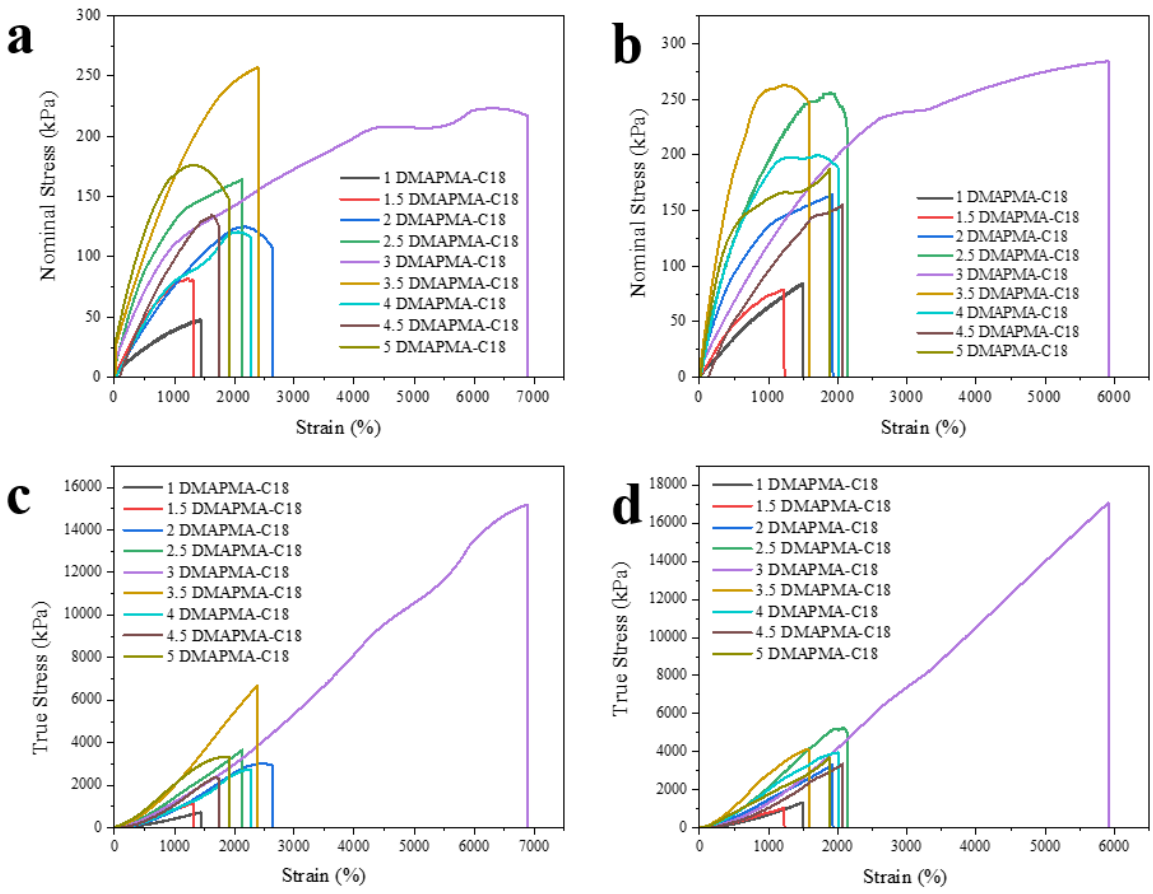

Figure 5. 15 Typical nominal stress-strain profiles for (a) CNC DPC hydrogels, (b) CNC-C8 DPC hydrogels and typical true stress-strain profiles for (c) CNC DPC hydrogels and (d) CNC-C8 DPC hydrogels.

5.2.5 Self-Recoverability

Figure 5.16shows the self-recoverability of CNC-P-DMAc-DMAPMA-C18 by applying THF between the cut surfaces at room temperature overnight. One block of DPC hydrogel product was cut into two blocks, one of which was colored as red while the other one was not. The pictures show that the DPC hydrogels could be recovered well.

The recovered hydrogel products could still be twisted, stretched and knotted like the initial conditions.

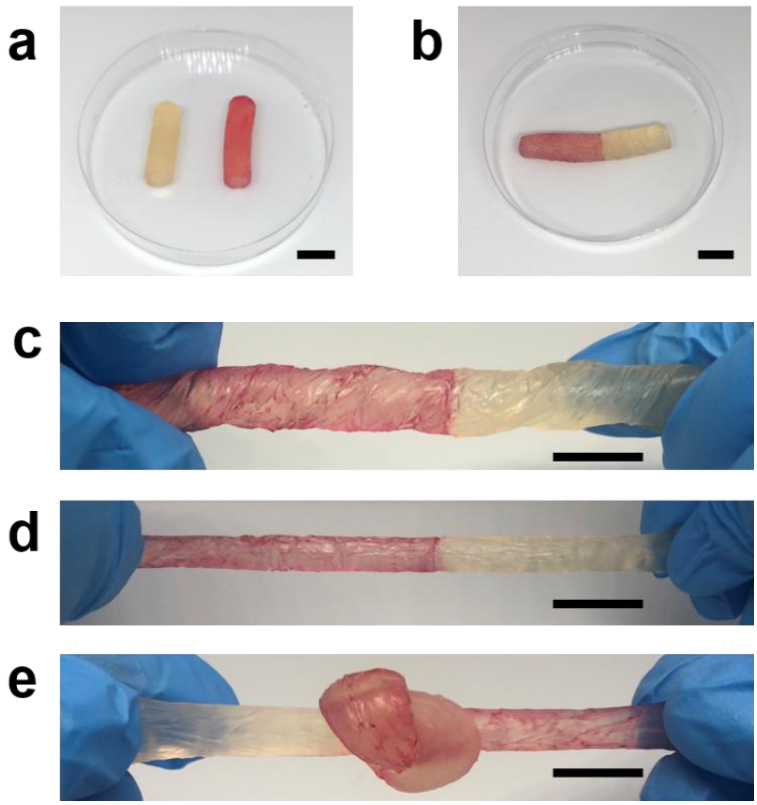

Figure 5.16 Photographs (a) and (b) demonstrating the self-healing behavior of CNC-P-DMAc-DMAPMA-C18 hydrogel with optimum contents of CNC and DMAPMA-C18 (a) cut into two hydrogel parts (b) self-recovered. Photographs (c-e) show the ability of hydrogel to withstand (c) twisting, (d) stretching, and (e) knotting.

Figure 5.17shows the stress and strain ratios of self-recovered CNC and CNC-C8 DPC hydrogels with optimal mechanical strength at different contents of DMAPMA-C18. For both the cases of CNC DPC hydrogels and CNC-C8 DPC hydrogels, the stress

self-recovery ratio increased with the increasing DMAPMA-C18 contents. The optimal stress self-recovery ratio of CNC DPC hydrogel is 89.96±1.29% at when the hydrogel contained 4 DMAPMA-C18 (0.09 w/v %). For the CNC-C8 DPC hydrogel, it was 76.32±1.08% at 5 DMAPMA-C18 (0.1125 w/v %) contents.

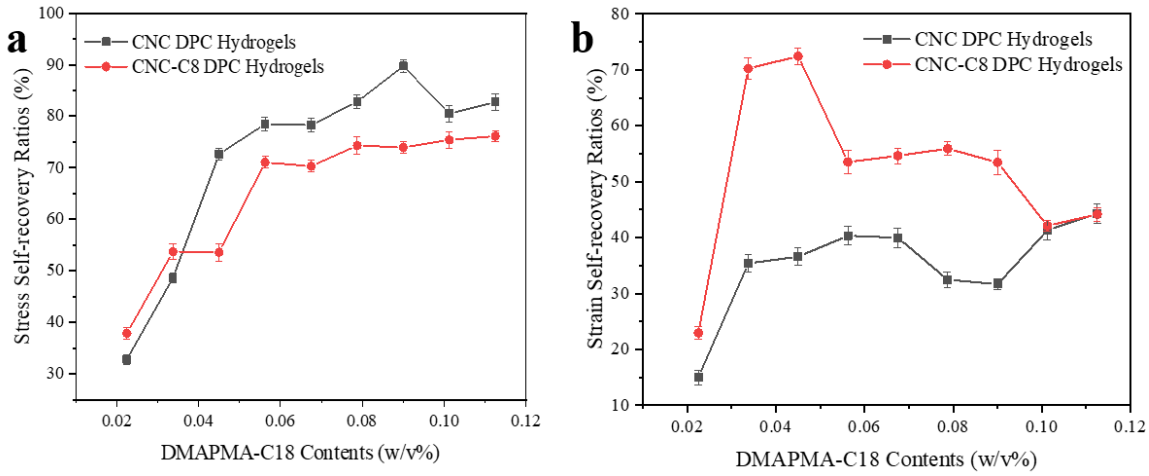

Figure 5. 17 The (a) stress and (b) strain self-recovery ratios of CNC DPC hydrogels and CNC-C8 DPC hydrogels with different DMAPMA-C18 contents.

The CNC DPC hydrogel showed the optimal elongation self-recovery ratio of 44.23±1.73% with 5 DMAPMA-C18 (0.1125 w/v %) and the optimal elongation self-recovery ratio of CNC-C8 DPC hydrogel was 72.46±1.46% when there were 2 DMAPMA-C18 (0.045 w/v %) in the hydrogel. In general, the CNC-C8 DPC hydrogels showed better elongations after self-recovery than that of CNC DPC hydrogels with different DMAPMA-C18 contents, due most likely to the enforcement of the hydrophobic interactions between the CNC-C8 and DMAPMA-C18.

Figure 5.18 showed the stress-strain curves of self-recovered CNC DPC hydrogel and CNC-C8 DPC hydrogel with 3 DMAPMA in the hydrogels**.** Owing to the hydrophobic interaction between CNC-18 and DMAPMA-C18, the self-recovered CNC-C8 DPC hydrogel showed better tensile strength than the self-recovered CNC DPC hydrogel.

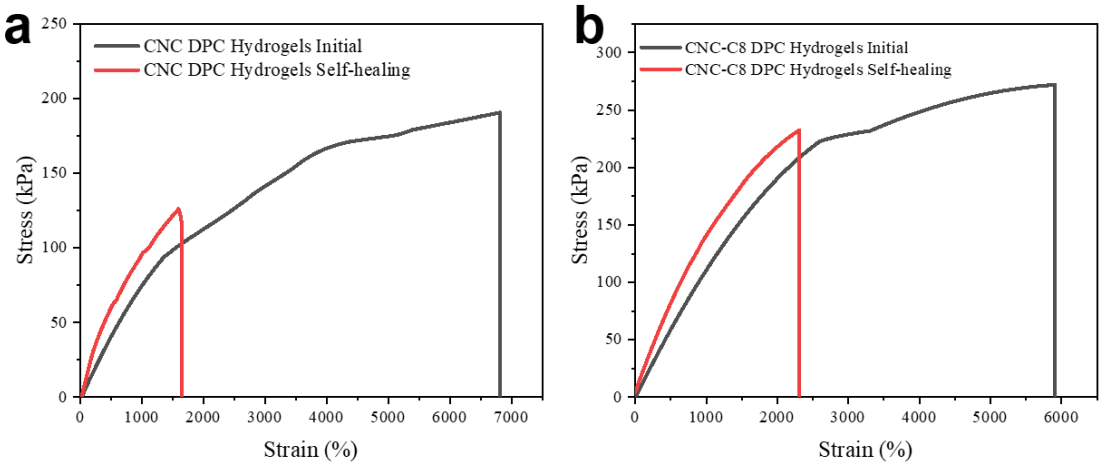

Figure 5.18 Typical stress-strain curves for self-repaired (a) CNC DPC hydrogel and (b) CNC-C8 DPC hydrogel with optimum content of DMAPMA-C18 and CNC or CNC-C8.

5.3 Swelling Test

5.3.1 Water Absorption

At the beginning of water absorption experiments, wet and freeze-dried CNC DPC hydrogels at 1 DMAPMA-C18 and different CNC contents of 0.0 w/v %, 0.2 w/v %, 0.4 w/v % and 0.6 w/v % were used for water absorption as shown in **Figure 5.19**. For both of the wet and freeze-dried samples, the water absorption capacities got increased rapidly

during the first day and improved gradually after that. The water absorption capacities for wet DPC hydrogels are obviously lower than that of freeze-dried hydrogels. The freeze-dried CNC DPC hydrogels were saturated earlier than wet CNC DPC hydrogels. For wet CNC DPC hydrogels, the one with no CNC showed optimal water absorption capacities while for freeze-dried CNC DPC hydrogels the one with 0.6 w/v % CNC contents showed better water absorption capacities.

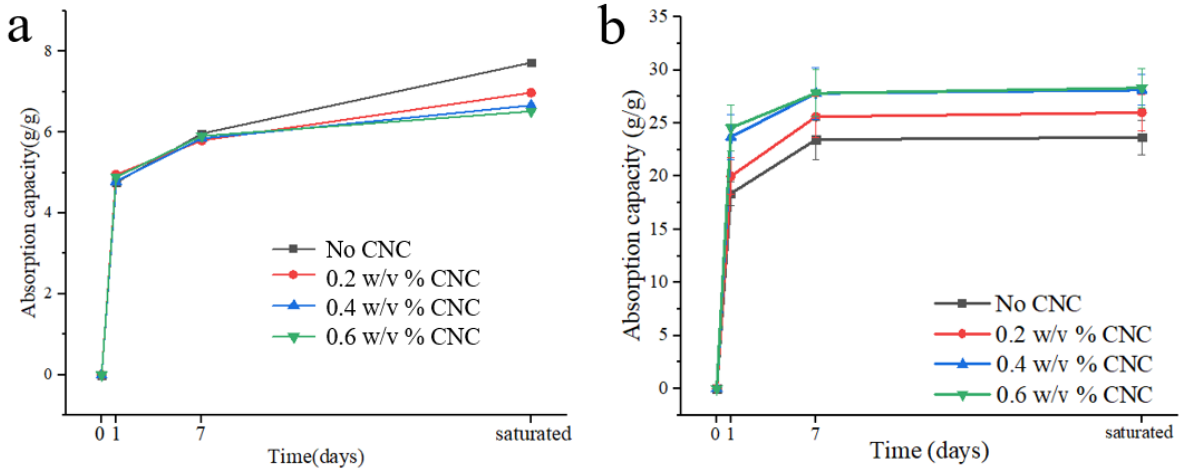

Figure 5. 19 Water absorption capacities for (a) wet and (b) freeze-dried CNC DPC hydrogels.

Four types of freeze-dried DPC hydrogels (CNC DPC hydrogels with 1 DMAPMA-C18, CNC-C8 DPC hydrogels with 1 DMAPMA-C18, CNC DPC hydrogels with 2 DMAPMA-C18 and CNC-C8 DPC hydrogels with 2 DMAPMA-C18) were used to absorb water for 168 hours at first and the results were shown in **Figure 5.20**.

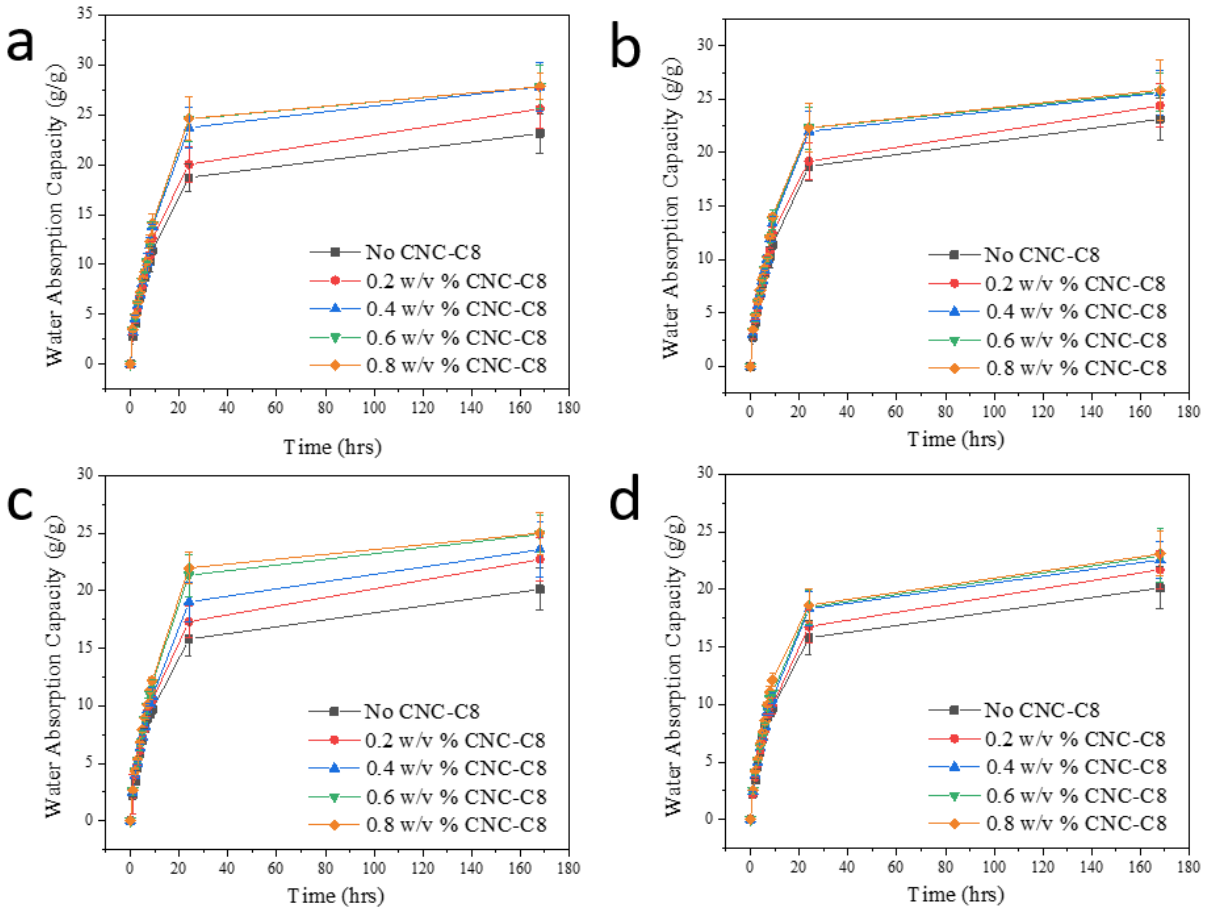

Figure 5. 20 Water absorption ability in hours of freeze-dried (a) CNC-P-DMAc-DMAPMA-C18, (b) CNC-C8-P-DMAc-DMAPMA-C18, (c) CNC-P-DMAc-2 DMAPMA-C18 and (d) CNC-C8-P-DMAc-2 DMAPMA-C18 hydrogels.

It could be observed that the water absorption capacities get increased sharply at the first 24 hours and grew gradually after that. In order to find out the saturation time, the water absorption capacities were recorded in days to make sure the time period for water absorption experiments. The four types of freeze-dried DPC hydrogels were used to adsorb water for 30 days and the results were shown in **Figure 5.21**.

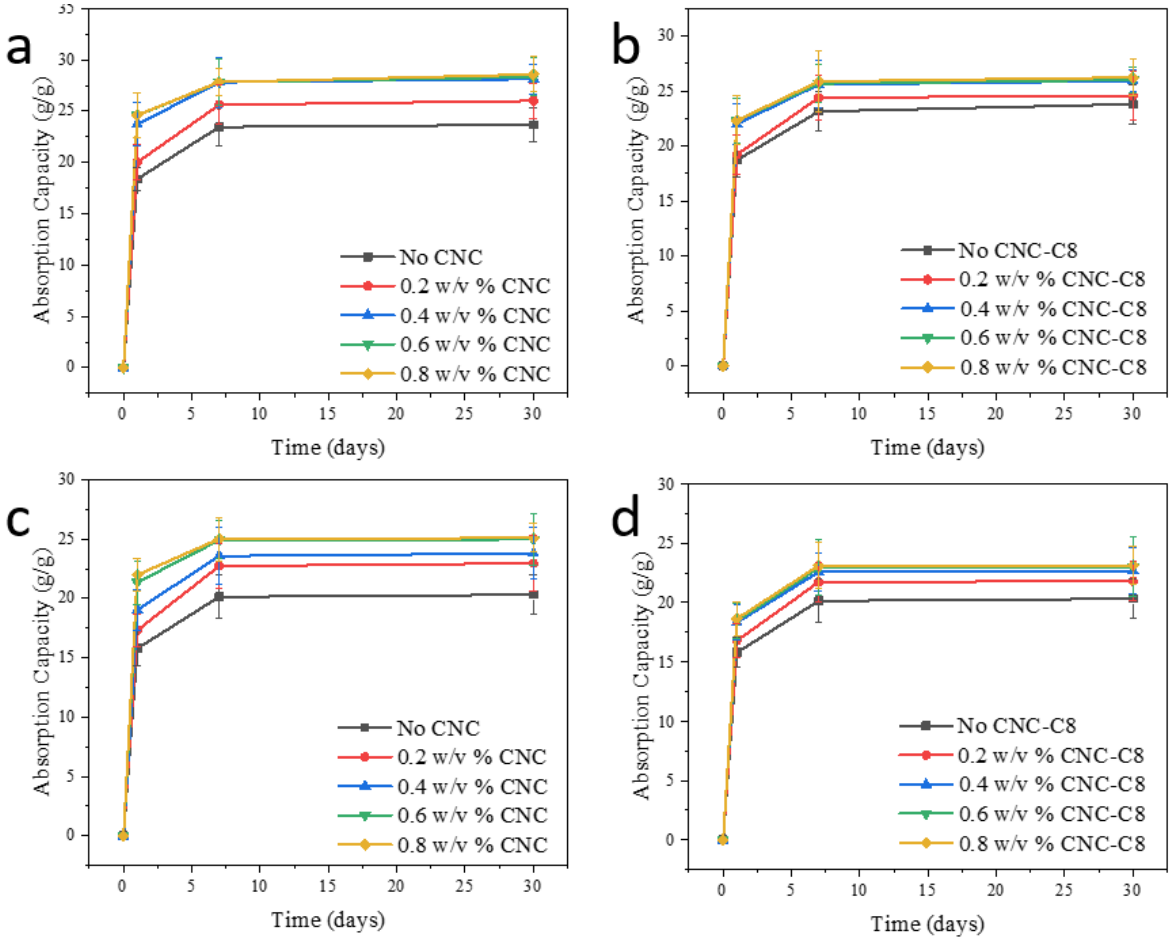

Figure 5. 21 Water absorption ability in days of freeze-dried (a) CNC-P-DMAc-DMAPMA-C18, (b) CNC-C8-P-DMAc-DMAPMA-C18, (c) CNC-P-DMAc-2 DMAPMA-C18 and (d) CNC-C8-P-DMAc-2 DMAPMA-C18 hydrogels.

For all the studied freeze-dried DPC hydrogels, their water absorption ability almost reached the highest when they contained 0.6 w/v % CNC. The further increase in the content of CNC showed a marginal increase on their water absorption ability. The reason is that CNC is abundant of hydrophilic hydroxyl groups. With the amount of CNC added,

the number of hydrophilic hydroxyl groups increased, so the water absorption was improved obviously at the beginning. But as the larger amount of CNC is added into the DPC hydrogels, it cannot be dispersed well in water as before but gathered together by the hydrogen bonds between the hydroxyl groups instead. The number of hydroxyl groups could be used to absorb water would be reduced. Therefore, the water absorption capacities of the four types of freeze-dried DPC hydrogels did not increase a lot after the CNC/CNC-C8 contents were higher than 0.6 w/v %.

It could be seen that the water absorption capacities increased fast in the first 7 days and negligible increase in their corresponding water absorption capacity was observed after 7 days. Based on the reason, a duration of 7 days was selected to determine the ability of hydrogel on adsorbing water with different contents of DMAPMA-C18, CNC and/or CNC-C8.The data of DPC hydrogel water absorption capacity (g/g) at different CNC contents and DMAPMA-C18 contents are shown in **Table 5.7**.

The optimal water absorption capacity was 27.8301±0.43 g/g of a CNC DPC hydrogel at 1 DMAPMA-C18 (0.0225 w/v %) content and 0.8 w/v % CNC content. This is because DMAPMA-C18 monomers were mainly hydrophobic, which would play negative effects on water absorption. However, as there were many hydrophilic hydroxyl groups on the surface of CNC, the addition of CNC in DPC hydrogels would be helpful for water absorption.

Table 5. 7 DPC hydrogel water absorption capacity (g/g) at different CNC contents (w/v %) and DMAPMA-C18 contents (w/v %)

Water Absorption Capacity (g/g) / DMAPMA-C18 Content (w/v %)	CNC Content (w/v %)				
	0	0.2	0.4	0.6	0.8
0.0225	23.1308	25.6101	27.8155	27.8226	**27.8301**
0.03375	21.0688	24.4336	26.5873	26.825	26.8316
0.045	20.1294	22.7261	23.5713	24.9084	25.0078
0.05625	18.9798	20.975	21.0593	22.7153	22.933
0.0675	17.6284	19.7189	19.9741	20.3519	20.4379
0.07875	15.2325	16.9179	17.801	18.8504	19.0213
0.09	13.651	15.6579	16.5724	17.1756	16.8001
0.10125	12.9442	13.5642	14.1973	14.5655	14.5032
0.1125	11.7262	12.1556	13.1371	13.3748	13.3501

Similarly, the data of DPC hydrogel water Absorption Capacity (g/g) at different CNC-C8 contents and DMAPMA-C18 contents are shown in **Table 5.8**. The optimal water absorption ability was also appeared at the one with maximum CNC-C8 contents while with the minimum DMAPMA-C18 contents. It is needed to be mentioned that although CNC-C8 had hydrophobic modifications, the C8 modification level for CNC used in

DPC hydrogels was only 5%. Therefore, the CNC-C8 was still be mainly hydrophilic.

Table 5. 8 DPC hydrogel water absorption capacity (g/g) at different CNC-C8 contents (w/v %) and DMAPMA-C18 contents (w/v %)

Water Absorption Capacity (g/g) / DMAPMA-C18 Content (w/v %)	CNC-C8Content (w/v %)				
	0	0.2	0.4	0.6	0.8
0.0225	23.1308	24.3876	25.5846	25.6809	**25.8638**
0.03375	21.0688	22.1672	23.649	24.5575	24.6575
0.045	20.1294	21.7261	22.5713	22.9084	23.0978
0.05625	18.9798	19.975	20.0593	20.7153	20.933
0.0675	17.6284	18.5011	19.8668	19.9035	19.9113
0.07875	15.2325	16.4642	17.0593	17.2413	17.5098
0.09	13.651	14.1259	14.8288	15.625	15.369
0.10125	12.9442	13.1639	13.5343	14.0049	14.0301
0.1125	11.7262	11.9764	12.0147	12.1673	12.1689

Figure 5.22 shows that increasing the content of CNC or CNC-C8 in the DPC hydrogels could obviously improve water absorption capacities when the content of CNC or CNC-C8 is less than 0.4 w/v %. With the increasing content of DMAPMA-C18, the

water absorption capacities of the hydrogel decreased due to the hydrophobicity of DMAPMA-C18.

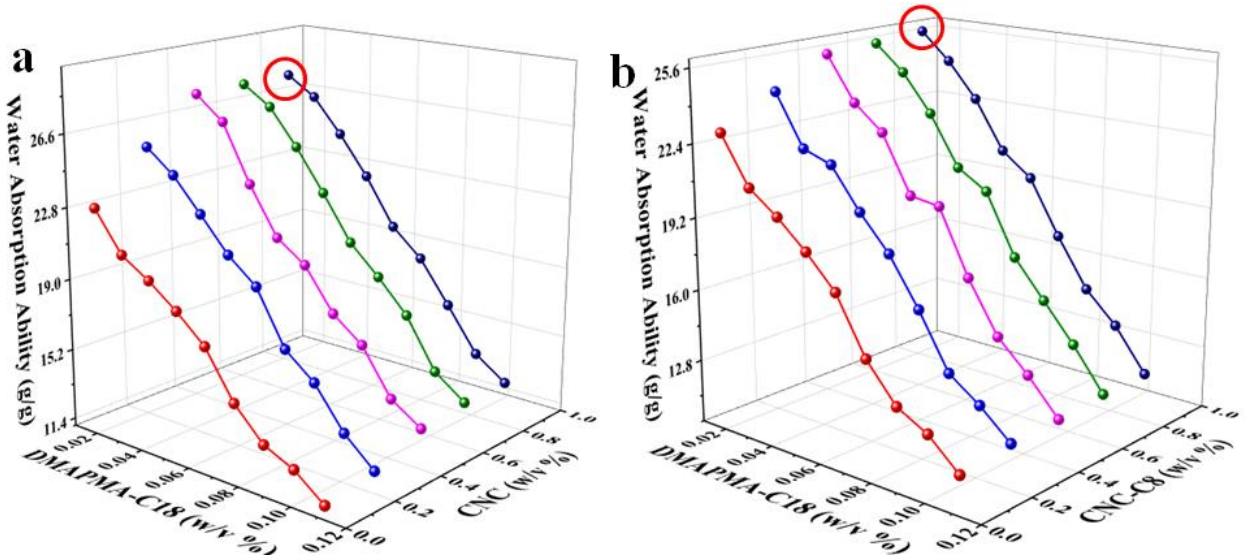

Figure 5. 22 Water absorption capacity of the DPC hydrogel as a function of the dosage of (a) CNC or (b) CNC-C8 and DMAPMA-C18. The points in red circles are the optimal water absorption capacity values.

Figure 5.23 showed water absorption capacity of the DPC hydrogels as a function of the dosages of CNC and CNC-C8 at each DMAPMA-C18 contents. The water absorption capacity of CNC DPC hydrogel was generally better than that of the CNC-C8 DPC hydrogel at the same content of DMAPMA-C18 and CNC or CNC-C8, resulting from the hydrophobic C8 chains on CNC. The hydrophilic monomers would play a positive role in water absorption while hydrophobic monomer would have negative effects on water absorption capacities.

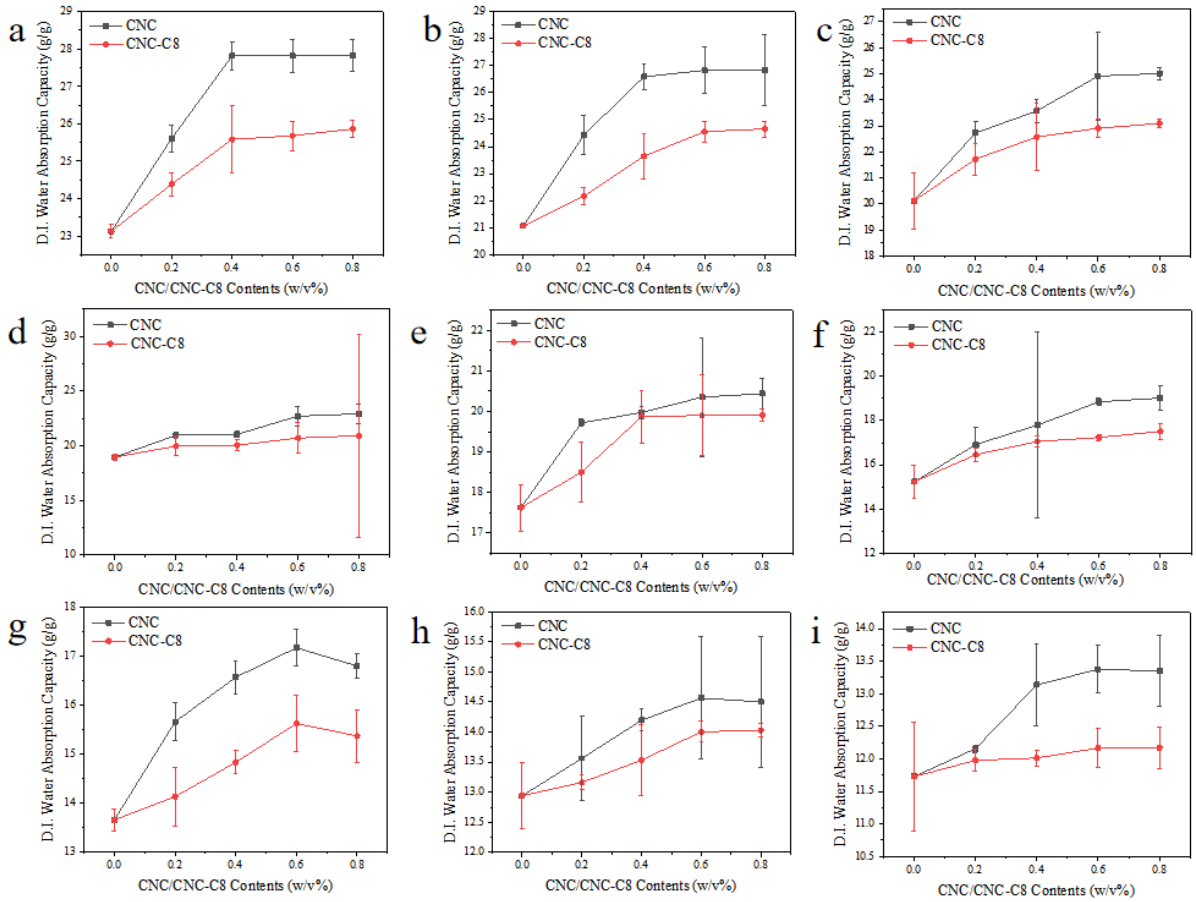

Figure 5. 23 Water absorption capacity of the DPC hydrogels as functions of the dosages of CNC and CNC-C8 at constant dosage of DMAPMA-C18 (a)0.0225 w/v % , (b)0.03375 w/v %, (c)0.045 w/v %, (d) 0.05625 w/v % , (e)0.0675 w/v %, (f)0.07875 w/v %, (g)0.09 w/v %, (h)0.10125 w/v % and (i) 0.1125 w/v %.

Figure 5.24 shows that, with the increasing content of DMAPMA-C18, the water absorption capacity of the hydrogel decreased, further confirming the negative effect of hydrophobic DMAPMA-C18 on the water absorption capacity of hydrogel.

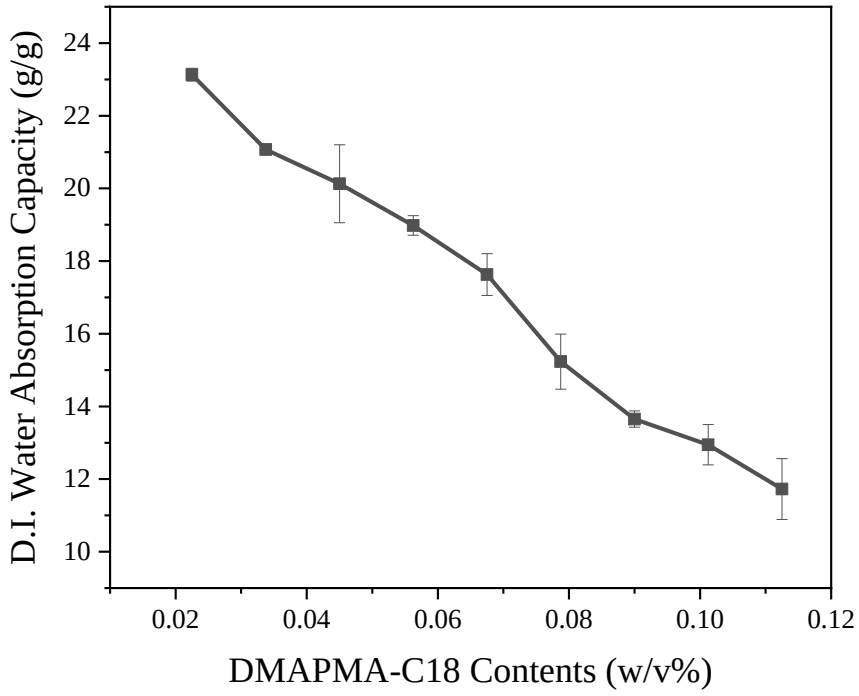

Figure 5. 24 Water absorption capacity of DPC hydrogels as a function of the dosage of DMAPMA-C18.

Then the CNC DPC hydrogel with 0.8 w/v % CNC and 1 DMAPMA-C18was used to do recycle water absorption tests. The water absorption process cycles were repeated for five times. The results were shown in **Figure 5.25**. It could be seen that the water absorption capacities for each water absorption cycle were similar with that of each other. With the number of cycles increased, the water absorption slightly decreased but not with obvious differences. The DPC hydrogel could be reused for at least five times for water absorption recycling at similar performances, which could be efficiently to help for saving the cost of DPC hydrogels.

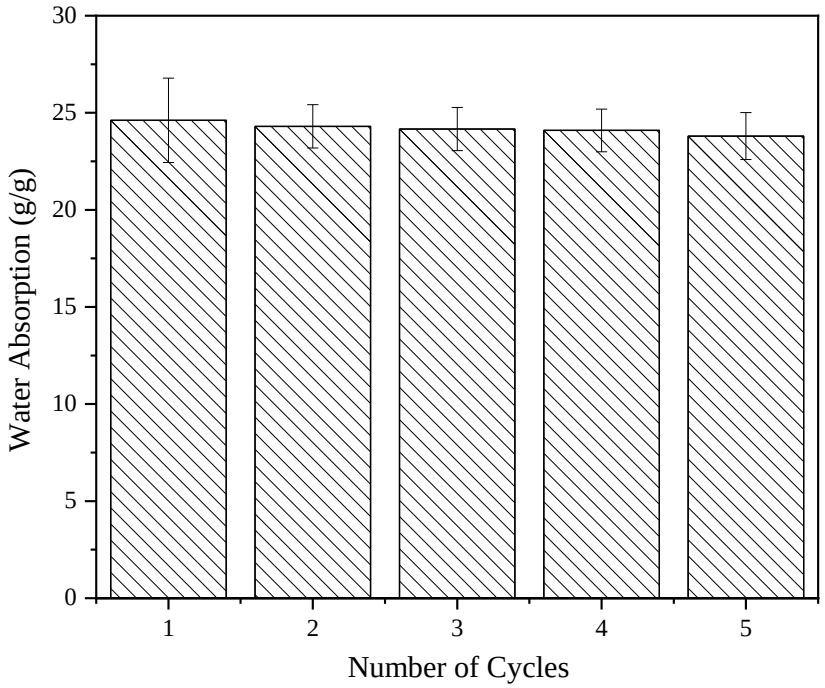

Figure 5. 25 Water absorption capacities cycling tests.

5.3.2 Olive Oil Absorption

The data of CNC DPC hydrogel olive oil absorption capacity (g/g) at different CNC contents and DMAPMA-C18 contents are shown in **Table 5.9.** The optimal olive oil absorption was0.5085±0.0055 g/g at 5 DMAPMA-C18 contents with no CNC additions. Generally, with the increase of DMAPMA-C18 contents, the olive oil absorption capacities increased. However, the increase of CNC addition would have negative effects on olive oil absorption capacities. The results were opposite to that of water swelling tests. This is because hydrophobic olive oil has low polarity and the hydrophobic DMAPMA-C18 with low polarity would have stronger interactions between olive molecules as compared with hydrophilic CNC or CNC-C8.

Table 5. 9 DPC hydrogel olive oil absorption capacity (g/g) at different CNC contents (w/v %) and DMAPMA-C18 contents (w/v %)

Olive Oil Absorption Capacity (g/g) / DMAPMA-C18 Content (w/v %)	CNC Content (w/v %)				
	0	0.2	0.4	0.6	0.8
0.0225	0.3236	0.2358	0.1792	0.1456	0.1256
0.03375	0.3378	0.3096	0.234	0.1875	0.1633
0.045	0.3407	0.3129	0.2464	0.2389	0.2098
0.05625	0.3643	0.3243	0.3059	0.2419	0.2173
0.0675	0.394	0.339	0.3195	0.2718	0.2399
0.07875	0.3977	0.3362	0.3228	0.292	0.2603
0.09	0.4179	0.3507	0.3323	0.2938	0.2727
0.10125	0.4383	0.3734	0.3453	0.3149	0.2729
0.1125	**0.5085**	0.4809	0.3822	0.3641	0.3257

Similarly, the data of DPC hydrogel olive oil absorption capacity (g/g) at different CNC-C8 contents and DMAPMA-C18 contents are shown in **Table 5.10**.Same to the olive oil absorption results for CNC DPC hydrogels, the optimal olive oil absorption for CNC-C8 DPC hydrogels was also 0.5085 g/g at the one with no CNC-C8 additions and 5 DMAPMA-C18 contents.

Table 5. 10 DPC hydrogel olive oil absorption capacity (g/g) at different CNC-C8 contents (w/v %) and DMAPMA-C18 contents (w/v %)

Olive Oil Absorption Capacity (g/g) / DMAPMA-C18 Content (w/v %)	CNC-C8 Content (w/v %)				
	0	0.2	0.4	0.6	0.8
0.0225	0.3236	0.3067	0.2733	0.2309	0.219
0.03375	0.3378	0.3134	0.3038	0.2775	0.2513
0.045	0.3407	0.3205	0.3063	0.2847	0.2508
0.05625	0.3643	0.3602	0.3254	0.3094	0.2897
0.0675	0.394	0.3795	0.3527	0.3083	0.2935
0.07875	0.3977	0.3762	0.3665	0.3306	0.3198
0.09	0.4179	0.4022	0.405	0.3859	0.3506
0.10125	0.4383	0.4314	0.4097	0.389	0.3699
0.1125	**0.5085**	0.4992	0.4589	0.3957	0.3721

As shown in **Figure 5.26**, the optimal olive oil absorption capacity for physically cross-linked hydrogels was 0.5085±0.0055 g/g at 5DMAPMA-C18 (0.1125 w/v %) contents without CNC or CNC-C8.

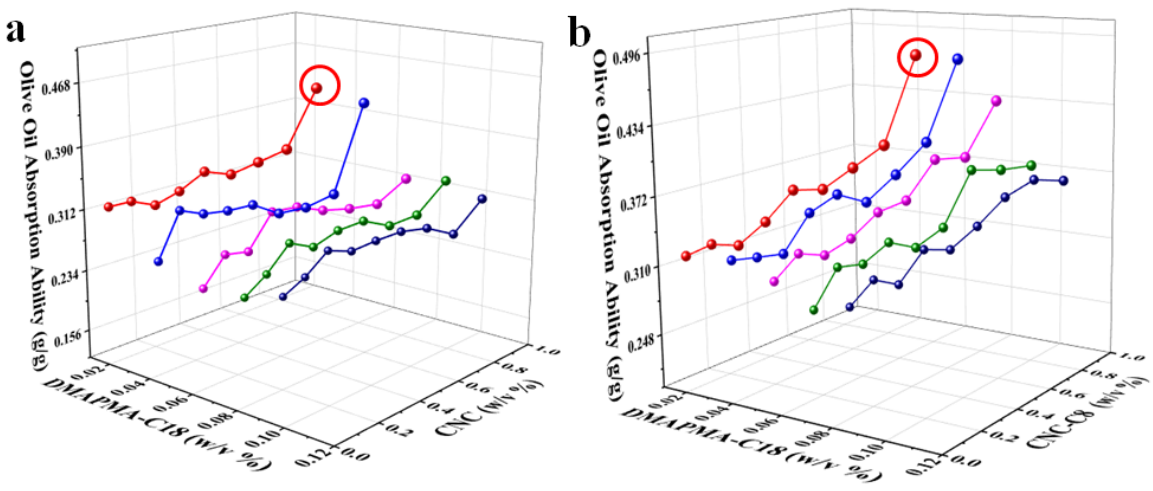

Figure 5. 26 Olive oil absorption capacity of DPC hydrogel as a function of the content of (a) CNC or (b) CNC-C8 and DMAPMA-C18. The points in red circles are the optimal olive oil absorption capacity values.

Figure 5.27 showed that the olive oil absorption capacity of CNC DPC hydrogels and CNC-C8 DPC hydrogels as functions of the dosages of CNC and CNC-C8 at each DMAPMA-C18 contents. Generally, for each DMAPMA-C18 contents and CNC or CNC-C8 contents combination, CNC-C8 DPC hydrogels would show better performances in olive oil absorptions than CNC DPC hydrogels. This is mainly because of the C8 alkane chains are hydrophobic, which could play a role in olive oil absorption process. But as CNC-C8 was only of 5% level of hydrophobic modifications on CNC, it is still mainly hydrophilic. The addition of CNC-C8 would play a negative role in olive oil absorption in general, which would be weaker than the negative effects of CNC on olive oil swelling tests.

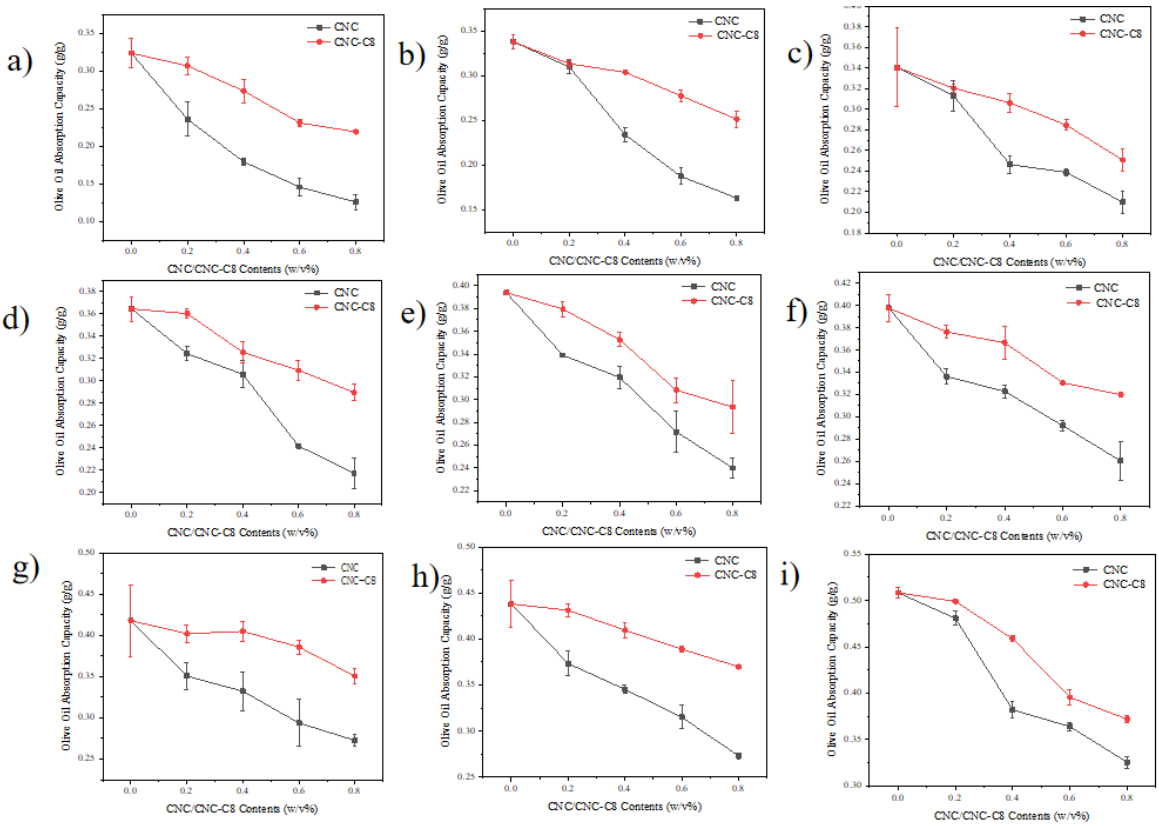

Figure 5. 27 Olive oil absorption capacity of the DPC hydrogels as a function of the dosages of CNC and CNC-C8 at each DMAPMA-C18 contents of (a) 0.0225 w/v % , (b) 0.03375 w/v %, (c) 0.045 w/v %, (d) 0.05625 w/v % , (e) 0.0675 w/v %, (f) 0.07875 w/v %, (g) 0.09 w/v %, (h) 0.10125 w/v % and (i) 0.1125 w/v % separately.

Figure 5.28 showed the increase of olive oil absorption capacities with the addition of DMAPMA-C18 contents. The C18 alkane chains on DMAPMA-C18 monomers are of hydrophobic properties, which could mainly have a positive effect on olive oil absorption tests.

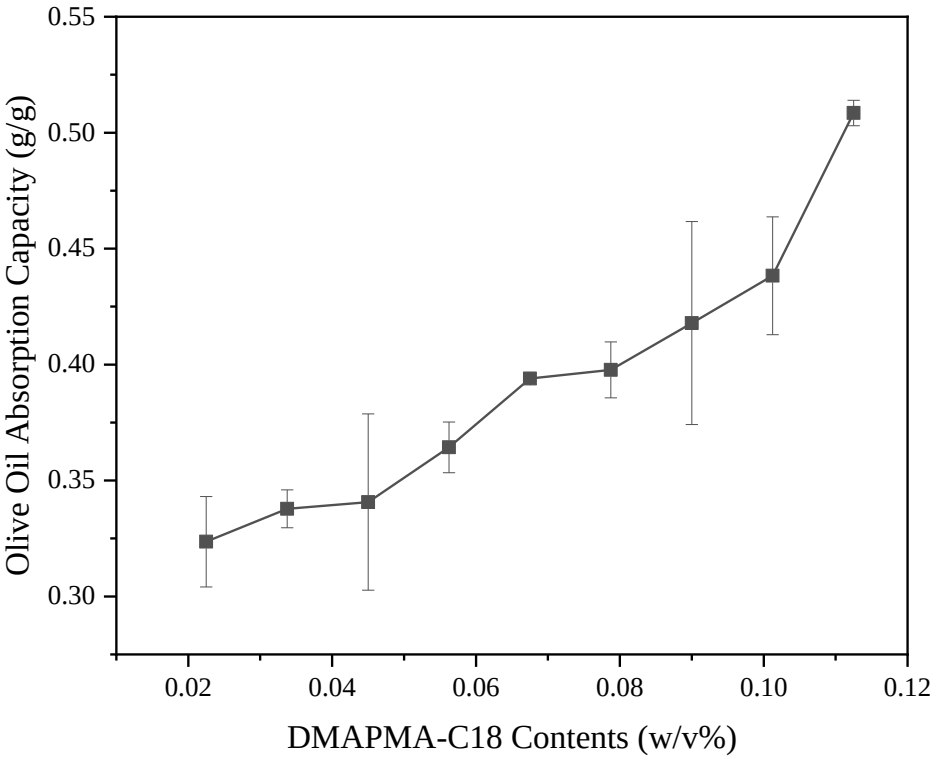

Figure 5. 28 Olive oil absorption capacity of DPC hydrogel with different contents of DMAPMA-C18.

5.3.3 Chloroform Absorption

At the beginning of chloroform absorption test, the wet and freeze-dried CNC DPC hydrogels at 1DMAPMA-C18 and different CNC contents of 0.0 w/v%, 0.14 w/v %, 0.2 w/v %, 0.4 w/v % and 0.6 w/v % were selected. The chloroform absorption results after ten minutes were shown in **Figure 5.29**. It could be observed that the chloroform absorption capacities for freeze-dried CNC DPC hydrogels were generally higher than wet DPC hydrogels at each CNC contents. The freeze-dried CNC DPC hydrogels showed an increase in chloroform absorption capacities with adding of CNC contents while wet

hydrogels did not show an obvious increase.

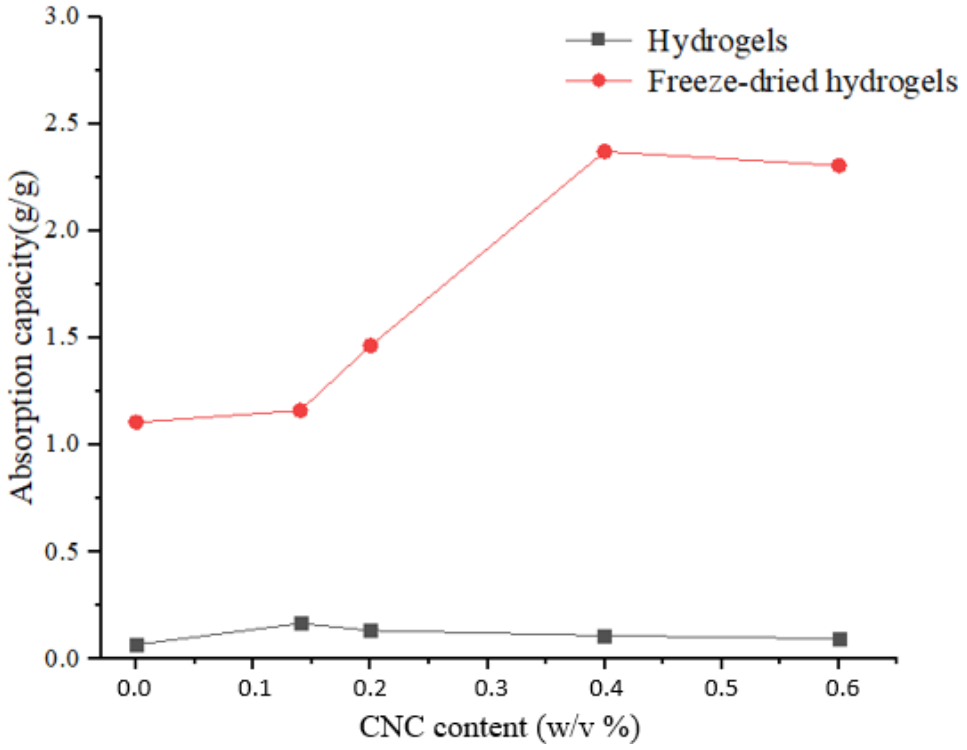

Figure 5. 29 Chloroform absorption capacities for wet and freeze-dried CNC DPC hydrogels at 1 DMAPMA-C18after ten minutes.

As shown in **Figure 5.30**, one block of physically cross-linked hydrogel was used to measure the increase of chloroform absorption capacities with the adding of time. It could be observed that with the increase of time in 180 minutes, the chloroform capacities got increased steadily. But as the shape of the hydrogel sample got changed after 80 minutes, the time period for chloroform absorption tests was selected as 80 minutes. Although the weight went on increasing after that, the changes of hydrogel shapes would make it hard to take the complete sample out of chloroform. As there were a great amount of chain

structures in hydrogels, the samples would be prone to be dissolved into chloroform.

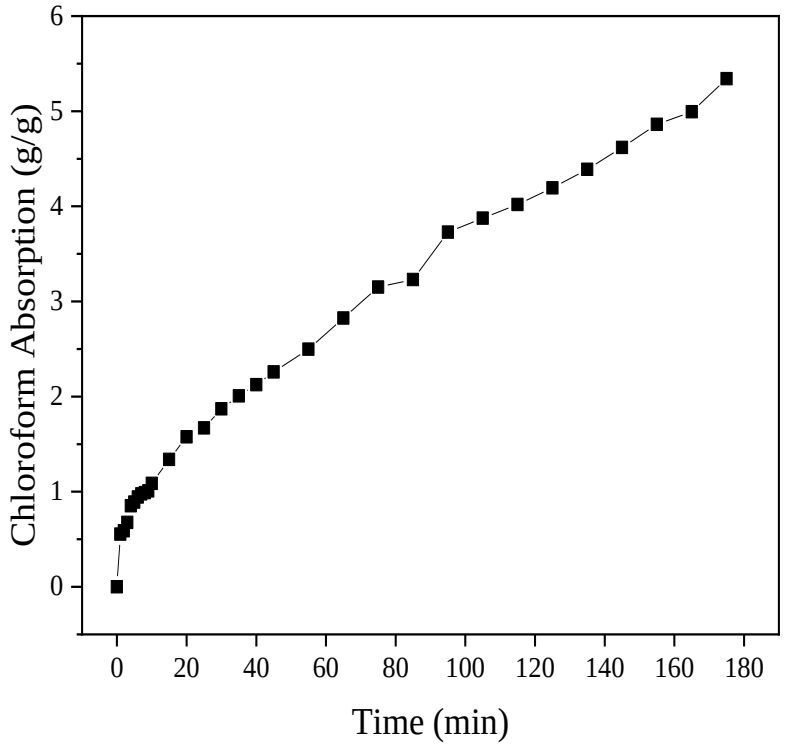

Figure 5. 30 The increase of chloroform absorption capacities for CNC DPC hydrogel with the increase of time.

The chloroform absorption experiment results for CNC DPC hydrogels and CNC-C8 DPC hydrogels were shown in **Table 5.11** and **Table 5.12**, respectively. However, the trend of chloroform absorption is not as simple as the water absorption and olive oil absorption tests. With the increase of CNC or CNC-C8 contents and DMAPMA-C18 contents, the chloroform absorption capacities get improved at first and then decreased after the optimal contents combination.

Table 5. 11 DPC hydrogel Chloroform Absorption Capacity (g/g) at different CNC Contents (w/v %) and DMAPMA-C18 contents (w/v %)

Chloroform Absorption Capacity (g/g) / DMAPMA-C18 Content (w/v %)	CNC Content (w/v %)				
	0	0.2	0.4	0.6	0.8
0.0225	1.5554	1.777	4.2719	4.8728	4.3124
0.03375	3.0308	3.3609	4.6044	5.1545	5.0133
0.045	4.3588	4.6828	**5.1699**	4.3141	4.2973
0.05625	1.6914	1.8532	2.6723	3.0319	2.9014
0.0675	1.6694	1.7245	1.7574	2.6245	2.5092
0.07875	1.6272	1.5038	1.8782	2.3142	2.1112
0.09	1.581	1.7756	2.0363	2.3308	2.0625
0.10125	1.5313	1.5925	1.84	1.1562	1.3064
0.1125	1.5482	1.513	1.2972	1.2316	1.0235

The optimal chloroform absorption for CNC DPC hydrogels was5.1699±0.1585 g/g with 0.4 w/v % CNC content and 2 DMAPMA-C18 contents while forCNC-C8 DPC hydrogel is 2.6403±0.1099 g/g with 0.2 w/v % CNC-C8 content and 1.5 DMAPMA-C18 content. In general, CNC DPC hydrogels would have better performances in chloroform absorption than CNC-C8 DPC hydrogels.

Table 5. 12 DPC hydrogel Chloroform Absorption Capacity (g/g) at different CNC-C8 contents (w/v %) and DMAPMA-C18 contents (w/v %)

Chloroform Absorption Capacity (g/g) DMAPMA-C18 Content (w/v %)	CNC-C8Content (w/v %)				
	0	0.2	0.4	0.6	0.8
0.0225	1.5554	1.7666	1.7624	1.6058	1.5877
0.03375	2.0308	**2.6403**	2.4858	2.2363	2.1902
0.045	2.3588	2.3478	2.1861	1.941	1.8826
0.05625	1.6914	1.778	1.7789	1.7416	1.6332
0.0675	1.6694	1.5084	1.3103	1.2958	1.1927
0.07875	1.6272	1.6535	1.3647	1.3055	1.1198
0.09	1.581	1.5792	1.3157	1.3579	1.1936
0.10125	2.1313	1.6703	1.3329	1.2895	1.2302
0.1125	1.5482	1.3915	1.3043	1.2229	1.1926

The results from **Figure 5.31**showed the three dimensional graphs of chloroform absorptions of CNC DPC hydrogels and CNC-C8 DPC hydrogels at different DMAPMA-C18 contents and CNC or CNC-C8 contents. The optimal values were circles in the graphs.

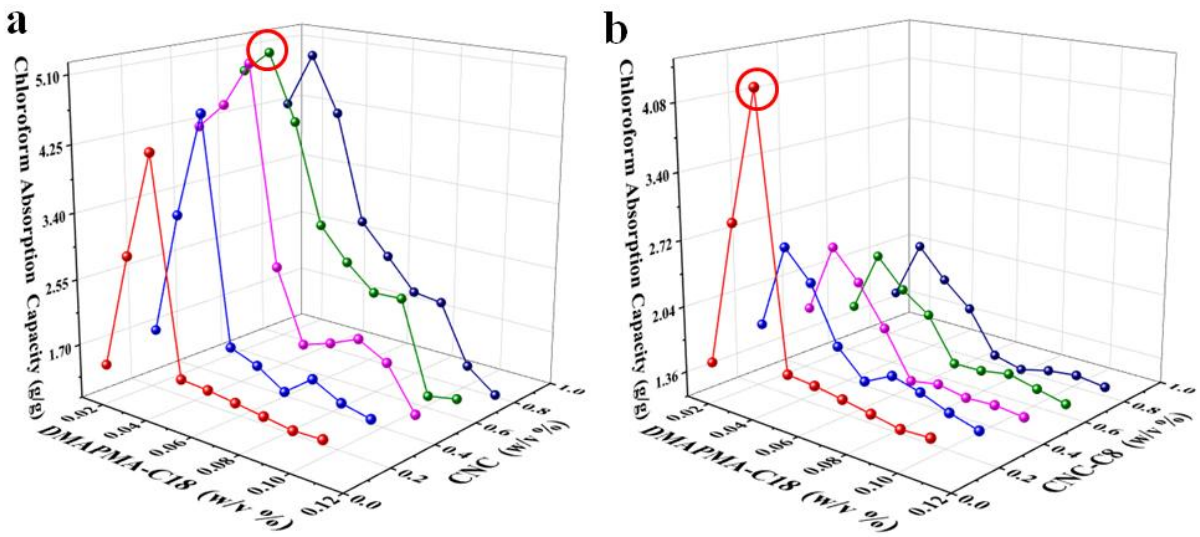

Figure 5. 31 Chloroform absorption capacity of DPC hydrogel as a function of the dosage of (a) CNC or (b) CNC-C8 and DMAPMA-C18. The points in red circles are the optimal chloroform absorption capacity values.

Figure 5.32 shows chloroform absorption capacity of the DPC hydrogels as a function of the dosages of CNC and CNC-C8 at each DMAPMA-C18 contents. The chloroform absorption capacities of CNC-C8 DPC hydrogels were generally lower than that of CNC DPC hydrogels at the same content of DMAPMA-C18 and CNC or CNC-C8.As chloroform could dissolve freeze-dried hydrogel samples, the time period was only selected as at the time the shape of hydrogels could keep the shape and were nor broken. Therefore the data obtained was just like a reference data but not the optimal chloroform absorption capacities for saturation conditions.

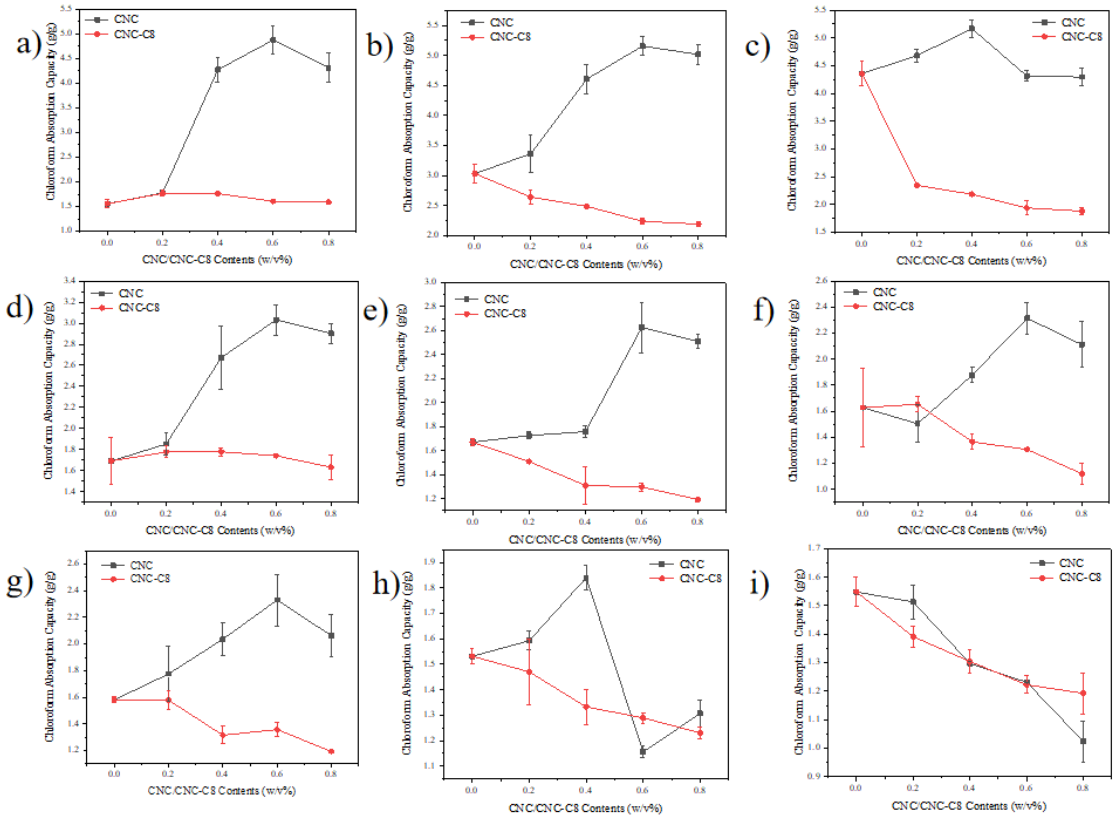

Figure 5. 32 Chloroform absorption capacity of the DPC hydrogels as a function of the dosages of CNC and CNC-C8 at each DMAPMA-C18 contents of (a)0.0225 w/v % , (b)0.03375 w/v %, (c)0.045 w/v %, (d) 0.05625 w/v % , (e)0.0675 w/v %, (f)0.07875 w/v %, (g)0.09 w/v %, (h)0.10125 w/v % and (i) 0.1125 w/v %.

If not consider CNC and CNC-C8 addition, we could see from **Figure 5.33** that 2 DMAPMA-C18 (0.045 w/v %) contents would be the optimal one with the chloroform absorption capacity of 4.3588±0.2182 g/g. The chloroform absorption capacities were increased with the increase of DMAPMA-C18 contents before 2 DMAPMA-C18, and decreased after that.

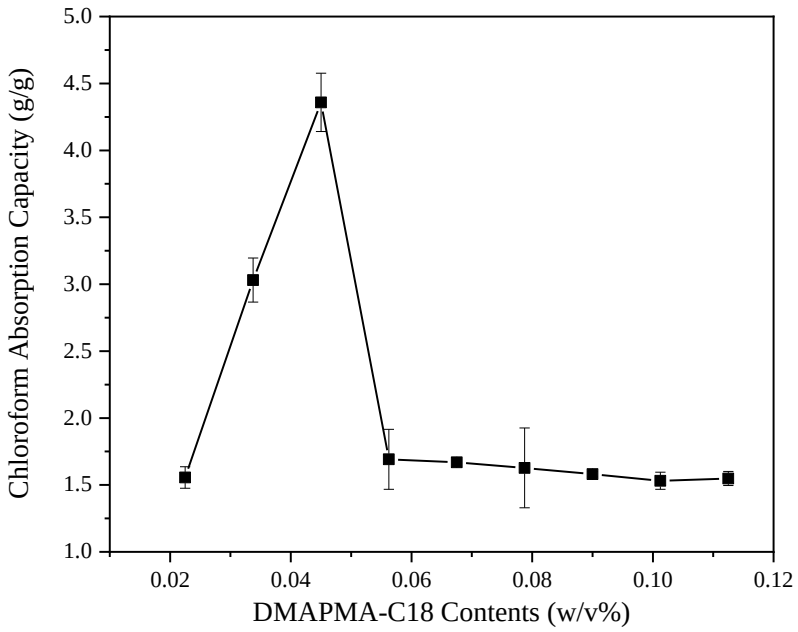

Figure 5. 33 Chloroform capacity of the DPC hydrogels as a function of the dosage of DMAPMA-C18.

5.4 Two-way ANOVA Analysis

5.4.1 Test of the Effects of CNC/CNC-C8 and DMAPMA-C18 Contents on Stress

The purpose of this section is statistically analyzing the effects of CNC/CNC-C8 contents andDMAPMA-C18 contents on Stress. There are five levels for the factor of CNC/CNC-C8 contents (0 w/v %, 0.2 w/v %, 0.4 w/v %, 0.6 w/v % and 0.8 w/v %) and 9 levels forDMAPMA-C18 contents (0.0225w/v %, 0.03375w/v %, 0.045w/v %, 0.05625w/v %, 0.0675w/v %, 0.07875w/v %, 0.09w/v %, 0.10125w/v % and 0.1125w/v %) as shown in **Table 5.13**. The parameters of reaction conditions were changed in turn to determine the optimum values for the experimental parameters of

CNC, CNC-C8 and DMAPMA-C18 contents. The Two-way ANOVA at 0.05 level of confidence is used to prove there is a difference in stress values due to CNC contents and DMAPMA-C18 contents with Minitab® 19.

Table 5. 13 CNC DPC hydrogels Minitab® 19 factor information for stress

Factor	Levels	Values
DMAPMA-C18Contents (w/v %)	9	0.02250, 0.03375, 0.04500, 0.05625, 0.06750, 0.07875,0.09000, 0.10125, 0.11250
CNC Contents (w/v %)	5	0.0, 0.2, 0.4, 0.6, 0.8

Table 5. 14 CNC DPC hydrogels Minitab® 19 Two-way ANOVA results for stress

Source	DF	Adj SS	Adj MS	F-Value	P-Value
Model	44	298652	6787.5	46.34	0.000
Linear	12	266389	22199.1	151.56	0.000
DMAPMA-C18 Contents (w/v %)	8	225081	28135.2	192.08	**0.000**
CNC Contents (w/v %)	4	41308	10327.0	70.50	**0.000**
2-Way Interactions	32	32262	1008.2	6.88	**0.000**
DMAPMA-C18 Contents (w/v %)*CNC Contents (w/v %)	32	32262	1008.2	6.88	**0.000**
Error	90	13183	146.5		
Total	134	311834			

From the Minitab® 19 Two-way ANOVA results outputs in **Table 5.14** we could see that the P-value of DMAPMA-C18 Contents (w/v %) (0.000) and CNC Contents (w/v %) (0.000) are both less than the significance level of 0.05. CNC contents and DMAPMA-C18 contents both have obvious effects on Stress values. The P-value of 2-Way Interactions (0.000) and DMAPMA-C18 Contents (w/v %)*CNC Contents (w/v %) (0.000) are both less than the significance level of 0.05 as well. It turned out that there is a significant interaction between CNC contents and DMAPMA-C18 contents on stress values.

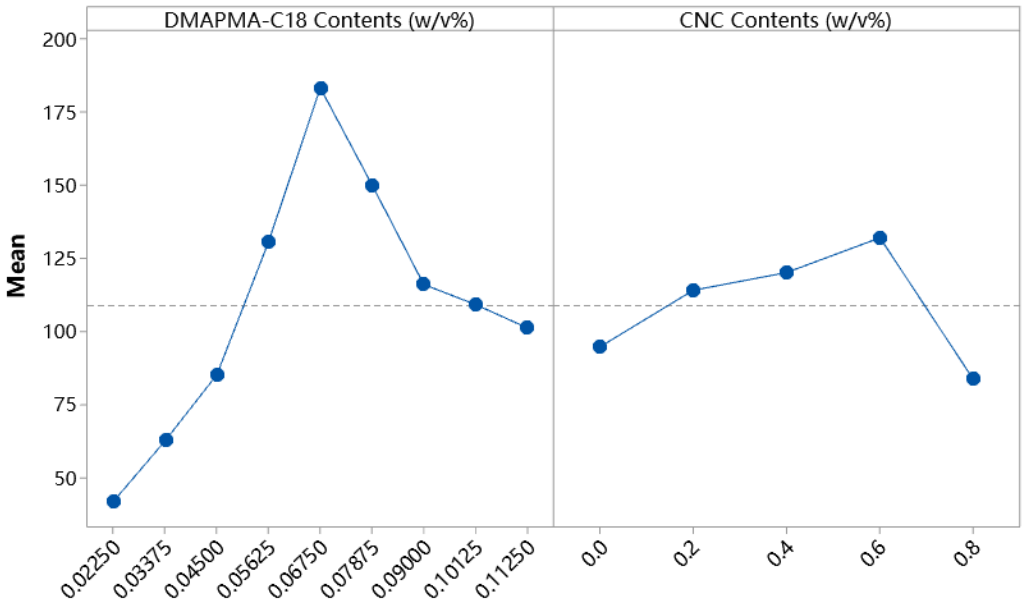

Figure 5. 34 CNC DPC hydrogels Minitab® 19 main effects plots for stress.

From the main effects plots for stress in **Figure 5.34** we could see that the CNC contents and DMAPMA-C18 contents both have positive effects on stress at low contents while have negative effects at relatively high content values. In addition, the effect of

DMAPMA-C18 contents is more obvious than that of CNC contents in general. The main effects plot shows that 0.06750 w/v % of DMAPMA-C18 content and 0.6 w/v % of CNC content would help to obtain optimal stress values for CNC DPC hydrogels.

Assume DMAPMA-C18 content (w/v %) is X_1, CNC content (w/v %) is X_2. The regression formula calculated by Minitab® 19is stress (kPa) = 45.3 + 955 X_1 + 44.4 X_2 - 689 X_1*X_2. The formula could be used to predict the stress values with other DMAPMA-C18 contents and CNC contents that were not shown in this study.

As for CNC-C8 DPC hydrogels, there are similar procedures as that of CNC DPC hydrogels to check the effects of CNC-C8 contents and DMAPMA-C18 contents on stress values. The Minitab® 19 factor information outputs are shown below in **Table 5.15.**

Table 5. 15 CNC-C8 DPC hydrogelsMinitab® 19 factor information for stress

Factor	Levels	Values
DMAPMA-C18 Contents (w/v %)	9	0.02250, 0.03375, 0.04500, 0.05625, 0.06750, 0.07875, 0.09000, 0.10125, 0.11250
CNC-C8 Contents (w/v %)	5	0.0, 0.2, 0.4, 0.6, 0.8

From the Minitab® 19 Two-way ANOVA results outputs in **Table 5.16** we could see that the P-value of DMAPMA-C18 Contents (w/v %) (0.000) and CNC-C8 Contents (w/v %) (0.000) are both less than the significance level of 0.05. CNC-C8 contents and DMAPMA-C18 contents both have obvious effects on Stress values separately. The

P-value of 2-Way Interactions (0.000) and DMAPMA-C18 Contents (w/v %)*CNC-C8 Contents (w/v %) (0.000) are both less than the significance level of 0.05 as well. It turned out that there is a significant interaction between CNC-C8 contents and DMAPMA-C18 contents on stress values.

Table 5. 16 CNC-C8 DPC hydrogels Minitab® 19 Two-way ANOVA results for stress

Source	DF	Adj SS	Adj MS	F-Value	P-Value
Model	44	574402	13054.6	233.19	0.000
Linear	12	509061	42421.8	757.78	0.000
DMAPMA-C18 Contents (w/v %)	8	390578	48822.2	872.11	**0.000**
CNC-C8 Contents (w/v %)	4	118484	29620.9	529.12	**0.000**
2-Way Interactions	32	65340	2041.9	36.47	**0.000**
DMAPMA-C18 Contents (w/v %)*CNC-C8 Contents (w/v %)	32	65340	2041.9	36.47	**0.000**
Error	90	5038	56.0		
Total	134	579440			

From the main effects plot for stress in **Figure 5.35** we could see that the CNC-C8 contents and DMAPMA-C18 contents both have positive effects on stress at low contents while have negative effects at relatively high content values. In addition, the effect of DMAPMA-C18 contents is more obvious than that of CNC contents in general. The main

effects plot shows that 0.06750 w/v % of DMAPMA-C18 content and 0.4 w/v % of CNC-C8 content would help to obtain optimal stress values for DPC hydrogels.

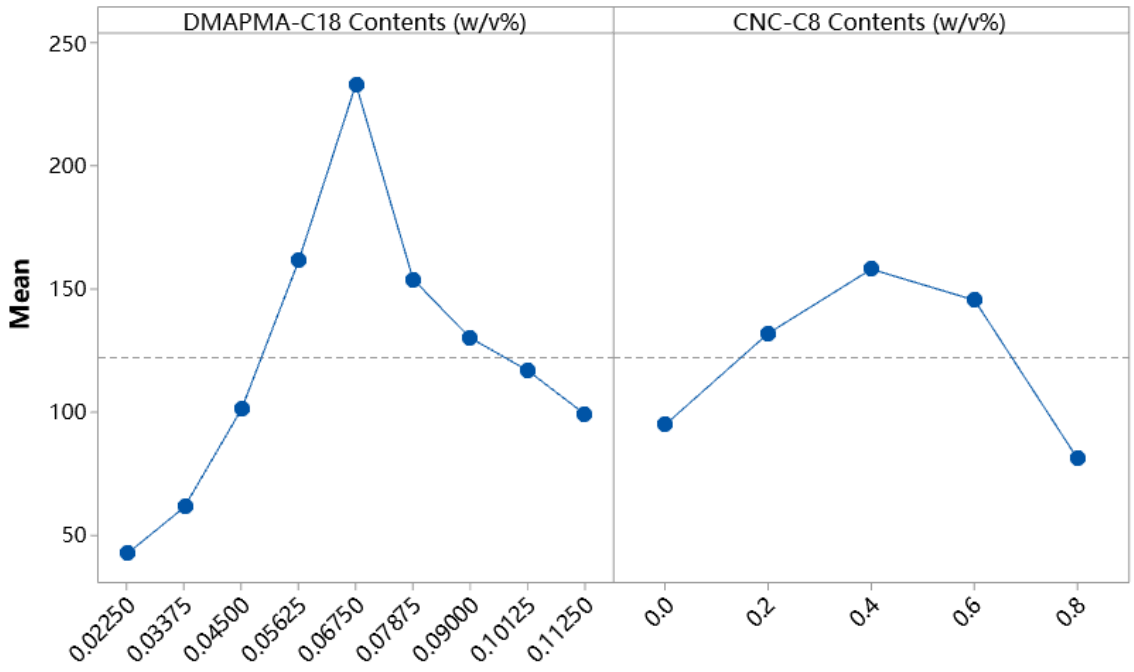

Figure 5. 35 CNC-C8 DPC hydrogels Minitab® 19 main effects plots for stress.

Assume DMAPMA-C18 content (w/v %) is X_1, CNC-C8 content (w/v %) is X_2. The regression formula calculated by Minitab® 19 is stress (kPa) = 66.5 + 867 X_1 + 28.2 X_2 - 522 X_1*X_2.

5.4.2 Test of the Effects of CNC/CNC-C8 and DMAPMA-C18 Contents on Strain

The purpose of this section is statistically analyzing the effects of CNC/CNC-C8 contents andDMAPMA-C18 contents on Elongations. There are five levels for the factor of CNC/CNC-C8 contents (0 w/v %, 0.2 w/v %, 0.4 w/v %, 0.6 w/v % and 0.8 w/v %) and 9

levels forDMAPMA-C18 contents (0.0225w/v %, 0.03375w/v %, 0.045w/v %, 0.05625w/v %, 0.0675w/v %, 0.07875w/v %, 0.09w/v %, 0.10125w/v % and 0.1125w/v %) as shown in **Table 5.17**.

Table 5. 17 CNC DPC hydrogels Minitab® 19 factor information for strain

Factor	Levels	Values
DMAPMA-C18 Contents (w/v %)	9	0.02250, 0.03375, 0.04500, 0.05625, 0.06750, 0.07875, 0.09000, 0.10125, 0.11250
CNC Contents (w/v %)	5	0.0, 0.2, 0.4, 0.6, 0.8

Table 5. 18 CNC DPC hydrogels Minitab® 19 Two-way ANOVA results for strain

Source	DF	Adj SS	Adj MS	F-Value	P-Value
Model	44	133350771	3030699	23.93	0.000
Linear	12	119193656	9932805	78.42	0.000
DMAPMA-C18 Contents (w/v %)	8	95629968	11953746	94.38	**0.000**
CNC Contents (w/v %)	4	23563689	5890922	46.51	**0.000**
2-Way Interactions	32	14157115	442410	3.49	**0.000**
DMAPMA-C18 Contents (w/v %)*CNC Contents (w/v %)	32	14157115	442410	3.49	**0.000**
Error	90	11398940	126655		
Total	134	144749711			

The parameters of reaction conditions were changed in turn to determine the optimum values for the experimental parameters of CNC, CNC-C8 and DMAPMA-C18 contents. The Two-way ANOVA at 0.05 level of confidence is used to prove there is a difference in elongation values due to CNC contents and DMAPMA-C18 contents with Minitab® 19.

From the Minitab® 19 Two-way ANOVA results outputs in **Table 5.18** we could see that the P-value of DMAPMA-C18 Contents (w/v %) (0.000) and CNC Contents (w/v %) (0.000) are both less than the significance level of 0.05. CNC contents and DMAPMA-C18 contents both have obvious effects on Elongation values separately. The P-value of Two-way Interactions (0.000) and DMAPMA-C18 Contents (w/v %)*CNC Contents (w/v %) (0.000) are both less than the significance level of 0.05 as well. It turned out that there is a significant interaction between CNC contents and DMAPMA-C18 contents on Elongation values.

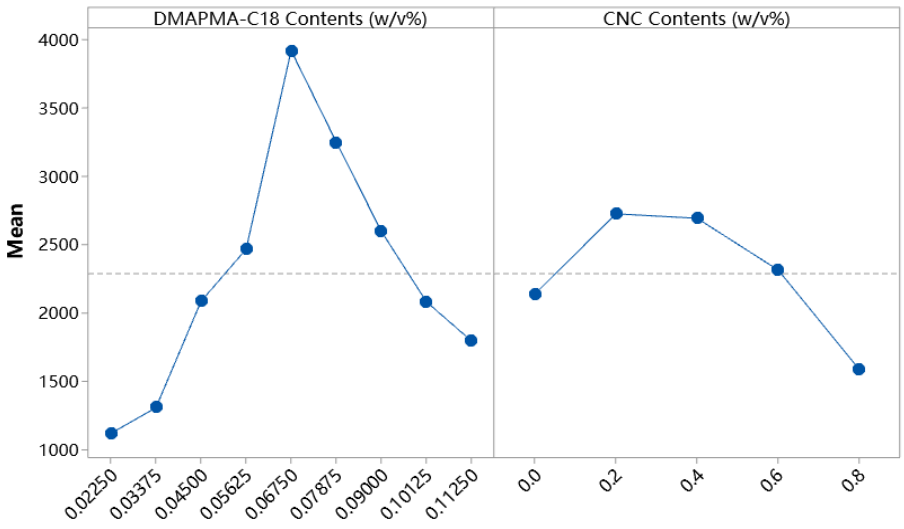

Figure 5. 36CNC DPC hydrogelsMinitab® 19 main effects plots for strain.

From the main effects plot in **Figure 5.36** for elongations we could see that the CNC contents and DMAPMA-C18 contents both have positive effects on elongations at low contents while have negative effects at relatively high content values. In addition, the effect of DMAPMA-C18 contents is more obvious than that of CNC contents in general. The main effects plot shows that 0.06750 w/v % of DMAPMA-C18 content and 0.2 w/v % of CNC content would help to obtain optimal elongation values for DPC hydrogels.

Assume DMAPMA-C18 content (w/v %) is X_1, CNC content (w/v %) is X_2. The regression formula calculated by Minitab® 19 is elongation (%) = $1596 + 14770\ X_1 + 24\ X_2 - 11599\ X_1*X_2$.

As for CNC-C8 DPC hydrogels, there are similar procedures as that of CNC DPC hydrogels to check the effects of CNC-C8 contents and DMAPMA-C18 contents on elongation values. The Minitab® 19 factor information outputs are shown below in **Table 5.19.**

Table 5. 19 CNC-C8 DPC hydrogels Minitab® 19 factor information for strain

Factor	Levels	Values
DMAPMA-C18 Contents (w/v %)	9	0.02250, 0.03375, 0.04500, 0.05625, 0.06750, 0.07875,0.09000, 0.10125, 0.11250
CNC-C8 Contents (w/v %)	5	0.0, 0.2, 0.4, 0.6, 0.8

From the Minitab® 19 Two-way ANOVA results outputs in **Table 5.20** we could see that the P-value of DMAPMA-C18 Contents (w/v %) (0.000) and CNC-C8 Contents (w/v %) (0.000) are both less than the significance level of 0.05. CNC-C8 contents and DMAPMA-C18 contents both have obvious effects on elongation values separately. The P-value of 2-Way Interactions (0.000) and DMAPMA-C18 Contents (w/v %)*CNC-C8 Contents (w/v %) (0.000) are both less than the significance level of 0.05 as well. It turned out that there is a significant interaction between CNC-C8 contents and DMAPMA-C18 contents on Elongation values.

Table 5. 20 CNC-C8 DPC hydrogels Minitab® 19 Two-way ANOVA results for strain

Source	DF	Adj SS	Adj MS	F-Value	P-Value
Model	44	88439089	2009979	32.76	0.000
Linear	12	78587188	6548932	106.73	0.000
DMAPMA-C18 Contents (w/v %)	8	64271218	8033902	130.93	**0.000**
CNC-C8 Contents (w/v %)	4	14315969	3578992	58.33	**0.000**
2-Way Interactions	32	9851901	307872	5.02	**0.000**
DMAPMA-C18 Contents (w/v %)*CNC-C8 Contents (w/v %)	32	9851901	307872	5.02	**0.000**
Error	90	5522485	61361		
Total	134	93961575			

From the main effects plot in **Figure 5.37** for elongations we could see that the CNC-C8 contents and DMAPMA-C18 contents both have positive effects on elongations at low contents while have negative effects at relatively high content values. In addition, the effect of DMAPMA-C18 contents is more obvious than that of CNC contents in general. The main effects plot shows that 0.06750 w/v % of DMAPMA-C18 content and 0.4 w/v % of CNC-C8 content would help to obtain optimal elongation values for DPC hydrogels.

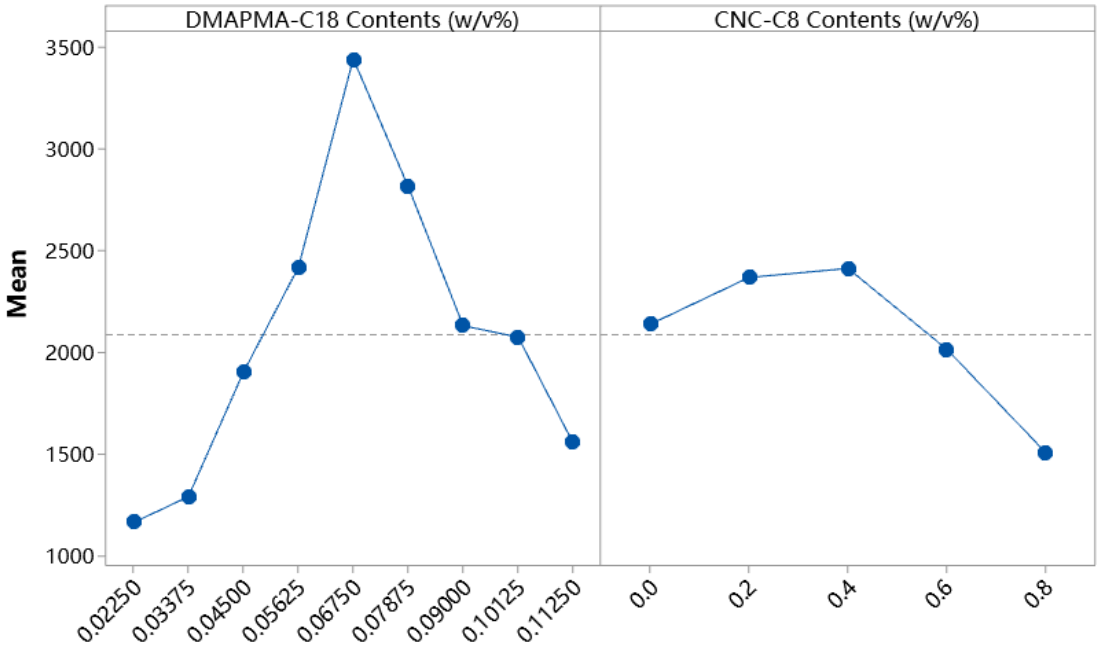

Figure 5. 37 CNC-C8 DPC hydrogels Minitab® 19 main effects plots for strain

Assume DMAPMA-C18 content (w/v %) is X_1, CNC-C8 content (w/v %) is X_2. The regression formula calculated by Minitab® 19 is elongation (%) = 1625 + 11634 X_1 - 40 X_2 - 11388 X_1*X_2.

5.4.3 Test of the Effects of CNC/CNC-C8 and DMAPMA-C18 Contents on Water Absorption

The purpose of this section is statistically analyzing the effects of CNC/CNC-C8 contents andDMAPMA-C18 contents on water absorption capacities. There are five levels for the factor of CNC/CNC-C8 contents (0 w/v %, 0.2 w/v %, 0.4 w/v %, 0.6 w/v % and 0.8 w/v %) and 9 levels forDMAPMA-C18 contents (0.0225w/v %, 0.03375w/v %, 0.045w/v %, 0.05625w/v %, 0.0675w/v %, 0.07875w/v %, 0.09w/v %, 0.10125w/v % and 0.1125w/v %) as shown in **Table 5.21**. The parameters of reaction conditions were changed in turn to determine the optimum values for the experimental parameters of CNC, CNC-C8 and DMAPMA-C18 contents. The Two-way ANOVA at 0.05 level of confidence is used to prove there is a difference in water absorption capacity values due to CNC contents and DMAPMA-C18 contents with Minitab 19.

Table 5. 21 CNC DPC hydrogels Minitab® 19 factor information for water absorption

Factor	Levels	Values
DMAPMA-C18 Contents (w/v %)	9	0.02250, 0.03375, 0.04500, 0.05625, 0.06750, 0.07875, 0.09000,0.10125, 0.11250
CNC Contents (w/v %)	5	0.0, 0.2, 0.4, 0.6, 0.8

From the Minitab® 19 Two-way ANOVA results outputs in **Table 5.22** we could see that

the P-value of DMAPMA-C18 Contents (w/v %) (0.000) and CNC Contents (w/v %) (0.000) are both less than the significance level of 0.05. CNC contents and DMAPMA-C18 contents both have obvious effects on water absorption capacity values separately. The P-value of 2-Way Interactions (0.035) and DMAPMA-C18 Contents (w/v %)*CNC Contents (w/v %) (0.035) are both less than the significance level of 0.05 as well. It turned out that there is a significant interaction between CNC contents and DMAPMA-C18 contents on water absorption capacity values.

Table 5. 22 CNC DPC hydrogels Minitab® 19 Two-way ANOVA results for water absorption

Source	DF	Adj SS	Adj MS	F-Value	P-Value
Model	44	3139.31	71.348	86.40	0.000
Linear	12	3095.79	257.982	312.42	0.000
DMAPMA-C18 Contents	8	2852.53	356.566	431.81	**0.000**
CNC Contents	4	243.26	60.816	73.65	**0.000**
2-Way Interactions	32	43.52	1.360	1.65	**0.035**
DMAPMA-C18 Contents*CNC Contents	32	43.52	1.360	1.65	**0.035**
Error	90	74.32	0.826		
Total	134	3213.62			

From the main effects plots for water absorption capacities in **Figure 5.38** we could see that the CNC contents are with positive effects on water absorption capacities and DMAPMA-C18 contents havenegative effects on water absorption capacities. The main reason is that DMAPMA-C18 is hydrophobic and CNC-C8 is mainly hydrophilic. There is only 5% level of hydrophobic group C8 on CNC. The main effects plot shows that 0.02250 w/v % of DMAPMA-C18 content and 0.6 w/v % of CNC content would help to obtain optimal water absorption capacity values for DPC hydrogels. 0.6 w/v % was selected as the optimal CNC content is because that the water absorption capacity values were similar to each other for 0.6 w/v % and 0.8 w/v %. Considering to save the cost 0.6 w/v % was chosen as the ideal CNC content.

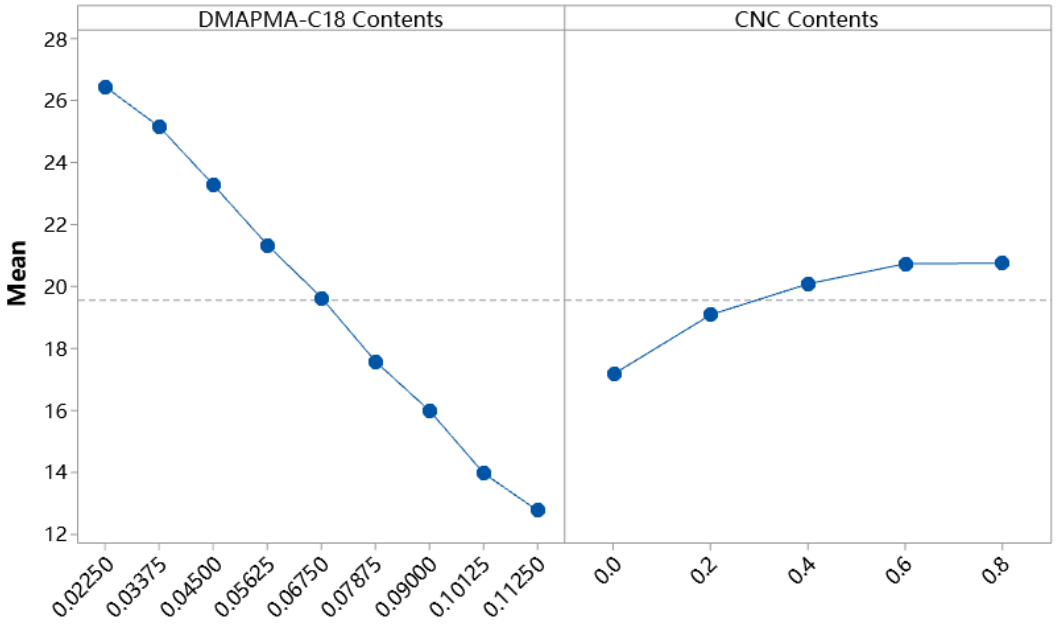

Figure 5. 38 CNC DPC hydrogels Minitab® 19 main effects plots for water absorption.

Assume DMAPMA-C18 content (w/v %) is X_1, CNC content (w/v %) is X_2. The regression formula calculated by Minitab® 19 is water absorption (g/g) = 27.145 - 138.44 X_1 + 7.722 X_2 - 49.2 X_1*X_2.

As for CNC-C8 DPC hydrogels, there are similar procedures as that of CNC DPC hydrogels to check the effects of CNC-C8 contents and DMAPMA-C18 contents on water absorption capacities. The Minitab® 19 factor information outputs are shown below in **Table 5.23**.

Table 5. 23 CNC-C8 DPC hydrogels Minitab® 19 Factor Information outputs for water absorption

Factor	Levels	Values
DMAPMA-C18 Contents (w/v %)	9	0.02250, 0.03375, 0.04500, 0.05625, 0.06750, 0.07875, 0.09000,0.10125, 0.11250
CNC-C8 Contents (w/v %)	5	0.0, 0.2, 0.4, 0.6, 0.8

From the Minitab®19 Two-way ANOVA results outputs in **Table 5.24** we could see that the P-value of DMAPMA-C18 contents (w/v %) (0.000) and CNC-C8 contents (w/v %) (0.000) are both less than the significance level of 0.05. CNC-C8 contents and DMAPMA-C18 contents both have obvious effects on water absorption capacity values separately. The P-value of 2-Way Interactions (1.000) and DMAPMA-C18 Contents

(w/v %)*CNC Contents (w/v %) (1.000) are both much more than the significance level of 0.05 as well. It turned out that there is no interaction between CNC contents and DMAPMA-C18 contents on water absorption capacity values.

Table 5. 24 CNC-C8 DPC hydrogels Minitab® 19 Two-way ANOVA results outputs for water absorption

Source	DF	Adj SS	Adj MS	F-Value	P-Value
Model	44	2562.75	58.244	26.31	0.000
Linear	12	2543.57	211.964	95.76	0.000
DMAPMA-C18 Contents	8	2457.99	307.248	138.81	**0.000**
CNC-C8 Contents	4	85.58	21.396	9.67	**0.000**
2-Way Interactions	32	19.17	0.599	0.27	**1.000**
DMAPMA-C18 Contents*CNC-C8 Contents	32	19.17	0.599	0.27	**1.000**
Error	90	199.21	2.213		
Total	134	2761.96			

From the main effects plot for water absorption capacities in **Figure 5.39**we could see that the CNC-C8 contents are with positive effects on water absorption capacities and DMAPMA-C18 contents have negative effects on water absorption capacities. The main reason is that DMAPMA-C18 is hydrophobic and CNC-C8 is mainly hydrophilic. There

is only 5% level of hydrophobic group C8 on CNC.In addition, the effect of DMAPMA-C18 contents is more obvious than that of CNC contents in general. The main effects plot shows that 0.02250 w/v % of DMAPMA-C18 content and 0.6 w/v % of CNC-C8 content would help to obtain optimal water absorption capacity values for DPC hydrogels. 0.6 w/v % was selected as the optimal CNC content is because that the water absorption capacity values were similar to each other for 0.6 w/v % and 0.8 w/v %. Considering to save the cost 0.6 w/v % was chosen as the ideal CNC content.

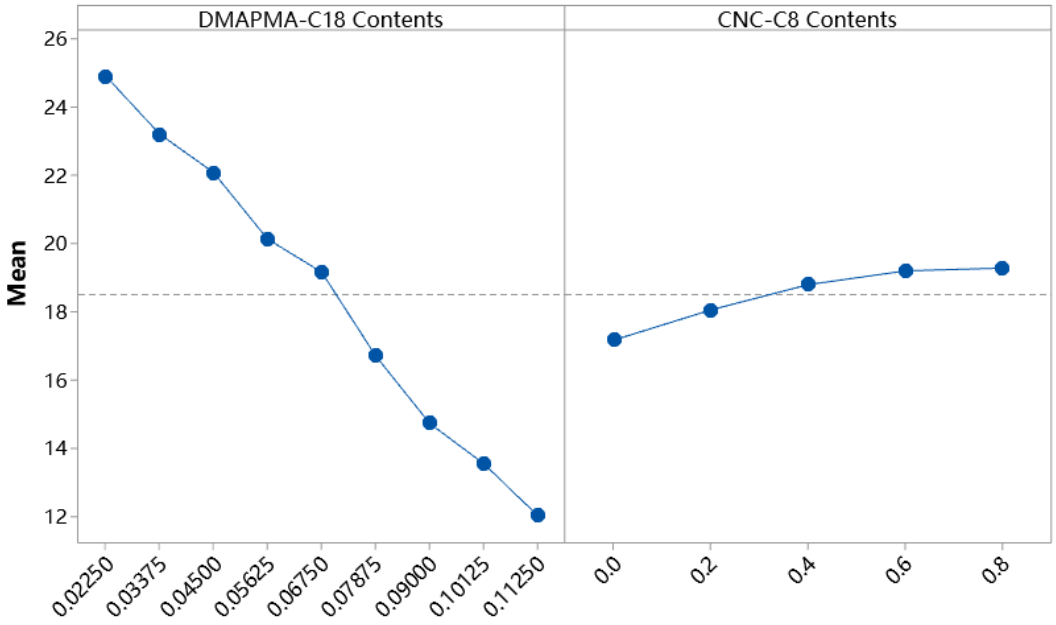

Figure 5. 39 CNC-C8 DPC hydrogels Minitab® 19 main effects plotsf or water absorption

Assume DMAPMA-C18 content (w/v %) is X_1, CNC-C8 content (w/v %) is X_2. The regression formula calculated by Minitab® 19 is water absorption (g/g)=27.313 - 146.51 X_1 + 2.690 X_2. Because the Two-way ANOVA results showed there are no

interactions between DMAPMA-C18 contents and CNC-C8 contents on water absorption abilities, there is no X_1*X_2 part in this formula.

5.4.4 Test of the Effects of CNC/CNC-C8 and DMAPMA-C18 Contents on Olive Oil Absorption

The purpose of this section is statistically analyzing the effects of CNC/CNC-C8 contents andDMAPMA-C18 contents on olive oil absorption capacities. There are five levels for the factor of CNC/CNC-C8 contents (0 w/v %, 0.2 w/v %, 0.4 w/v %, 0.6 w/v % and 0.8 w/v %) and 9 levels forDMAPMA-C18 contents (0.0225w/v %, 0.03375w/v %, 0.045w/v %, 0.05625w/v %, 0.0675w/v %, 0.07875w/v %, 0.09w/v %, 0.10125w/v % and 0.1125w/v %) as shown in **Table 5.25**.

Table 5. 25 CNC DPC hydrogels Minitab® 19 factor information for olive oil absorption

Factor	Levels	Values
DMAPMA-C18 Contents (w/v %)	9	0.02250, 0.03375, 0.04500, 0.05625, 0.06750, 0.07875, 0.09000,0.10125, 0.11250
CNC Contents (w/v %)	5	0.0, 0.2, 0.4, 0.6, 0.8

The parameters of reaction conditions were changed in turn to determine the optimum values for the experimental parameters of CNC, CNC-C8 and DMAPMA-C18 contents. The Two-way ANOVA at 0.05 level of confidence is used to prove there is a difference in

olive oil absorption capacity values due to CNC contents and DMAPMA-C18 contents with Minitab® 19.

Table 5. 26CNC DPC hydrogels Minitab® 19 Two-way ANOVA results for olive oil absorption

Source	DF	Adj SS	Adj MS	F-Value	P-Value
Model	44	0.90953	0.020671	95.92	0.000
Linear	12	0.88449	0.073707	342.01	0.000
DMAPMA-C18 Contents	8	0.45127	0.056408	261.74	**0.000**
CNC Contents	4	0.43322	0.108306	502.54	**0.000**
2-Way Interactions	32	0.02505	0.000783	3.63	**0.000**
DMAPMA-C18 Contents*CNC Contents	32	0.02505	0.000783	3.63	**0.000**
Error	90	0.01940	0.000216		
Total	134	0.92893			

From the Minitab® 19 Two-way ANOVA results outputs in **Table 5.26** we could see that the P-value of DMAPMA-C18 Contents (w/v %) (0.000) and CNC Contents (w/v %) (0.000) are both less than the significance level of 0.05. CNC contents and DMAPMA-C18 contents both have obvious effects on olive oil absorption capacity values separately. The P-value of Two-way Interactions (0.000) and DMAPMA-C18

Contents (w/v %)*CNC Contents (w/v %) (0.000) are both less than the significance level of 0.05 as well. It turned out that there is a significant interaction between CNC contents and DMAPMA-C18 contents on olive oil absorption capacity values.

From the main effects plot for olive oil absorption capacities in **Figure 5.40**we could see that the DMAPMA-C18 contents are with positive effects on olive oil absorption capacities while CNC contents are with negative effects. The main effects plot shows that 0.11250 w/v % of DMAPMA-C18 content and 0.0 w/v % of CNC content would help to obtain optimal olive oil absorption capacity values for DPC hydrogels. The olive oil absorption capacity values may still go higher and higher with the increase of DMAPMA-C18 contents and without CNC addition.

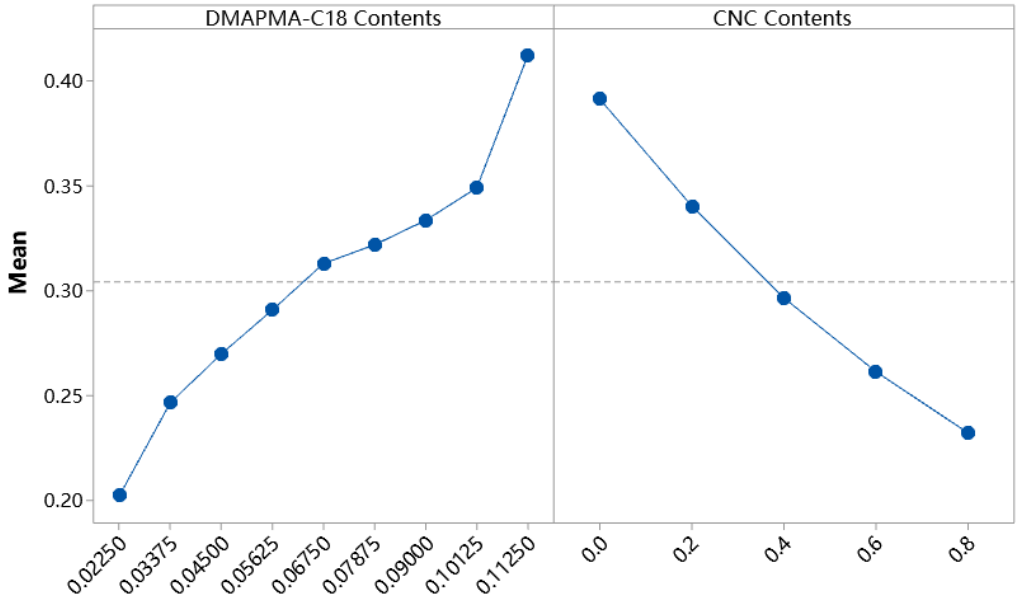

Figure 5. 40 CNC DPC hydrogels Minitab® 19 main effects plot outputs for olive oil absorption.

Assume DMAPMA-C18 content (w/v %) is X_1, CNC content (w/v %) is X_2. The regression formula calculated by Minitab® 19 is olive oil absorption (g/g) = 0.2590 + 1.849 X_1 - 0.2138 X_2 + 0.219 X_1*X_2.

As for CNC-C8 DPC hydrogels, there are similar procedures as that of CNC DPC hydrogels to check the effects of CNC-C8 contents and DMAPMA-C18 contents on olive oil absorption capacities. The Minitab® 19 factor information outputs are shown below in **Table 5.27.**

Table 5. 27 CNC-C8 DPC hydrogels Minitab® 19 factor information for olive oil absorption

Factor	Levels	Values
DMAPMA-C18 Contents (w/v %)	9	0.02250, 0.03375, 0.04500, 0.05625, 0.06750, 0.07875, 0.09000,0.10125, 0.11250
CNC-C8 Contents (w/v %)	5	0.0, 0.2, 0.4, 0.6, 0.8

From the Minitab® 19 Two-way ANOVA results outputs in **Table 5.28** we could see that the P-value of DMAPMA-C18 Contents (w/v %) (0.000) and CNC-C8 Contents (w/v %) (0.000) are both less than the significance level of 0.05. CNC-C8 contents and DMAPMA-C18 contents both have obvious effects on olive oil absorption capacity values separately. The P-value of 2-Way Interactions (0.000) and DMAPMA-C18 Contents (w/v %)*CNC-C8 Contents (w/v %) (0.000) are both less than the significance

level of 0.05 as well. It turned out that there is a significant interaction between CNC-C8 contents and DMAPMA-C18 contents on olive oil absorption capacity values.

Table 5. 28 CNC-C8 DPC hydrogels Minitab® 19 Two-way ANOVA results for olive oil absorption

Source	DF	Adj SS	Adj MS	F-Value	P-Value
Model	44	0.561686	0.012766	192.96	0.000
Linear	12	0.546140	0.045512	687.92	0.000
DMAPMA-C18 Contents	8	0.398377	0.049797	752.70	**0.000**
CNC-C8 Contents	4	0.147763	0.036941	558.37	**0.000**
2-Way Interactions	32	0.015547	0.000486	7.34	**0.000**
DMAPMA-C18 Contents*CNC-C8 Contents	32	0.015547	0.000486	7.34	**0.000**
Error	90	0.005954	0.000066		
Total	134	0.567641			

From the main effects plot for olive oil absorption capacities in **Figure 5.41**we could see that the DMAPMA-C18 contents are with positive effects on olive oil absorption capacities while CNC contents are with negative effects. The main effects plot shows that 0.11250 w/v % of DMAPMA-C18 content and 0.0 w/v % of CNC content would help to obtain optimal olive oil absorption capacity values for DPC hydrogels. Similar to the

CNC DPC hydrogels, the olive oil absorption capacity values may still go higher and higher with the increase of DMAPMA-C18 contents and with no CNC addition.

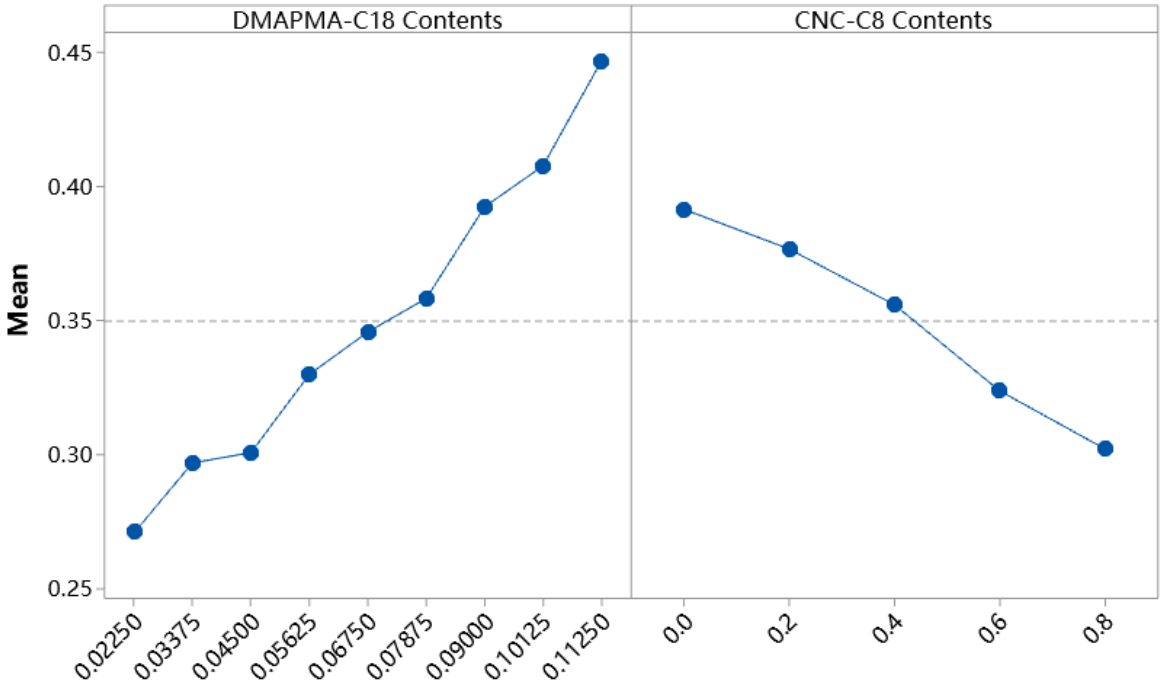

Figure 5. 41 CNC-C8 DPC hydrogels Minitab® 19 main effects plots for olive oil absorption

Assume DMAPMA-C18 content (w/v %) is X_1, CNC-C8 content (w/v %) is X_2. The regression formula calculated by Minitab® 19 is olive oil absorption (g/g) = 0.26838 + 1.895 X_1 - 0.1087 X_2 - 0.110 X_1*X_2.

5.4.5 Test of the Effects of CNC/CNC-C8 and DMAPMA-C18 Contents on Chloroform Absorption

The purpose of this section is statistically analyzing the effects of CNC/CNC-C8 contents

andDMAPMA-C18 contents on chloroform absorption capacities. There are five levels for the factor of CNC/CNC-C8 contents (0 w/v %, 0.2 w/v %, 0.4 w/v %, 0.6 w/v % and 0.8 w/v %) and 9 levels forDMAPMA-C18 contents (0.0225w/v %, 0.03375w/v %, 0.045w/v %, 0.05625w/v %, 0.0675w/v %, 0.07875w/v %, 0.09w/v %, 0.10125w/v % and 0.1125w/v %) as shown in **Table 5.29**. The parameters of reaction conditions were changed in turn to determine the optimum values for the experimental parameters of CNC, CNC-C8 and DMAPMA-C18 contents.The Two-way ANOVA at 0.05 level of confidence is used to prove there is a difference in chloroform absorption capacity values due to CNC contents and DMAPMA-C18 contents with Minitab 19.

Table 5. 29 CNC DPC hydrogels Minitab® 19 factor information for chloroform absorption

Factor	Levels	Values
DMAPMA-C18 Contents (w/v %)	9	0.02250, 0.03375, 0.04500, 0.05625, 0.06750, 0.07875, 0.09000,0.10125, 0.11250
CNC Contents (w/v %)	5	0.0, 0.2, 0.4, 0.6, 0.8

From the Minitab® 19 Two-way ANOVA results outputs in **Table 5.30** we could see that the P-value of DMAPMA-C18 Contents (w/v %) (0.000) and CNC Contents (w/v %) (0.000) are both less than the significance level of 0.05. CNC contents and DMAPMA-C18 contents both have obvious effects on chloroform absorption capacity

values separately. The P-value of 2-Way Interactions (0.000) and DMAPMA-C18 Contents (w/v %)*CNC Contents (w/v %) (0.000) are both less than the significance level of 0.05 as well. It turned out that there is a significant interaction between CNC contents and DMAPMA-C18 contents on chloroform absorption capacity values.

Table 5. 30 CNC DPC hydrogels Minitab® 19 Two-way ANOVA results for chloroform absorption

Source	DF	Adj SS	Adj MS	F-Value	P-Value
Model	44	221.64	5.0374	36.70	0.000
Linear	12	187.74	15.6450	113.97	0.000
DMAPMA-C18 Contents (w/v %)	8	168.27	21.0341	153.23	**0.000**
CNC Contents (w/v %)	4	19.47	4.8669	35.46	**0.000**
2-Way Interactions	32	33.90	1.0595	7.72	**0.000**
DMAPMA-C18 Contents (w/v %)*CNC Contents (w/v %)	32	33.90	1.0595	7.72	**0.000**
Error	90	12.35	0.1373		
Total	134	234.00			

Fromthe main effects plot for CNC DPC hydrogels chloroform absorption capacities in **Figure 5.42**we could see that the DMAPMA-C18 contents are mainly with negative

effects on chloroform absorption capacities while CNC contents are mainly with positive effects. The DMAPMA-C18 contents are with a more obvious effect on chloroform absorption capacities than CNC contents. The main effects plot shows that 0.04500 w/v % of DMAPMA-C18 content and 0.6 w/v % of CNC content would help to obtain optimal chloroform absorption capacity values for DPC hydrogels.

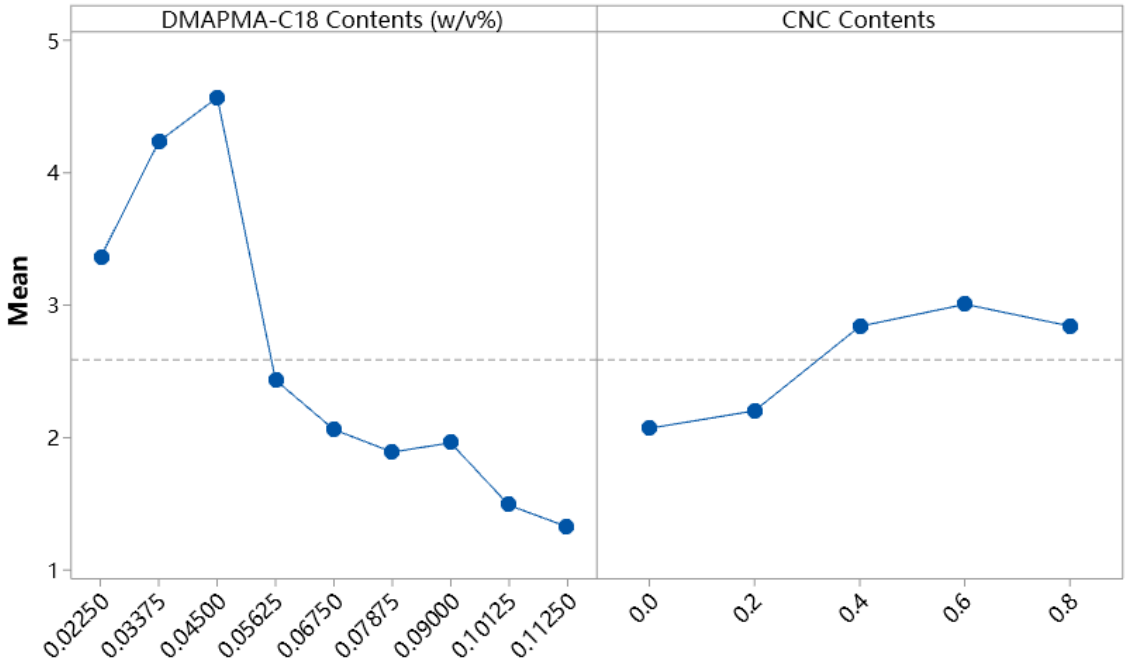

Figure 5. 42 CNC DPC hydrogels Minitab® 19 main effects plots for chloroform absorption.

Assume DMAPMA-C18 content (w/v %) is X_1, CNC content (w/v %) is X_2. The regression formula calculated by Minitab® 19 is chloroform absorption (g/g) = 3.183 - 15.77 X_1+ 4.049 X_2 - 42.6 X_1*X_2.

As for CNC-C8 DPC hydrogels, there are similar procedures as that of CNC DPC hydrogels to check the effects of CNC-C8 contents and DMAPMA-C18 contents on chloroform absorption capacity values. The Minitab® 19 factor information outputs are shown below in **Table 5.31**.

Table 5. 31 CNC-C8 DPC hydrogels Minitab® 19 factor information for chloroform absorption

Factor	Levels	Values
DMAPMA-C18 Contents (w/v %)	9	0.02250, 0.03375, 0.04500, 0.05625, 0.06750, 0.07875, 0.09000,0.10125, 0.11250
CNC-C8 Contents (w/v %)	5	0.0, 0.2, 0.4, 0.6, 0.8

From the Minitab® 19 Two-way ANOVA results outputs in **Table 5.32** we could see that the P-value of DMAPMA-C18 Contents (w/v %) (0.000) and CNC-C8 Contents (w/v %) (0.000) are both less than the significance level of 0.05. CNC-C8 contents and DMAPMA-C18 contents both have obvious effects on chloroform absorption capacity values separately. The P-value of 2-Way Interactions (0.000) and DMAPMA-C18 Contents (w/v %)*CNC-C8 Contents (w/v %) (0.000) are both less than the significance level of 0.05 as well. It turned out that there is a significant interaction between CNC-C8 contents and DMAPMA-C18 contents on chloroform absorption capacity values.

Table 5. 32 CNC-C8 DPC hydrogels Minitab® 19 Two-way ANOVA results for chloroform absorption

Source	DF	Adj SS	Adj MS	F-Value	P-Value
Model	44	19.6548	0.44670	81.61	0.000
Linear	12	17.2833	1.44028	263.15	0.000
DMAPMA-C18 Contents (w/v %)	8	14.8279	1.85348	338.64	**0.000**
CNC-C8 Contents (w/v %)	4	2.4554	0.61386	112.16	**0.000**
2-Way Interactions	32	2.3715	0.07411	13.54	**0.000**
DMAPMA-C18 Contents (w/v %)*CNC-C8 Contents (w/v %)	32	2.3715	0.07411	13.54	**0.000**
Error	90	0.4926	0.00547		
Total	134	20.1474			

From the main effects plot for CNC-C8 DPC hydrogels chloroform absorption capacities in **Figure 5.43**we could see that the DMAPMA-C18 contents and CNC-C8 contents are both mainly with negative effects on chloroform absorption capacities. The DMAPMA-C18 contents are with a more obvious effect on chloroform absorption capacities than CNC-C8 contents. The main effects plot shows that 0.03375 w/v % of DMAPMA-C18 content and 0.0 w/v % of CNC content would help to obtain optimal

chloroform absorption capacity values for DPC hydrogels. The mean of chloroform absorption capacities at 0.0w/v % CNC-C8 contentis similar to that at 0.2 w/v % CNC-C8 content, therefore 0.0 w/v % was selected as the optimal CNC-C8 content.

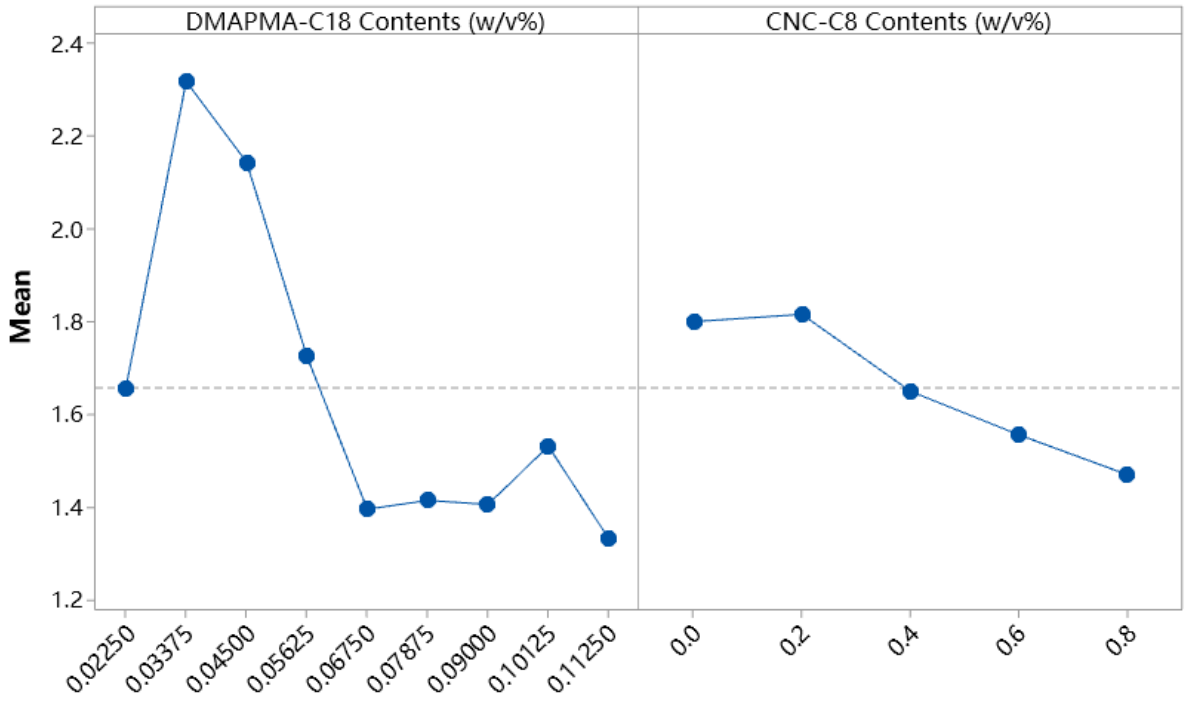

Figure 5. 43 CNC-C8 DPC hydrogels Minitab® 19 main effects plots for chloroform absorption.

Assume DMAPMA-C18 content (w/v %) is X_1, CNC-C8 content (w/v %) is X_2. The regression formula calculated by Minitab® 19 is chloroform absorption (g/g) = 2.187 - 5.12 X_1 + 0.036 X_2 - 7.34 X_1*X_2.

5.5 SEM Analysis

We could see several holes in the DPC hydrogels cutting surface SEM graph in **Figure 5.44**, which means the water in wet hydrogels has already been removed after freeze-dry process and the holes are the previous positions where the water existed. The hole diameters on the cutting surface were generally less than 5 microns.

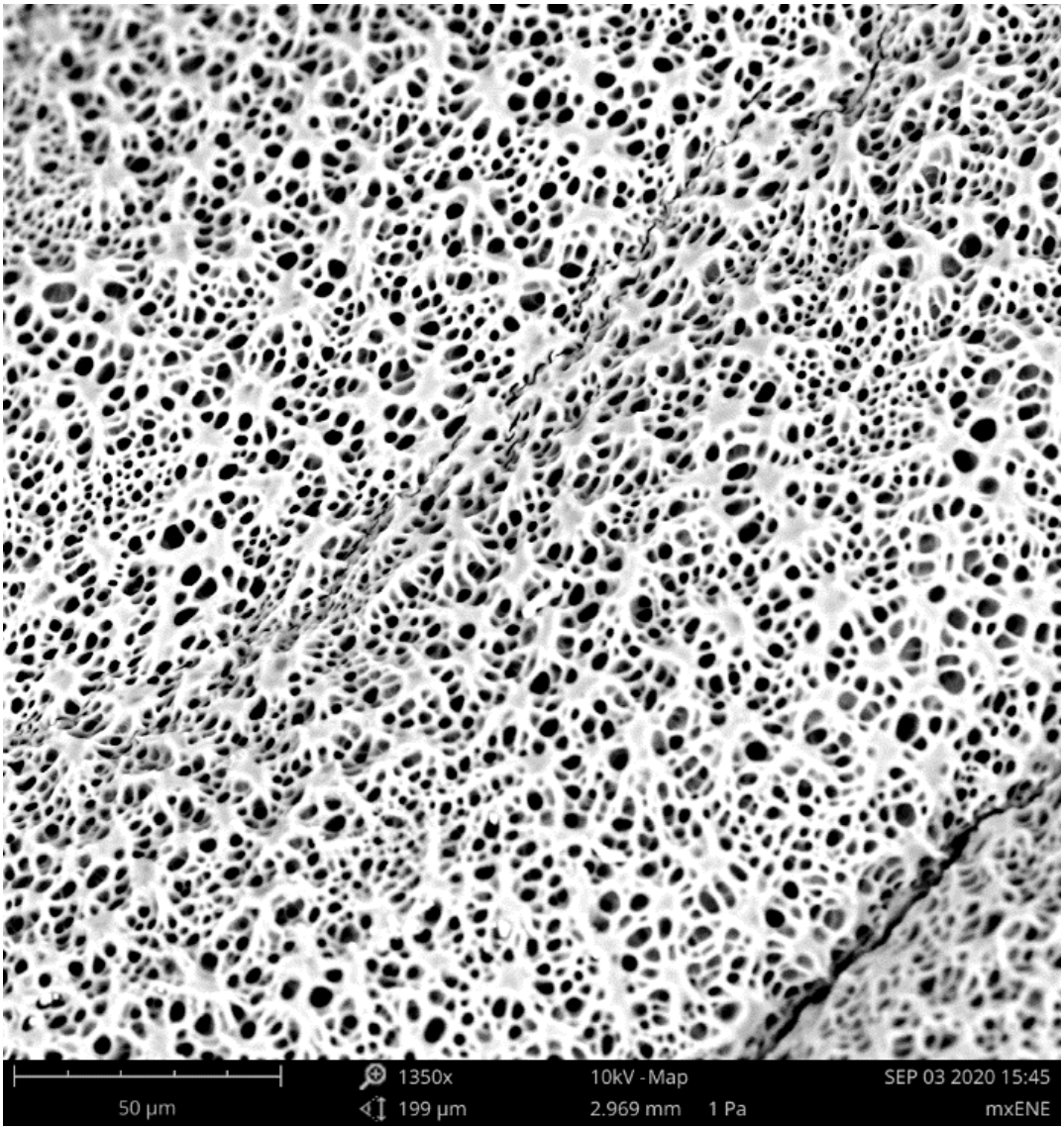

Figure 5. 44 SEM graphs for freeze-dried DPC hydrogels cutting surface.

Chapter 6 Conclusion and Future Work

6.1 Conclusion

In this study, we designed a synthesis method to prepare a type of self-recoverable dual physically cross-linked DPC hydrogels. The engineered hydrogels had DMAc-DMAPMA-C18 polymer forming the first network physically cross-linked mainly by hydrophobic interactions, on which the secondary cross-link points were formed by hydrophobic interactions between CNC-C8 and DMAPMA-C18, electrostatic interactions between negatively charged CNC and positively charged DMAPMA, as well as the hydrogen bonding between CNC (CNC-C8)and DMAc side chains of polymers.

The tensile test showed the hydrophobic forces could play a role in improving the physical properties of stresses and elongations of DPC hydrogels at low DMAPMA-C18and CNC or CNC-C8 contents. The addition of CNC and CNC-C8 could also help to enhance the mechanical strengths at low contents but not as obviously as the addition of DMAPMA-C18 did. The mechanical property of DPC hydrogel could be readily tuned in an extensive range for different applications by changing the CNC or CNC-C8 and DMAPMA-C18contents in DPC hydrogels. At the optimal formulation, the DPC hydrogel possessed optimal average nominal stress(331.05±32.06 kPa), true stress(14463.99±2939.98 kPa), compressive tress (2822.77 kPa) at the strain of 90% and

elongation (4267.85%) at the contents of 3 DMAPMA-C18 of 0.0675 w/v % and 0.4 w/v % CNC-C8 contents. The initial wet DPC hydrogels could be pressed and recover their shaped after releasing the stress.

Furthermore, because of its unique physically reversible network structures, the DPC hydrogels could sufficiently reconstruct its network structures, resulting in good self-recovery properties by applying THF between the cut surfaces overnight. The self-recovery test showed ideal self-recoverability in CNC DPC hydrogels and CNC-C8 DPC hydrogels. The optimal stress self-recovery ratio of CNC DPC hydrogel is 78.22% when the hydrogel contained 2.5 DMAPMA-C18 (0.05625 w/v %). For the CNC-C8 DPC hydrogel, it was 74.97% at 3.5 DMAPMA-C18 (0.07875 w/v %) contents. The CNC DPC hydrogel showed the optimal elongation self-recovery ratio of 40.49% with 2.5 DMAPMA-C18 (0.05625 w/v %) and the optimal elongation self-recovery ratio of CNC-C8 DPC hydrogel was 55.54% when there were 3.5 DMAPMA-C18 (0.07875 w/v %) in the hydrogel.

For water absorption, the shape of DPC hydrogels would not change and even if it has already expanded to much larger than the initial condition and saturated. The optimal water absorption capacity was 27.8301 g/g of a CNC DPC hydrogel at 1 DMAPMA-C18 (0.0225 w/v %) content and 0.8 w/v % CNC content and25.8638 g/g for a CNC-C8 DPC hydrogel at1 DMAPMA-C18 (0.0225 w/v %) content and 0.8 w/v % CNC-C8

content.CNC DPC hydrogels showed better water absorption abilities than CNC-C8 DPC hydrogels because there are more hydrophilic hydroxyl groups on CNC than CNC-C8. For this reason CNC would be more hydrophilic and help to absorb water. CNC (CNC-C8) DPC hydrogels with higher DMAPMA-C18 contents are usually with better olive oil absorption abilities according to the tests results. The cycling water absorption tests showed that the freeze-dried hydrogel could be used to absorb water for at least five times with similar performances. The optimal olive oil absorption capacity for DPC hydrogels was 0.5085g/g at 5DMAPMA-C18 (0.1125 w/v %) contents without CNC or CNC-C8. CNC and CNC-C8 would be mainly with positive effects in water absorption while with negative effects in olive oil absorption. Nevertheless, DMAPMA-C18 would be opposite to CNC and CNC-C8, which could decrease water absorption capacities while increase olive oil absorption capacities.

The absorption time period for water and olive oil swelling is according to the saturation with 7 days and 5 mins separately. While as the shape of DPC hydrogels in chloroform would get changed, so the time period of 80 mins for chloroform absorption was selected according to the shape containing. The optimal chloroform absorption capacity for CNC DPC hydrogel was 5.1699g/g with 2 DMAPMA-C18 (0.045 w/v %) and 0.4 w/v % CNC. The chloroform absorption capacity of the CNC-C8 DPC hydrogels were generally lower than that of CNC DPC hydrogels at the same content of DMAPMA-C18 and CNC or CNC-C8.

The SEM graphs showed there are holes on the cutting surface of freeze-dried DPC hydrogel samples, where are the positions that the water exited previously in initial wet DPC hydrogel products.

The results highlight that:

1) The introduction of hydrophobic force and CNC addition could help to increase the mechanical strength and elongations of DPC hydrogels in certain contents range.
2) The hydrophobic chains and CNC contents cannot be added too much in the DPC hydrogels because they would gather together to form inhomogeneous hydrogels which could even be easier to break than the lower dosage ones.
3) DPC hydrogels are with ideal self-healing abilities as a type of non-autonomic self-healing materials. For stress recovery, CNC DPC hydrogels are better than CNC-C8 DPC hydrogels, while for elongation recovery, CNC-C8 DPC hydrogels would be optimal. For both of CNC DPC hydrogels and CNC-C8 DPC hydrogels, the stress self-recovery ratio increased with increasing DMAPMA-C18 contents.
4) The addition of CNC and CNC-C8 would help to improve water absorption abilities while DMAPMA-C18 monomer would have negative effects. The influence on olive oil absorption is totally opposite.
5) Minitab® 19 was used do Two-way ANOVA tests. It was approved that DMAPMA-C18 contents have effects on stress, elongation, water absorption, olive

oil absorption and chloroform absorption separately at 0.05 level of significance. So do the CNC or CNC-C8 contents. Exceptfor CNC-C8 DPC hydrogels for water absorption, there areallwith interaction effects between DMAPMA-C18 contents and CNC or CNC-C8 contents on stress, elongation, water absorption, olive oil absorption and chloroform absorption.

6.2 Future Work

Currently, the DPC hydrogel products show good mechanical properties. However, they are only with simple applications of swelling tests. In order to broaden the application areas of DPC hydrogels, more future works are worthwhile to try.

Compared with other ideal hydrogel materials with the stresses over MPa, the optimal stress in this study of 331.05 kPa seems still not high enough. Future efforts could be made to add other types of hydrophobic groups (such as rigid aromatic groups) or nanoparticles including other forces such as cation-pi and pi-pi interactions to see if the mechanical properties could be improved until better than the current conditions. Other types of polymer chain monomers could also be introduced into this system to form a triple physically cross-linked hydrogels to see if stronger physical interactions would appear to improve the mechanical strengths and self-healing abilities.

Another problem is that the DPC hydrogel is a type of non-autonomic self-healing material. Its self-healing process needs THF as a trigger, which is with toxicity. However,

one common potential application for hydrogels with high mechanical properties is artificial tissue, which requires safe and autonomic self-recoverable characteristics. So it would be important to find other safe trigger for self-healing or add some modifications to the current DPC hydrogels to make them autonomic self-healing hydrogels. If the DPC hydrogel samples are going to be used for absorption activities on industry, it would be a common phenomenon that the hydrogel would be easily to reach wastes and get contaminated during the absorption process. It would also be worthwhile to study on the self-healing abilities of DPC hydrogels between two contaminated cutting surfaces, the contaminants may include organic solvents, dusts and so on.

The reaction temperature in DPC hydrogel synthesis process is 65℃, which is high. If the DPC hydrogel is going to be used in industry, the high temperature would cause a great amount of energy waste every year. Therefore another valuable work is to search a better polymerization initiator to replace current KPS. The ideal polymerization initiator would be better to play a role at room temperature or just need a trigger like light, which could be helpful to save the production costs.

References

Akay, G., Hassan-Raeisi, A., Tuncaboylu, D. C., Orakdogen, N., Abdurrahmanoglu, S., Oppermann, W., & Okay, O. (2013). Self-healing hydrogels formed in catanionic surfactant solutions. *Soft Matter*, *9*, 2254–2261. https://doi.org/10.1039/c2sm27515e

Akhavan, B., Jarvis, K., & Majewski, P. (2013). Hydrophobic plasma polymer coated silica particles for petroleum hydrocarbon removal. *ACS Applied Materials and Interfaces*, *5*, 8563−8571. https://doi.org/10.1021/am4020154

Amendola, V., & Meneghetti, M. (2009). Self-healing at the nanoscale. *Nanoscale*, *1*(1), 74-88. https://doi.org/10.1039/b9nr00146h

Arunan, E., Desiraju, G. R., Klein, R. A., Sadlej, J., Scheiner, S., Alkorta, I., … Nesbitt, D. J. (2011). Definition of the hydrogen bond (IUPAC Recommendations 2011). *Pure and Applied Chemistry*, *83*(8), 1637–1641. https://doi.org/10.1351/PAC-REC-10-01-02

Ashton, N. N., & Stewart, R. J. (2015). Self-recovering caddisfly silk: Energy dissipating, Ca2+-dependent, double dynamic network fibers. *Soft Matter*, *11*, 1667–1676. https://doi.org/10.1039/c4sm02435d

Bardajee, G. R., Pourjavadi, A., Ghavami, S., Soleyman, R., & Jafarpour, F. (2011). UV-prepared salep-based nanoporous hydrogel for controlled release of tetracycline

hydrochloride in colon. *Journal of Photochemistry and Photobiology B: Biology*, *102*, 232–240. https://doi.org/10.1016/j.jphotobiol.2010.12.008

Berthomieu, C., & Hienerwadel, R. (2009). Fourier transform infrared (FTIR) spectroscopy. *Photosynthesis Research*, pp. 157–170. https://doi.org/10.1007/s11120-009-9439-x

Blanco, A., Monte, M. C., Campano, C., Balea, A., Merayo, N., & Negro, C. (2018). Nanocellulose for industrial use: Cellulose nanofibers (CNF), cellulose nanocrystals (CNC), and bacterial cellulose (BC). In *Handbook of Nanomaterials for Industrial Applications* (pp. 74–126). https://doi.org/10.1016/B978-0-12-813351-4.00005-5

Burattini, S., Greenland, B. W., Merino, D. H., Weng, W., Seppala, J., Colquhoun, H. M., … Rowan, S. J. (2010). A healable supramolecular polymer blend based on aromatic π-π Stacking and hydrogen-bonding interactions. *Journal of the American Chemical Society*, *132*, 12051–12058. https://doi.org/10.1021/ja104446r

Busseron, E., Ruff, Y., Moulin, E., & Giuseppone, N. (2013). Supramolecular self-assemblies as functional nanomaterials. *Nanoscale*, pp. 7098–7140. https://doi.org/10.1039/c3nr02176a

Chandler, D. (2005). Interfaces and the driving force of hydrophobic assembly. *Nature*, pp. 640–647. https://doi.org/10.1038/nature04162

Chandramouli, N., Ferrand, Y., Lautrette, G., Kauffmann, B., MacKereth, C. D., Laguerre, M., … Huc, I. (2015). Iterative design of a helically folded aromatic oligoamide sequence for the selective encapsulation of fructose. *Nature Chemistry*, *7*, 334–341. https://doi.org/10.1038/nchem.2195

Chen, C., Li, D., Abe, K., & Yano, H. (2018). Formation of high strength double-network gels from cellulose nanofiber/polyacrylamide via NaOH gelation treatment. *Cellulose*, *25*(9), 5089–5097. https://doi.org/10.1007/s10570-018-1938-5

Chen, H., Chen, Q., Hu, R., Wang, H., Newby, B. M. Z., Chang, Y., & Zheng, J. (2015). Mechanically strong hybrid double network hydrogels with antifouling properties. *Journal of Materials Chemistry B*, *3*, 5426–5435. https://doi.org/10.1039/c5tb00681c

Chen, Q., Zhu, L., Chen, H., Yan, H., Huang, L., Yang, J., & Zheng, J. (2015). A novel design strategy for fully physically linked double network hydrogels with tough, fatigue resistant, and self- Healing properties. *Advanced Functional Materials*, *25*, 1598–1607. https://doi.org/10.1002/adfm.201404357

Cipriano, B. H., Banik, S. J., Sharma, R., Rumore, D., Hwang, W., Briber, R. M., & Raghavan, S. R. (2014). Superabsorbent hydrogels that are robust and highly stretchable. *Macromolecules*, *47*, 4445−4452. https://doi.org/10.1021/ma500882n

Dai, X., Zhang, Y., Gao, L., Bai, T., Wang, W., Cui, Y., & Liu, W. (2015). A

mechanically strong, highly stable, thermoplastic, and self-healable supramolecular polymer hydrogel. *Advanced Materials*, *27*, 3566–3571. https://doi.org/10.1002/adma.201500534

De France, K. J., Hoare, T., & Cranston, E. D. (2017). Review of Hydrogels and Aerogels Containing Nanocellulose. *Chemistry of Materials*, *29*, 4609−4631. https://doi.org/10.1021/acs.chemmater.7b00531

Fan, J., Shi, Z., Lian, M., Li, H., & Yin, J. (2013). Mechanically strong graphene oxide/sodium alginate/polyacrylamide nanocomposite hydrogel with improved dye absorption capacity. *Journal of Materials Chemistry A*, *1*, 7433–7443. https://doi.org/10.1039/c3ta10639j

Fung, Y. C., & Skalak, R. (1982). Biomechanics. Mechanical Properties of Living Tissues. *Journal of Applied Mechanics*, *49*(2), 464–465. https://doi.org/10.1115/1.3162171

Gessner, T., & Mayer, U. (2000). Triarylmethane and Diarylmethane Dyes. In *Ullmann's Encyclopedia of Industrial Chemistry*. https://doi.org/10.1002/14356007.a27_179

Gong, J. P. (2006). Friction and lubrication of hydrogels - Its richness and complexity. *Soft Matter*, pp. 544-552. https://doi.org/10.1039/b603209p

Gong, J. P. (2010). Why are double network hydrogels so tough? *Soft Matter*, pp.

2583–2590. https://doi.org/10.1039/b924290b

Gong, J. P. (2014). Materials both tough and soft. *Science*, pp. 161–162. https://doi.org/10.1126/science.1252389

Gong, J. P., Katsuyama, Y., Kurokawa, T., & Osada, Y. (2003). Double-network hydrogels with extremely high mechanical strength. *Advanced Materials*, *15*(14), 1155–1158. https://doi.org/10.1002/adma.200304907

Gousséé, C., Chanzy, H., Excoffier, G., Soubeyrand, L., & Fleury, E. (2002). Stable suspensions of partially silylated cellulose whiskers dispersed in organic solvents. *Polymer*, *43*, 2645–2651. https://doi.org/10.1016/S0032-3861(02)00051-4

Gribova, V., Crouzier, T., & Picart, C. (2011). A material's point of view on recent developments of polymeric biomaterials: Control of mechanical and biochemical properties. *Journal of Materials Chemistry*, p. 14354. https://doi.org/10.1039/c1jm11372k

Griffiths, P. R., & De Haseth, J. A. (2006). Fourier Transform Infrared Spectrometry: Second Edition. In *Fourier Transform Infrared Spectrometry: Second Edition*. https://doi.org/10.1002/047010631X

Habibi, Y., Lucia, L. A., & Rojas, O. J. (2010). Cellulose nanocrystals: Chemistry, self-assembly, and applications. *Chemical Reviews*, *110*, 3479–3500.

https://doi.org/10.1021/cr900339w

Hager, M. D., Greil, P., Leyens, C., Van Der Zwaag, S., & Schubert, U. S. (2010). Self-healing materials. *Advanced Materials*, 5424–5430. https://doi.org/10.1002/adma.201003036

Hao, J., & Weiss, R. A. (2011). Viscoelastic and mechanical behavior of hydrophobically modified hydrogels. *Macromolecules*, *44*(23), 9390–9398. https://doi.org/10.1021/ma202130u

Haque, M. A., Kurokawa, T., & Gong, J. P. (2012). Super tough double network hydrogels and their application as biomaterials. *Polymer*, pp. 1805–1822. https://doi.org/10.1016/j.polymer.2012.03.013

Haraguchi, K., & Takehisa, T. (2002). Nanocomposite hydrogels: A unique organic-inorganic network structure with extraordinary mechanical, optical, and swelling/De-swelling properties. *Advanced Materials*, *14*, 1120. https://doi.org/10.1002/1521-4095(20020816)14:16<1120::AID-ADMA1120>3.0.CO;2-9

House, J. E., & House, K. A. (2010). Descriptive inorganic chemistry: Second edition. In *Descriptive Inorganic Chemistry: Second Edition*. https://doi.org/10.1016/C2009-0-05861-9

Hu, J., Zhang, G., & Liu, S. (2012). Enzyme-responsive polymeric assemblies, nanoparticles and hydrogels. *Chemical Society Reviews*, *41*, 5933–5949. https://doi.org/10.1039/c2cs35103j

Hu, X., Xiong, L., Wang, T., Zhu, M., Liu, X., & Tong, Z. (2011). Ultrahigh tensibility and stimuli-response of polymer-hectorite nanocomposite hydrogels. *Macromolecular Symposia*, 49–58. https://doi.org/10.1002/masy.201000131

Hu, Y., Du, Z., Deng, X., Wang, T., Yang, Z., Zhou, W., & Wang, C. (2016). Dual Physically Cross-Linked Hydrogels with High Stretchability, Toughness, and Good Self-Recoverability. *Macromolecules*, *49*, 5660–5668. https://doi.org/10.1021/acs.macromol.6b00584

Idris, A. M., & El-Zahhar, A. A. (2019). Indicative properties measurements by SEM, SEM-EDX and XRD for initial homogeneity tests of new certified reference materials. *Microchemical Journal*, *146*, 429–433. https://doi.org/10.1016/j.microc.2019.01.032

Iyer, B. V. S., Salib, I. G., Yashin, V. V., Kowalewski, T., Matyjaszewski, K., & Balazs, A. C. (2013). Modeling the response of dual cross-linked nanoparticle networks to mechanical deformation. *Soft Matter*, *9*, 109–121. https://doi.org/10.1039/c2sm27121d

Jane Reece, Urry, L. A., Cain, M. L., Wasserman, S. A., Minorsky, P. V., Jackson, R. B.,

& Campbell, N. A. (2011). Campbell Biology: Global Edition. In *Campbell Biology*.

Jiang, G., Liu, C., Liu, X., Zhang, G., Yang, M., & Liu, F. (2009). Construction and properties of hydrophobic association hydrogels with high mechanical strength and reforming capabilitya. *Macromolecular Materials and Engineering*, *294*, 815–820. https://doi.org/10.1002/mame.200900160

Khabibullin, A., Alizadehgiashi, M., Khuu, N., Prince, E., Tebbe, M., & Kumacheva, E. (2017). Injectable Shear-Thinning Fluorescent Hydrogel Formed by Cellulose Nanocrystals and Graphene Quantum Dots. *Langmuir*, *33*, 12344–12350. https://doi.org/10.1021/acs.langmuir.7b02906

Klemm, D., Kramer, F., Moritz, S., Lindström, T., Ankerfors, M., Gray, D., & Dorris, A. (2011). Nanocelluloses: A new family of nature-based materials. *Angewandte Chemie - International Edition*, pp. 5438–5466. https://doi.org/10.1002/anie.201001273

Kolmakov, G. V., Revanur, R., Tangirala, R., Emrick, T., Russell, T. P., Crosby, A. J., & Balazs, A. C. (2010). Using nanoparticle-filled microcapsules for site-specific healing of damaged substrates: Creating a “repair-and-go” system. *ACS Nano*, 1115–1123. https://doi.org/10.1021/nn901296y

Lee, K. Y., Tammelin, T., Schulfter, K., Kiiskinen, H., Samela, J., & Bismarck, A. (2012). High performance cellulose nanocomposites: Comparing the reinforcing ability of

bacterial cellulose and nanofibrillated cellulose. *ACS Applied Materials and Interfaces*, *4*(8), 4078–4086. https://doi.org/10.1021/am300852a

Levine, M. D., Ramsey, P. P., & Smldt, K. R. (2001). *Applied Statistics for Engineers and Scientists*. Prentice Hall.

Lewis, G. N. (1916). The atom and the molecule. *Journal of the American Chemical Society*, *38*(4), 762–785. https://doi.org/10.1021/ja02261a002

Li, B., Zhang, Y., Wu, C., Guo, B., & Luo, Z. (2018). Fabrication of mechanically tough and self-recoverable nanocomposite hydrogels from polyacrylamide grafted cellulose nanocrystal and poly (acrylic acid). *Carbohydrate Polymers*, *198*, 1–8. https://doi.org/10.1016/j.carbpol.2018.06.047

Li, C., Mu, C., Lin, W., & Ngai, T. (2015). Gelatin Effects on the Physicochemical and Hemocompatible Properties of Gelatin/PAAm/Laponite Nanocomposite Hydrogels. *ACS Applied Materials and Interfaces*, *7*, 18732−18741. https://doi.org/10.1021/acsami.5b05287

Li, F., Su, Y., Wang, J., Wu, G., & Wang, C. (2010). Influence of dynamic load on friction behavior of human articular cartilage, stainless steel and polyvinyl alcohol hydrogel as artificial cartilage. *Journal of Materials Science: Materials in Medicine*, *21*, 147–154. https://doi.org/10.1007/s10856-009-3863-5

Li, H., Choi, Y. S., Rutland, M. W., & Atkin, R. (2020). Nanotribology of hydrogels with similar stiffness but different polymer and crosslinker concentrations. *Journal of Colloid and Interface Science*, *563*, 347–353. https://doi.org/10.1016/j.jcis.2019.12.045

Li, L., Yan, B., Yang, J., Huang, W., Chen, L., & Zeng, H. (2017). Injectable Self-Healing Hydrogel with Antimicrobial and Antifouling Properties. *ACS Applied Materials and Interfaces*, pp. 9221–9225. https://doi.org/10.1021/acsami.6b16192

Li, Xuefei, Qin, H., Zhang, X., & Guo, Z. (2019). Triple-network hydrogels with high strength, low friction and self-healing by chemical-physical crosslinking. *Journal of Colloid and Interface Science*, *556*, 549–556. https://doi.org/10.1016/j.jcis.2019.08.100

Li, Xuefeng, Yang, Q., Zhao, Y., Long, S., & Zheng, J. (2017). Dual physically crosslinked double network hydrogels with high toughness and self-healing properties. *Soft Matter*, *13*, 911–920. https://doi.org/10.1039/c6sm02567f

Li, Y., Rodrigues, J., & Tomás, H. (2012). Injectable and biodegradable hydrogels: Gelation, biodegradation and biomedical applications. *Chemical Society Reviews*, *41*, 2193–2221. https://doi.org/10.1039/c1cs15203c

Lim, L. S., Rosli, N. A., Ahmad, I., Mat Lazim, A., & Mohd Amin, M. C. I. (2017). Synthesis and swelling behavior of pH-sensitive semi-IPN superabsorbent hydrogels

based on poly (acrylic acid) reinforced with cellulose nanocrystals. *Nanomaterials, 7*, 399. https://doi.org/10.3390/nano7110399

Lin, N., Huang, J., & Dufresne, A. (2012). Preparation, properties and applications of polysaccharide nanocrystals in advanced functional nanomaterials: A review. *Nanoscale*, pp. 3274–3294. https://doi.org/10.1039/c2nr30260h

Loessner, D., Meinert, C., Kaemmerer, E., Martine, L. C., Yue, K., Levett, P. A., … Hutmacher, D. W. (2016). Functionalization, preparation and use of cell-laden gelatin methacryloyl-based hydrogels as modular tissue culture platforms. *Nature Protocols, 11*(4), 727–746. https://doi.org/10.1038/nprot.2016.037

Mihajlovic, M., Staropoli, M., Appavou, M. S., Wyss, H. M., Pyckhout-Hintzen, W., & Sijbesma, R. P. (2017). Tough Supramolecular Hydrogel Based on Strong Hydrophobic Interactions in a Multiblock Segmented Copolymer. *Macromolecules, 50*, 3333−3346. https://doi.org/10.1021/acs.macromol.7b00319

Miquelard-Garnier, G., Demeures, S., Creton, C., & Hourdet, D. (2006). Synthesis and rheological behavior of new hydrophobically modified hydrogels with tunable properties. *Macromolecules, 39*, 8128–8139. https://doi.org/10.1021/ma061361n

Moon, R. J., Martini, A., Nairn, J., Simonsen, J., & Youngblood, J. (2011). Cellulose nanomaterials review: Structure, properties and nanocomposites. *Chemical Society Reviews, 40*, 3941–3994. https://doi.org/10.1039/c0cs00108b

Na, Y. H., Tanaka, Y., Kawauchi, Y., Furukawa, H., Sumiyoshi, T., Gong, J. P., & Osada, Y. (2006). Necking phenomenon of double-network gels. *Macromolecules*, *39*(14), 4641–4645. https://doi.org/10.1021/ma060568d

Naficy, S., Spinks, G. M., & Wallace, G. G. (2014). Thin, tough, pH-sensitive hydrogel films with rapid load recovery. *ACS Applied Materials and Interfaces*, *6*, 4109–4114. https://doi.org/10.1021/am405708v

Odom, S. A., Caruso, M. M., Finke, A. D., Prokup, A. M., Ritchey, J. A., Leonard, J. H., … Moore, J. S. (2010). Restoration of conductivity with TTF-TCNQ charge-transfer salts. *Advanced Functional Materials*, *20*(11), 1721–1727. https://doi.org/10.1002/adfm.201000159

Pethes, I., Bakó, I., & Pusztai, L. (2020). Chloride ions as integral parts of hydrogen bonded networks in aqueous salt solutions: The appearance of solvent separated anion pairs. *Physical Chemistry Chemical Physics*, *22*, 11038–11044. https://doi.org/10.1039/d0cp01806f

Phadke, A., Zhang, C., Arman, B., Hsu, C. C., Mashelkar, R. A., Lele, A. K., … Varghese, S. (2012). Rapid self-healing hydrogels. *Proceedings of the National Academy of Sciences of the United States of America*, *109*(12), 4383–4388. https://doi.org/10.1073/pnas.1201122109

Phanthong, P., Reubroycharoen, P., Kongparakul, S., Samart, C., Wang, Z., Hao, X., …

Guan, G. (2018). Fabrication and evaluation of nanocellulose sponge for oil/water separation. *Carbohydrate Polymers*, *190*, 184–189. https://doi.org/10.1016/j.carbpol.2018.02.066

Plackett, D., Letchford, K., Jackson, J., & Burt, H. (2014). A review of nanocellulose as a novel vehicle for drug delivery. *Nordic Pulp & Paper Research Journal*, *29*(1), 105–118. https://doi.org/10.3183/npprj-2014-29-01-p105-118

Rao, P., Sun, T. L., Chen, L., Takahashi, R., Shinohara, G., Guo, H., … Gong, J. P. (2018). Tough Hydrogels with Fast, Strong, and Reversible Underwater Adhesion Based on a Multiscale Design. *Advanced Materials*, *30*, 1801884. https://doi.org/10.1002/adma.201801884

Ryu, J. H., Koo Han, N., Lee, J. S., & Jeong, Y. G. (2019). Microstructure, thermal and mechanical properties of composite films based on carboxymethylated nanocellulose and polyacrylamide. *Carbohydrate Polymers*, *211*, 84–90. https://doi.org/10.1016/j.carbpol.2019.01.109

Seiffert, S., & Sprakel, J. (2012). Physical chemistry of supramolecular polymer networks. *Chemical Society Reviews*, *41*, 909–930. https://doi.org/10.1039/c1cs15191f

Seuring, J., & Agarwal, S. (2010). Non-ionic homo- and copolymers with H-donor and H-acceptor units with an UCST in water. *Macromolecular Chemistry and Physics*,

211(19), 2109–2117. https://doi.org/10.1002/macp.201000147

Shi, F. K., Wang, X. P., Guo, R. H., Zhong, M., & Xie, X. M. (2015). Highly stretchable and super tough nanocomposite physical hydrogels facilitated by the coupling of intermolecular hydrogen bonds and analogous chemical crosslinking of nanoparticles. *Journal of Materials Chemistry B*, *3*, 1187–1192. https://doi.org/10.1039/c4tb01654h

Sirό, I., & Plackett, D. (2010). Microfibrillated cellulose and new nanocomposite materials: A review. *Cellulose*, pp. 459–494. https://doi.org/10.1007/s10570-010-9405-y

Smulders, M. M. J., Zarra, S., & Nitschke, J. R. (2013). Quantitative understanding of guest binding enables the design of complex host-guest behavior. *Journal of the American Chemical Society*, *135*, 7039−7046. https://doi.org/10.1021/ja402084x

Sun, J. Y., Zhao, X., Illeperuma, W. R. K., Chaudhuri, O., Oh, K. H., Mooney, D. J., … Suo, Z. (2012). Highly stretchable and tough hydrogels. *Nature*, *489*, 133–136. https://doi.org/10.1038/nature11409

Sun, T. L., Kurokawa, T., Kuroda, S., Ihsan, A. Bin, Akasaki, T., Sato, K., … Gong, J. P. (2013). Physical hydrogels composed of polyampholytes demonstrate high toughness and viscoelasticity. *Nature Materials*, *12*, 932–937. https://doi.org/10.1038/nmat3713

Sun, W., Xue, B., Li, Y., Qin, M., Wu, J., Lu, K., … Wang, W. (2016). Polymer-Supramolecular Polymer Double-Network Hydrogel. *Advanced Functional Materials*, *26*, 9044–9052. https://doi.org/10.1002/adfm.201603512

Tamesue, S., Ohtani, M., Yamada, K., Ishida, Y., Spruell, J. M., Lynd, N. A., … Aida, T. (2013). Linear versus dendritic molecular binders for hydrogel network formation with clay nanosheets: Studies with ABA triblock copolyethers carrying guanidinium ion pendants. *Journal of the American Chemical Society*, *135*, 15650−15655. https://doi.org/10.1021/ja408547g

Thomas, B., Raj, M. C., Athira, B. K., Rubiyah, H. M., Joy, J., Moores, A., … Sanchez, C. (2018). Nanocellulose, a Versatile Green Platform: From Biosources to Materials and Their Applications. *Chemical Reviews*, pp. 11575–11625. https://doi.org/10.1021/acs.chemrev.7b00627

Tingaut, P., Zimmermann, T., & Sèbe, G. (2012). Cellulose nanocrystals and microfibrillated cellulose as building blocks for the design of hierarchical functional materials. *Journal of Materials Chemistry*, *22*, 20105–20111. https://doi.org/10.1039/c2jm32956e

Tuncaboylu, D. C., Sari, M., Oppermann, W., & Okay, O. (2011). Tough and self-healing hydrogels formed via hydrophobic interactions. *Macromolecules*, *44*, 4997–5005. https://doi.org/10.1021/ma200579v

Ureña-Benavides, E. E., Ao, G., Davis, V. A., & Kitchens, C. L. (2011). Rheology and phase behavior of lyotropic cellulose nanocrystal suspensions. *Macromolecules*, *44*(22), 8990-8998. https://doi.org/10.1021/ma201649f

Van Der Zwaag, S., Van Dijk, N. H., Jonkers, H. M., Mookhoek, S. D., & Sloof, W. G. (2009). Self-healing behaviour in Man-made engineering materials: Bioinspired but taking into account their intrinsic character. *Philosophical Transactions of the Royal Society A: Mathematical, Physical and Engineering Sciences*, *367*(1894), 1689-1704. https://doi.org/10.1098/rsta.2009.0020

Wang, J., Lin, L., Cheng, Q., & Jiang, L. (2012). A strong bio-inspired layered PNIPAM-clay nanocomposite hydrogel. *Angewandte Chemie - International Edition*, *51*, 4676–4680. https://doi.org/10.1002/anie.201200267

Wang, T., Zheng, S., Sun, W., Liu, X., Fu, S., & Tong, Z. (2014). Notch insensitive and self-healing PNIPAm-PAM-clay nanocomposite hydrogels. *Soft Matter*, *10*, 3506–3512. https://doi.org/10.1039/c3sm52961d

Wang, X. H., Song, F., Qian, D., He, Y. D., Nie, W. C., Wang, X. L., & Wang, Y. Z. (2018). Strong and tough fully physically crosslinked double network hydrogels with tunable mechanics and high self-healing performance. *Chemical Engineering Journal*, *349*, 588–594. https://doi.org/10.1016/j.cej.2018.05.081

Wang, Y., Niu, J., Hou, J., Wang, Z., Wu, J., Meng, G., … Guo, X. (2018). A novel

design strategy for triple-network structure hydrogels with high-strength, tough and self-healing properties. *Polymer*, *135*, 16–24. https://doi.org/10.1016/j.polymer.2017.11.076

Wei, J., Wang, J., Su, S., Wang, S., & Qiu, J. (2015). Tough and fully recoverable hydrogels. *Journal of Materials Chemistry B*, *3*, 5284–5290. https://doi.org/10.1039/c5tb00504c

Weinhold, F., & Klein, R. A. (2014). What is a hydrogen bond? Resonance covalency in the supramolecular domain. *Chemistry Education Research and Practice*, *15*, 276–285. https://doi.org/10.1039/c4rp00030g

White, S. R., Sottos, N. R., Geubelle, P. H., Moore, J. S., Kessler, M. R., Sriram, S. R., … Viswanathan, S. (2001). Autonomic healing of polymer composites. *Nature*, pp. 794–797. https://doi.org/10.1038/35057232

Wu, C. J., Gaharwar, A. K., Chan, B. K., & Schmidt, G. (2011). Mechanically tough Pluronic F127/Laponite nanocomposite hydrogels from covalently and physically cross-linked networks. *Macromolecules*, *44*, 8215–8224. https://doi.org/10.1021/ma200562k

Wu, S., Dong, H., Li, Q., Wang, G., & Cao, X. (2017). High strength, biocompatible hydrogels with designable shapes and special hollow-formed character using chitosan and gelatin. *Carbohydrate Polymers*, *168*, 147–152.

https://doi.org/10.1016/j.carbpol.2017.03.069

Xu, D., Bhatnagar, D., Gersappe, D., Sokolov, J. C., Rafailovich, M. H., & Lombardi, J. (2015). Rheology of poly (N-isopropylacrylamide)-clay nanocomposite hydrogels. *Macromolecules*, *48*, 840–846. https://doi.org/10.1021/ma502111p

Xu, K., An, H., Lu, C., Tan, Y., Li, P., & Wang, P. (2013). Facile fabrication method of hydrophobic-associating cross-linking hydrogel with outstanding mechanical performance and self-healing property in the absence of surfactants. *Polymer*, *54*, 5665–5672. https://doi.org/10.1016/j.polymer.2013.07.079

Yang, C. H., Wang, M. X., Haider, H., Yang, J. H., Sun, J. Y., Chen, Y. M., … Suo, Z. (2013). Strengthening alginate/polyacrylamide hydrogels using various multivalent cations. *ACS Applied Materials and Interfaces*, *5*, 10418−1042. https://doi.org/10.1021/am403966x

Yang, J., Han, C. R., Duan, J. F., Ma, M. G., Zhang, X. M., Xu, F., & Sun, R. C. (2013). Synthesis and characterization of mechanically flexible and tough cellulose nanocrystals-polyacrylamide nanocomposite hydrogels. *Cellulose*, *20*, 227–237. https://doi.org/10.1007/s10570-012-9841-y

Yang, J., Han, C. R., Xu, F., & Sun, R. C. (2014). Simple approach to reinforce hydrogels with cellulose nanocrystals. *Nanoscale*, *6*, 5934–5943. https://doi.org/10.1039/c4nr01214c

Yang, X., Zhang, G., & Zhang, D. (2012). Stimuli responsive gels based on low molecular weight gelators. *Journal of Materials Chemistry*, *22*, 38–50. https://doi.org/10.1039/c1jm13205a

Yao, H., Ke, H., Zhang, X., Pan, S. J., Li, M. S., Yang, L. P., … Jiang, W. (2018). Molecular Recognition of Hydrophilic Molecules in Water by Combining the Hydrophobic Effect with Hydrogen Bonding. *Journal of the American Chemical Society*, *140*, 13466–13477. https://doi.org/10.1021/jacs.8b09157

Youngblood, J. P., & Sottos, N. R. (2008). Bioinspired Materials for Self-Cleaning and Self-Healing. *MRS Bulletin*, *33*(8), 732–741. https://doi.org/10.1557/mrs2008.158

Yu, L., Chen, G. Y., Xu, H., & Liu, X. (2016). Substrate-independent, transparent oil-repellent coatings with self-healing and persistent easy-sliding oil repellency. *ACS Nano*, *10*, 1076−1085. https://doi.org/10.1021/acsnano.5b06404

Yuan, N., Xu, L., Wang, H., Fu, Y., Zhang, Z., Liu, L., … Rong, J. (2016). Dual Physically Cross-Linked Double Network Hydrogels with High Mechanical Strength, Fatigue Resistance, Notch-Insensitivity, and Self-Healing Properties. *ACS Applied Materials and Interfaces*, *8*, 34034−3404. https://doi.org/10.1021/acsami.6b12243

Zhang, T., Cheng, Q., Ye, D., & Chang, C. (2017). Tunicate cellulose nanocrystals reinforced nanocomposite hydrogels comprised by hybrid cross-linked networks.

Carbohydrate Polymers, *169*, 139–148. https://doi.org/10.1016/j.carbpol.2017.04.007

Zhao, D., Huang, J., Zhong, Y., Li, K., Zhang, L., & Cai, J. (2016). High-Strength and High-Toughness Double-Cross-Linked Cellulose Hydrogels: A New Strategy Using Sequential Chemical and Physical Cross-Linking. *Advanced Functional Materials*, *26*, 6279–6287. https://doi.org/10.1002/adfm.201601645

Zhao, X. (2014). Multi-scale multi-mechanism design of tough hydrogels: Building dissipation into stretchy networks. *Soft Matter*, pp. 672–687. https://doi.org/10.1039/c3sm52272e

Zhao, Z., Fang, R., Rong, Q., & Liu, M. (2017). Bioinspired Nanocomposite Hydrogels with Highly Ordered Structures. *Advanced Materials*, p. 1703045. https://doi.org/10.1002/adma.201703045

Zhong, M., Liu, Y. T., & Xie, X. M. (2015). Self-healable, super tough graphene oxide-poly (acrylic acid) nanocomposite hydrogels facilitated by dual cross-linking effects through dynamic ionic interactions. *Journal of Materials Chemistry B*, *3*, 4001–4008. https://doi.org/10.1039/c5tb00075k

Appendix

The copyright permissions are listed as follows:

JOHN WILEY AND SONS LICENSE
TERMS AND CONDITIONS

Jul 26, 2020

This Agreement between Ms. XINYAO LIU ("You") and John Wiley and Sons ("John Wiley and Sons") consists of your license details and the terms and conditions provided by John Wiley and Sons and Copyright Clearance Center.

License Number: 4876821254963
License date: Jul 26, 2020
Licensed Content Publisher: John Wiley and Sons
Licensed Content Publication: Advanced Materials
Licensed Content Title: Self‐Healing Materials
Licensed Content Author: Ulrich S. Schubert, Sybrand van der Zwaag, Christoph Leyens, et al
Licensed Content Date: Sep 13, 2010
Licensed Content Volume: 22
Licensed Content Issue: 47
Licensed Content Pages: 7
Type of use: Dissertation/Thesis
Requestor type: University/Academic
Format: Electronic
Portion: Figure/table
Number of figures/tables: 2
Will you be translating?:No
Title: Self-Recoverable Dual Physically Cross-Linked Hydrogels Incorporating Hydrophobic Interactions
Institution name: University of Calgary
Expected presentation date: Aug 2020
Portions: Figure 1 and Figure 2 on page 5425
Requestor Location: Ms. XINYAO LIU250 Collegiate BV NW0445B Crowsnest HallCalgary, AB T2N 5A6, Canada
Attn: Ms. XINYAO LIU
Publisher Tax ID: EU826007151
Total: 0.00 CAD
Terms and Conditions

TERMS AND CONDITIONS

This copyrighted material is owned by or exclusively licensed to John Wiley & Sons, Inc. or one of its group companies (each a "Wiley Company") or handled on behalf of a society with which a Wiley Company has exclusive publishing rights in relation to a particular work (collectively "WILEY"). By clicking "accept" in connection with completing this licensing transaction, you agree that the following terms and conditions apply to this transaction (along with the billing and payment terms and conditions established by the Copyright Clearance Center Inc., ("CCC's Billing and Payment terms and conditions"), at the time that you opened your Rights Link account (these are available at any time at http://myaccount.copyright.com).

Terms and Conditions

- The materials you have requested permission to reproduce or reuse (the "Wiley Materials") are protected by copyright.

- You are hereby granted a personal, non-exclusive, non-sub licensable (on a stand-alone basis), non-transferable, worldwide, limited license to reproduce the Wiley Materials for the purpose specified in the licensing process. This license, **and any CONTENT (PDF or image file) purchased as part of your order,** is for a one-time use only and limited to any maximum distribution number specified in the license. The first instance of republication or reuse granted by this license must be completed within two years of the date of the grant of this license (although copies prepared before the end date may be distributed thereafter). The Wiley Materials shall not be used in any other manner or for any other purpose, beyond what is granted in the license. Permission is granted subject to an appropriate acknowledgement given to the author, title of the material/book/journal and the publisher. You shall also duplicate the copyright notice that appears in the Wiley publication in your use of the Wiley Material. Permission is also granted on the understanding that nowhere in the text is a previously published source acknowledged for all or part of this Wiley Material. Any third party content is expressly excluded from this permission.

- With respect to the Wiley Materials, all rights are reserved. Except as expressly granted by the terms of the license, no part of the Wiley Materials may be copied, modified, adapted (except for minor reformatting required by the new Publication), translated, reproduced, transferred or distributed, in any form or by any means, and no derivative works may be made based on the Wiley Materials without the prior permission of the respective copyright owner. **For STM Signatory Publishers clearing permission under the terms of the STM Permissions Guidelines only, the terms of the license are extended to include subsequent editions and for editions in other languages, provided such editions are for the work as a whole in situ and does not involve the separate exploitation of the permitted figures or extracts,** You may not alter, remove or suppress in any manner any copyright, trademark or other notices displayed by the Wiley Materials. You may not license, rent, sell, loan, lease,

pledge, offer as security, transfer or assign the Wiley Materials on a stand-alone basis, or any of the rights granted to you hereunder to any other person.

- The Wiley Materials and all of the intellectual property rights therein shall at all times remain the exclusive property of John Wiley & Sons Inc, the Wiley Companies, or their respective licensors, and your interest therein is only that of having possession of and the right to reproduce the Wiley Materials pursuant to Section 2 herein during the continuance of this Agreement. You agree that you own no right, title or interest in or to the Wiley Materials or any of the intellectual property rights therein. You shall have no rights hereunder other than the license as provided for above in Section 2. No right, license or interest to any trademark, trade name, service mark or other branding ("Marks") of WILEY or its licensors is granted hereunder, and you agree that you shall not assert any such right, license or interest with respect thereto

- NEITHER WILEY NOR ITS LICENSORS MAKES ANY WARRANTY OR REPRESENTATION OF ANY KIND TO YOU OR ANY THIRD PARTY, EXPRESS, IMPLIED OR STATUTORY, WITH RESPECT TO THE MATERIALS OR THE ACCURACY OF ANY INFORMATION CONTAINED IN THE MATERIALS, INCLUDING, WITHOUT LIMITATION, ANY IMPLIED WARRANTY OF MERCHANTABILITY, ACCURACY, SATISFACTORY QUALITY, FITNESS FOR A PARTICULAR PURPOSE, USABILITY, INTEGRATION OR NON-INFRINGEMENT AND ALL SUCH WARRANTIES ARE HEREBY EXCLUDED BY WILEY AND ITS LICENSORS AND WAIVED BY YOU.

- WILEY shall have the right to terminate this Agreement immediately upon breach of this Agreement by you.

- You shall indemnify, defend and hold harmless WILEY, its Licensors and their respective directors, officers, agents and employees, from and against any actual or threatened claims, demands, causes of action or proceedings arising from any breach of this Agreement by you.

- IN NO EVENT SHALL WILEY OR ITS LICENSORS BE LIABLE TO YOU OR ANY OTHER PARTY OR ANY OTHER PERSON OR ENTITY FOR ANY SPECIAL, CONSEQUENTIAL, INCIDENTAL, INDIRECT, EXEMPLARY OR PUNITIVE DAMAGES, HOWEVER CAUSED, ARISING OUT OF OR IN CONNECTION WITH THE DOWNLOADING, PROVISIONING, VIEWING OR USE OF THE MATERIALS REGARDLESS OF THE FORM OF ACTION, WHETHER FOR BREACH OF CONTRACT, BREACH OF WARRANTY, TORT, NEGLIGENCE, INFRINGEMENT OR OTHERWISE (INCLUDING, WITHOUT LIMITATION, DAMAGES BASED ON LOSS OF PROFITS, DATA, FILES, USE, BUSINESS OPPORTUNITY OR CLAIMS OF THIRD PARTIES), AND WHETHER OR NOT THE PARTY HAS BEEN ADVISED OF THE POSSIBILITY

OF SUCH DAMAGES. THIS LIMITATION SHALL APPLY NOTWITHSTANDING ANY FAILURE OF ESSENTIAL PURPOSE OF ANY LIMITED REMEDY PROVIDED HEREIN.

- Should any provision of this Agreement be held by a court of competent jurisdiction to be illegal, invalid, or unenforceable, that provision shall be deemed amended to achieve as nearly as possible the same economic effect as the original provision, and the legality, validity and enforceability of the remaining provisions of this Agreement shall not be affected or impaired thereby.

- The failure of either party to enforce any term or condition of this Agreement shall not constitute a waiver of either party's right to enforce each and every term and condition of this Agreement. No breach under this agreement shall be deemed waived or excused by either party unless such waiver or consent is in writing signed by the party granting such waiver or consent. The waiver by or consent of a party to a breach of any provision of this Agreement shall not operate or be construed as a waiver of or consent to any other or subsequent breach by such other party.

- This Agreement may not be assigned (including by operation of law or otherwise) by you without WILEY's prior written consent.

- Any fee required for this permission shall be non-refundable after thirty (30) days from receipt by the CCC.

- These terms and conditions together with CCC's Billing and Payment terms and conditions (which are incorporated herein) form the entire agreement between you and WILEY concerning this licensing transaction and (in the absence of fraud) supersedes all prior agreements and representations of the parties, oral or written. This Agreement may not be amended except in writing signed by both parties. This Agreement shall be binding upon and inure to the benefit of the parties' successors, legal representatives, and authorized assigns.

- In the event of any conflict between your obligations established by these terms and conditions and those established by CCC's Billing and Payment terms and conditions, these terms and conditions shall prevail.

- WILEY expressly reserves all rights not specifically granted in the combination of (i) the license details provided by you and accepted in the course of this licensing transaction, (ii) these terms and conditions and (iii) CCC's Billing and Payment terms and conditions.

- This Agreement will be void if the Type of Use, Format, Circulation, or Requestor Type was misrepresented during the licensing process.

- This Agreement shall be governed by and construed in accordance with the laws of the State of New York, USA, without regards to such state's conflict of law rules. Any legal action, suit or proceeding arising out of or relating to these Terms and Conditions or the breach thereof shall be instituted in a court of competent jurisdiction in New York County in the State of New York in the United States of America and each party hereby consents and submits to the personal jurisdiction of such court, waives any objection to venue in such court and consents to service of process by registered or certified mail, return receipt requested, at the last known address of such party.

WILEY OPEN ACCESS TERMS AND CONDITIONS

Wiley Publishes Open Access Articles in fully Open Access Journals and in Subscription journals offering Online Open. Although most of the fully Open Access journals publish open access articles under the terms of the Creative Commons Attribution (CC BY) License only, the subscription journals and a few of the Open Access Journals offer a choice of Creative Commons Licenses. The license type is clearly identified on the article.

The Creative Commons Attribution License

The Creative Commons Attribution License (CC-BY) allows users to copy, distribute and transmit an article, adapt the article and make commercial use of the article. The CC-BY license permits commercial and non-

Creative Commons Attribution Non-Commercial License

The Creative Commons Attribution Non-Commercial (CC-BY-NC)Licensepermits use, distribution and reproduction in any medium, provided the original work is properly cited and is not used for commercial purposes.(see below)

Creative Commons Attribution-Non-Commercial-No Derivs License

The Creative Commons Attribution Non-Commercial-NoDerivs License (CC-BY-NC-ND) permits use, distribution and reproduction in any medium, provided the original work is properly cited, is not used for commercial purposes and no modifications or adaptations are made. (see below)

Use by commercial "for-profit" organizations

Use of Wiley Open Access articles for commercial, promotional, or marketing purposes requires further explicit permission from Wiley and will be subject to a fee.
